

**PREPARATION OF POLY(VINYL PYRROLIDONE) NANOGELS  
BY RADIATION-INDUCED CROSSLINKING  
OF DILUTE AQUEOUS SOLUTIONS**

**POLİ(VİNİL PİROLİDON)'UN SEYRELTİK SULU  
ÇÖZELTİLERİNDEN RADYASYONLA BAŞLATILAN ÇAPRAZ  
BAĞLANMA YÖNTEMİ İLE NANOJEL ELDE EDİLMESİ**

**SEMİHA DUYGU IŞIK**

Submitted to the Institute for Graduate Studies  
in Pure & Applied Sciences of Hacettepe University  
as a partial fulfillment of the requirements for the degree of

**MASTER OF SCIENCE  
in  
CHEMISTRY**

**2011**

To the Institute for Graduate Studies in Pure and Applied Sciences,

This study has been accepted as a THESIS of MASTER of SCIENCE in CHEMISTRY by our examining committee.

Chair :.....  
Prof. Dr. Nesrin HASIRCI

Member (Supervisor) :.....  
Prof. Dr. Olgun GÜVEN

Member :.....  
Prof. Dr. Piotr ULANSKI

Member :.....  
Prof. Dr. Adil DENİZLİ

Member :.....  
Prof. Dr. Murat ŞEN

#### APPROVEMENT

This thesis has been found in compliance with the relevant rules and regulations of the Graduate School of Hacettepe University and approved on 07/01/2011 by the members of the above listed jury members and further confirmed on ...../...../2011 by the Board of the Institute for Graduate Studies in Pure and Applied Sciences.

...../...../2011

Prof. Dr. Adil DENİZLİ

Director of the Institute for Graduate  
Studies in Pure and Applied Sciences

*To my dear family,*

*my nephew,*

*and to*

*Music*



# PREPARATION OF POLY(VINYL PYRROLIDONE) NANOGELS BY RADIATION-INDUCED CROSSLINKING OF DILUTE AQUEOUS SOLUTIONS

Semiha Duygu IŞIK

## ABSTRACT

Nanogels are intramolecularly crosslinked particles with equivalent diameters of approximately 1 to 100 nm exhibiting network structures that can swell in a suitable solvent. Radiation induced synthesis method was chosen to prepare poly(vinyl pyrrolidone) (PVP) ( $M_w = (1.278 \pm 0.023) \times 10^6 \text{ g mol}^{-1}$ ) nanogels because of not requiring monomers or additives (initiator, catalyst, etc.), thus providing the possibility to produce clean materials and to control the degree of crosslinking. PVP nanogels were synthesized by using either electron beam (e-beam) or gamma irradiation from its dilute aqueous solutions. Nanogels synthesized were characterized by using dynamic light scattering (DLS), gel permeation chromatography (GPC), scanning electron microscopy (SEM) and atomic force microscopy (AFM) techniques.

A novel approach to control the particle size of PVP nanogels, which is of great importance for their applications in biomedical field, is proposed. Controlling the solution thermodynamics of aqueous PVP solutions is a way to control the size of polymer coils which will be the precursor of corresponding gels. In order to have a control on the sizes of polymeric coils in solution, in separate studies, guanidinium sulfate (GS) as a denaturing agent, and acetone (Ac) as a non-solvent were used. GS was chosen to be the most effective denaturing agent among the others, thiourea and guanidinium carbonate. Viscosimetric measurements of PVP solutions prepared in the presence of GS showed that there was a clear decrease in limiting viscosity numbers with increasing concentration of GS from 12.61 (water) to 2.87 (2.0 M GS) dL/g due to the disruption of hydrogen bonds between PVP and water molecules. PVP nanogels were prepared from corresponding solutions with e-beam irradiation. The DLS results showed that however there was no systematical change in the sizes of nanogels with the increasing concentration of GS. Moreover acetone was used as a non-solvent and its effect on unirradiated PVP coil sizes was determined by DLS

technique. A decrease in coil size was observed from 63 nm (0.0 Ac/w) to 51 nm (0.66 Ac/w) for unirradiated PVP. Nanogels were prepared from acetone/water mixtures by using gamma irradiation. As the amount of non-solvent increases polymer-polymer interactions are increased and the contraction of coils help the system prefer intramolecular crosslinking due to shorter inter-radical distances on the same PVP backbone, thus, smaller nanogels were obtained with increasing amount of acetone. It was observed that the total absorbed dose didn't affect the size or size based polydispersity index (PDI) of PVP nanogels. For 2 mg/mL concentration, PVP nanogels prepared in water underwent intermolecular crosslinking and microgelation was observed reaching sizes of approximately 230 nm. However all the nanogels prepared in binary mixtures ended up with nanogelation and obtained in the size range 56 to 44 nm. Additionally, PDI values were between 0.20 and 0.23 for PVP nanogels prepared from binary mixtures, but for the nanogels prepared in water they were between 0.31 and 0.38. This decrease in size and polydispersity was also observed by GPC analysis. For the first time, nanogel formation was characterized by using GPC technique. GPC results perfectly fit with the experimental data taken from DLS.

Effect of polymer concentration and effect of type of radiation source was studied for aqueous systems. For the first time a comparative study of gamma and e-beam irradiation was made on the same polymer. The sizes of 1 mg/mL, e-beam irradiated samples showed a systematical decrease from 59 to 46 nm with increasing total absorbed dose. On the other hand, sizes of 1 mg/mL, gamma irradiated samples showed no sensitivity to total absorbed dose. Furthermore, different polymer concentrations were studied and for concentrations higher than 1 mg/mL intermolecular crosslinking was observed. 1 mg/mL samples irradiated with either e-beam or gamma were characterized by AFM and SEM. The AFM and SEM micrographs of 1 mg/mL, gamma irradiated sample showed that the nanogels are spherical and very homogeneous with diameters of approximately 80 nm. AFM and SEM results were also consistent with DLS data.

**Keywords:** Poly(vinyl pyrrolidone) (PVP), nanogel, microgel, theta solvent, denaturing agent, gamma irradiation, electron beam irradiation

**Supervisor:** Prof. Dr. Olgun GÜVEN, Hacettepe University, Department of Chemistry

# POLİ(VİNİL PİROLİDON)'UN SEYRELTİK SULU ÇÖZELTİLERİNDEN RADYASYONLA BAŞLATILAN ÇAPRAZ BAĞLANMA YÖNTEMİ İLE NANOJEL ELDE EDİLMESİ

**Semiha Duygu IŞIK**

## **ÖZET**

Nanojeller çapları yaklaşık 1-100 nm arası olan ve uygun çözücüde şişebilen molekül-içi çapraz bağlı yapılardır. Poli(vinil pirolidon) (PVP) ( $M_w = 1.278 \pm 0.023 \times 10^6 \text{ g mol}^{-1}$ ) nanojellerinin hazırlanmasında radyasyonla başlatılan çapraz bağlanma yöntemi, herhangi bir monomer, başlatıcı, çapraz-bağlayıcı ajan ya da diğer katkı maddelerinin kullanım gerekliliğinin ortadan kaldırılması sayesinde daha temiz materyaller elde edilmesine ve çapraz bağlanma derecesinin kontrolüne olanak sağladığı için tercih edilmiştir. PVP nanojelleri seyreltik sulu çözeltilerinden elektron demeti (e-demeti) ve gama ışınlamasıyla elde edilmiştir. Hazırlanan nanojeller dinamik ışık saçılması (DLS), büyüklükçe ayırma kromatografisi (GPC) teknikleri, taramalı elektron mikroskobu (SEM) ve atomik kuvvet mikroskobu kullanılarak karakterize edilmiştir.

Nanojellerin parçacık boyutu özellikle biyomedikal alandaki uygulamaları için oldukça önemlidir. Bu çalışmada, PVP nanojellerinin parçacık boyutunu kontrol etmek için yeni bir yaklaşım önerilmiştir. Sulu PVP çözeltilerinin çözelti termodinamiğini kontrol etmek polimer yumak boyutlarının kontrol edilebilmesini sağlar. Polimer yumakları, elde edilecek PVP nanojellerinin başlangıç noktası olduğundan, bu kontrol aynı zamanda nanojellerin boyut kontrolünü de mümkün kılmaktadır. Çözeltideki polimer yumaklarının boyutlarını kontrol etmek amacıyla, ayrı çalışmalarda, denatüre edici ajan olan guanidinyum sülfat (GS) ve PVP için çöktürücü olan aseton (Ac) kullanılmıştır. GS varlığında hazırlanan PVP çözeltilerinin viskozimetrik ölçümleri sonucunda limit viskozite sayısında 12.61'den (su) 2.87 dL/g'a (2.0 M GS) keskin bir düşüş gözlenmiştir. Kullanılan denatüre edici ajanlar içerisinde (tiyoüre, guanidinyum karbonat ve GS) en keskin düşüşün

GS'ta gözlenmesi sebebiyle deneylere GS ile devam edilmiştir. Limit viskozite sayısındaki bu düşüş, PVP ve su molekülleri arasındaki hidrojen bağlarının bozulması ve polimer yumağının büzülmesi sonucu gözlenmiştir. Sonrasında, ilgili polimer çözeltilerinden e-demeti ışınlaması ile PVP nanojelleri hazırlanmıştır. Ancak, DLS sonuçları nanojellerin büyüklüklerinin artan GS derişimleri ile sistematik bir deęişim göstermediğini ortaya koymuştur.

Çalışmanın dięer aşamasında, aseton çöktürücü olarak kullanılmış ve asetonun ışınlanmamış PVP yumak boyutları üzerindeki etkisi DLS teknięi kullanılarak tespit edilmiştir. Işınlanmamış PVP için yumak boyutlarında 63 nm'den (0.0 Ac/su) 51 nm'ye (0.66 Ac/su) bir düşüş gözlenmiştir. Aseton/su ikili sistemleri varlığında PVP çözeltilerinden gama ışınlamasıyla nanojeller hazırlanmıştır. Çöktürücü miktarının artmasıyla polimer-polimer etkileşimleri artar ve polimer yumağında büzülme gerçekleşir. Sonuçta, aynı PVP zinciri üzerinde radikaller arası uzaklığın daha az olması sistemin molekül-içi çapraz bağlanmayı tercih etmesine yardımcı olur. Bu nedenle, artan aseton miktarıyla daha küçük boyutlarda nanojeller elde edilmiştir. Toplam absorplanan dozun nanojel boyutunu veya boyuta dayalı polidispersite indeksini (PDI) deęiştirmedięi gözlenmiştir. 2 mg/mL derişime sahip, sadece su içerisinde hazırlanmış PVP çözeltilerinin ışınlanması sonucu moleküller-arası çapraz bağlanma ve mikrojelleşme nedeniyle boyutları yaklaşık 230 nm olan nanojeller elde edilmiştir. Ancak, çözücü/çöktürücü sistemler içerisinde hazırlanmış olan tüm nanojellerin boyutları 56-44 nm arasındadır; sistem sadece nanojelleşme ile sonuçlanmıştır. Ek olarak, ikili sistemlerden hazırlanan nanojellerin PDI deęerleri 0.20-0.23 arası deęişirken su içerisinde hazırlanan nanojeller için PDI deęerleri 0.31-0.38 arasındadır. Nanojellerin boyutları ve PDI deęerlerindeki bu düşüş aynı zamanda GPC sonuçlarında da gözlenmiştir. Nanojel oluşumu ilk defa GPC teknięi kullanılarak karakterize edilmiştir. GPC sonuçları DLS analizlerinden alınan sonuçlarla tamamen örtüşmektedir.

Sadece su içerisinde hazırlanan PVP nanojelleri için polimer derişiminin ve radyasyon kaynaęı türünün etkisi araştırılmıştır. İlk defa aynı polimer için gama ve e-demeti ışınlamasının nanojel boyutuna etkisi kıyaslamalı olarak çalışılmıştır. e-demeti ile

ışınlanmış örneklerde artan toplam absorplanan doz ile nanojel boyutlarında 59 nm'den 46 nm'ye sistematik bir düşüş gözlemiştir. Diğer yandan, gama ile ışınlanmış örnekler için nanojel boyutlarının toplam absorplanan doza duyarlı olmadığı gözlenmiştir. Ayrıca, farklı polimer derişimlerinde çalışılmış ve 1 mg/mL'den daha yüksek derişime sahip örneklerde önemli ölçüde moleküller-arası çapraz bağlanma gözlenmiştir. 1 mg/mL derişime sahip, e-demeti ve gama ile ışınlanmış örnekler AFM ve SEM kullanılarak karakterize edilmiştir. 1 mg/mL, gama ile ışınlanmış örneğin AFM ve SEM görüntüleri, hazırlanan nanojellerin yaklaşık 80 nm çapa sahip, küresel ve oldukça homojen olduklarını göstermiştir. AFM ve SEM sonuçları da DLS verileriyle uyumludur.

**Anahtar Sözcükler:** Poli(vinil piroolidon) (PVP), nanojel, mikrojel, teta çözücü, denature edici ajan, gama ışınlaması, elektron demeti ışınlaması

**Danışman:** Prof. Dr. Olgun GÜVEN, Hacettepe Üniversitesi, Kimya Bölümü



## *Acknowledgements*

First, I would like to express my deepest gratitude to my supervisor, Prof. Dr. Olgun GÜVEN, for his encouragement, inspiration, and endless patience throughout this thesis. He has always been my strongest supporter; with his sage guidance, unconfined knowledge and scientific insight that allowed me to investigate a subject from a fundamental aspect.

I would like to thank Prof. Dr. Piotr ULANSKI for his agreement to be on my dissertation committee. My researches and experiments on this topic mostly progressed in the light of his studies which are highly important due to their novelty and comprehensiveness.

I extend my thanks to every member of Polymer Chemistry Division of Chemistry Department of Hacettepe University for their support and help. I also owe thanks to Prof. Dr. Murat ŞEN for his thoughtful suggestions and empathy and the valuable discussions, especially about GPC, LS and AFM analysis. I would like to acknowledge Prof. Dr. Mohamad AL-SHEIKHLY for his technical support in using the Radiation Facilities at the University of Maryland and Assoc. Prof. Dr. Adnan SEVİL for helping me use the gamma facility at Sarayköy Nuclear Research and Training Center. I also owe thanks to National Nanotechnology Research Center, UNAM at Bilkent University for DLS and SEM experiments. This work was supported by Hacettepe University, Scientific Research Unit (Project No: 5216).

Last, but certainly not least, I wish to express my most sincere thanks to my family, for being always with me. Over the years they have done their best for me. Their helps, guidance, encouragement and unlimited support have led me to the place I stand now.

## TABLE OF CONTENTS

ABSTRACT .....	i
ÖZET .....	iii
ACKNOWLEDGEMENTS.....	vi
TABLE OF CONTENTS .....	vii
FIGURE INDEX.....	x
TABLE INDEX.....	xvi
<b>1. INTRODUCTION.....</b>	<b>1</b>
<b>2. NANOGELS AND MICROGELS.....</b>	<b>4</b>
2.1. Synthesis Methods of Nanogels.....	7
2.1.1. Crosslinking Polymerization .....	8
2.1.1.1. Free-Radical Polymerization.....	9
2.1.1.2. Anionic Polymerization .....	11
2.1.1.3. Emulsion Polymerization .....	11
2.1.1.4. Crosslinking Polymerization in Bulk.....	14
2.1.1.5. Polymerization with Non-classical Initiation .....	15
2.1.2. Intramolecular Crosslinking of Polymers.....	15
2.1.2.1. Chemical Intramolecular Crosslinking.....	15
2.1.2.2. Radiation Induced Intramolecular Crosslinking.....	16
2.2. Applications of Nanogels.....	20

<b>3. RADIATION INDUCED SYNTHESIS OF NANOGELS.....</b>	<b>29</b>
3.1. Radiation Chemistry of Aqueous Systems .....	29
3.2. Reaction Mechanisms of $e_{aq}^-$ and $\cdot OH$ with PVP.....	35
3.3. Effect of Acetone.....	37
<b>4. POLYMER SOLUTION THERMODYNAMICS.....</b>	<b>38</b>
<b>5. EXPERIMENTAL .....</b>	<b>42</b>
5.1. Materials .....	42
5.2. Method.....	43
5.3. Preliminary Studies .....	44
5.3.1. Static Light Scattering.....	44
5.3.2. Viscosity measurements .....	44
5.4. Characterization of PVP nanogels .....	44
5.4.1. Dynamic Light Scattering (DLS) Analysis .....	44
5.4.2. Gel Permeation Chromatography (GPC) Analysis.....	46
5.4.3. Atomic Force Microscopy (AFM) Analysis.....	46
5.4.4. Scanning Electron Microscopy (SEM) Analysis .....	47
<b>6. RESULTS and DISCUSSION.....</b>	<b>48</b>
6.1. Determination of Weight Average Molecular Weight of PVP by Static Light Scattering.....	51

6.2. Effect of Denaturing Agents .....	52
<i>Viscosity Measurements</i> .....	53
<i>Dynamic Light Scattering Analysis</i> .....	56
6.3. Effect of a Non-solvent, Acetone.....	60
<i>Dynamic Light Scattering Analysis</i> .....	60
<i>Gel Permeation Chromatography (GPC) Analysis</i> .....	65
<i>Scanning Electron Microscopy (SEM) Analysis</i> .....	67
6.4. PVP Nanogels Prepared in Water: Effect of Total Absorbed Dose, Polymer Concentration and Type of Radiation Source .....	68
<i>Dynamic Light Scattering Analysis</i> .....	69
<i>Gel Permeation Chromatography (GPC) Analysis</i> .....	72
<i>Atomic Force Microscopy (AFM) Analysis</i> .....	75
<i>Scanning Electron Microscopy (SEM) Analysis</i> .....	77
<b>7. CONCLUSIONS</b> .....	<b>81</b>
<b>8. REFERENCES</b> .....	<b>84</b>
<b>CURRICULUM VITAE</b> .....	<b>104</b>

## FIGURE INDEX

<b>Figure 1.1.</b> Evolution of the number of publications on nanogels/microgels since 1950 (Sanson and Rieger, 2010). .....	1
<b>Figure 2.1.</b> Macromolecules of different forms: a) linear, b) branched, c) network, d) microgel (Greenley, 1980).....	5
<b>Figure 2.2.</b> Microgels of different forms: a) random (homogeneous), b) core-shell.....	6
<b>Figure 2.3.</b> Factors affecting nanogel swelling (Kabanov and Vinogradov, 2009). .....	6
<b>Figure 2.4.</b> List of synthesis methods of nano- and microgels (Ulanski and Rosiak, 2004). .....	7
<b>Figure 2.5.</b> Types of polymer crosslinking: a) intermolecular crosslinking, final product is a macroscopic gel, b) intramolecular crosslinking (crosslinks are represented by red dots), final product is a microgel (or nanogel). .....	9
<b>Figure 2.6.</b> Classical emulsion polymerization process. ....	12
<b>Figure 2.7.</b> Reaction path for the radiation induced synthesis of nanogels from polymer solutions, where the system can end up with either a nanogel (via intramolecular crosslinking) or a macroscopic gel (via intermolecular crosslinking). .....	17
<b>Figure 2.8.</b> Change in intrinsic viscosity and weight average molecular weight with the total absorbed dose of PVA solution (Ulanski et al., 1998).....	18

<b>Figure 2.9.</b> Apparent hydrodynamic radius ( $R_{h,app}$ ) of PVME microgel vs. temperature [total dose: 20 kGy ( $\Delta$ ), 80 kGy (o)] (A) and the SEM image of PMVE microgel in its swollen state after irradiation with a dose of 80 kGy (B) (Arndt et al., 2001).....	19
<b>Figure 2.10.</b> Weight average molecular weight ( $\blacksquare$ ) and intrinsic viscosity, $[\eta]$ ( $\bullet$ ) of pulse irradiated PAA solutions as a function of total absorbed dose (Ulanski et al., 2002).....	20
<b>Figure 2.11.</b> Different architectures of polymers that are mainly used in biomedical applications: A) Liposome, B) Nanosphere and Nanocapsule, C) Micelle, D) Dendrimer, E) Nanogel. ....	21
<b>Figure 2.12.</b> Schematic illustration of nanoparticle passing through tumor tissue through EPR effect (Wang et al., 2009).....	23
<b>Figure 2.13.</b> Schematic illustration of multifunctional core-shell hybrid nanogels (Wu et al., 2010-b).....	24
<b>Figure 2.14.</b> Therapeutic efficacies of photothermal, chemo, and combined chemo-photo-thermal treatments with AgeAu@PEGeHA hybrid nanogels as drug carriers, respectively (Wu et al., 2010-b). ....	24
<b>Figure 2.15.</b> Fluorescent nanogel thermometer: Schematic diagram and chemical structures of the components (A), Fluorescence responses to temperature variation in water and in KCl solutions (B), Insensitivity to pH variation (C) (Gota, 2009). ....	26
<b>Figure 2.16.</b> Schematic illustration of the formation of porous hollow PAA nanogels (Chen, 2010).....	27
<b>Figure 2.17.</b> Crosslinked electrospun nanofibers: (a) fibers with high PNIPAM concentration, (b) fibers with high PNIPAM concentration after immersion in water for 4 days (Sinha-Ray, 2010).....	28

<b>Figure 3.1.</b> Scheme of reactions of transient species produced by irradiation in water without or with a diluted S acting as a radical scavenger (Buxton, 2008).....	32
<b>Figure 3.2.</b> Reaction of $\bullet\text{OH}$ with poly(vinyl pyrrolidone) (Rosiak et al., 1990).....	36
<b>Figure 3.3.</b> Reaction of $e_{\text{aq}}^-$ with poly(vinyl pyrrolidone) (An, 2007). ....	36
<b>Figure 4.1.</b> $R_h$ of PVP polymer chains as a function of temperature (An, 2010). .	41
<b>Figure 4.2.</b> Change of $R_h$ of the synthesized PVP nanohydrogels, using e-beam with a total absorbed dose, 5kGy, as a function of irradiation temperature at different pulse repetition rates (An, 2010). ....	41
<b>Figure 5.1.</b> Successive DLS analyses for a single sample (1 mg/mL PVP in water, 15 kGy).....	45
<b>Figure 6.1.</b> Change in radius of gyration and weight average molecular weight with the total absorbed dose of PVP solution (Ulanski and Rosiak, 1999).....	48
<b>Figure 6.2.</b> Particle size effects on bioavailability and circulation time (An, 2007).....	50
<b>Figure 6.3.</b> Static light scattering result for poly(vinyl pyrrolidone) in water by constructing the Zimm plot. ....	51
<b>Figure 6.4.</b> PVP molecule in aqueous solution (A), and PVP molecule in thiourea solution (B). ....	53
<b>Figure 6.5.</b> Change of reduced viscosity, $\eta_{\text{sp}}/c$ of aqueous PVP solutions with concentration, c, for different guanidinium carbonate concentrations at 25°C. ....	54

<b>Figure 6.6.</b> Change of reduced viscosity, $\eta_{sp}/c$ of aqueous PVP solutions with concentration, $c$ , for different thiourea concentrations at 25°C.....	54
<b>Figure 6.7.</b> Change of reduced viscosity, $\eta_{sp}/c$ of aqueous PVP solutions with concentration, $c$ , for different guanidinium sulfate concentrations at 25°C. ....	55
<b>Figure 6.8.</b> Effect of denaturing agent concentration and total absorbed dose on the peak mean diameters of PVP nanogels that are synthesized from 1 mg/mL aqueous PVP solutions by e-beam irradiation.....	56
<b>Figure 6.9.</b> Effect of denaturing agent concentration and total absorbed dose on the peak mean diameters of PVP nanogels that are synthesized from 2 mg/mL aqueous PVP solutions by e-beam irradiation.....	57
<b>Figure 6.10.</b> Effect of acetone amount in the acetone/water binary mixture on the peak mean diameter of unirradiated PVP.....	61
<b>Figure 6.11.</b> Irradiated PVP in water - a blurry solution, and a transparent solution that consists of PVP nanogels synthesized in acetone/water mixture. ....	63
<b>Figure 6.12.</b> Effect of acetone amount in the acetone/water binary mixture on the peak mean diameter of PVP nanogels that are synthesized from 2 mg/mL PVP solutions by gamma radiation with a total absorbed dose of 15 kGy.....	64
<b>Figure 6.13.</b> Effect of acetone amount in the acetone/water binary mixture on the peak mean diameter of PVP nanogels, as compared to unirradiated PVP coil sizes.....	64
<b>Figure 6.14.</b> Normalized chromatograms of unirradiated PVP and PVP nanogels prepared in acetone/water mixtures with acetone ratios 0.60, 0.62, 0.64 and 0.66 from 2 mg/mL PVP solution using gamma rays with a total absorbed dose of 15 kGy.....	66



<b>Figure 6.15.</b> Size distribution graph based on scattered light intensities of unirradiated PVP (blue) and PVP nanogels prepared in acetone/water mixtures with acetone ratios 0.60 (red), 0.62 (black), 0.64 (pink) and 0.66 (green) from 2 mg/mL PVP solutions using gamma rays with a total absorbed dose of 15 kGy.....	66
<b>Figure 6.16.</b> Scanning electron micrographs of PVP nanogels prepared in 0.66 acetone/water mixture from 2 mg/mL solution PVP using gamma rays with a total absorbed dose of 15 kGy, with a magnification of 13000x (A) and 50000x (B). .....	67
<b>Figure 6.17.</b> Factors promoting intramolecular crosslinking.....	68
<b>Figure 6.18.</b> Effect of total absorbed dose on the peak mean diameter of PVP nanogels that are synthesized from 1 mg/mL aqueous PVP solutions by gamma radiation.....	69
<b>Figure 6.19.</b> Effect of total absorbed dose on the peak mean diameter of PVP nanogels that are synthesized from 2 mg/mL aqueous PVP solutions by gamma radiation.....	71
<b>Figure 6.20.</b> Effect of total absorbed dose on the peak mean diameter of PVP nanogels that are synthesized from 1 mg/mL aqueous PVP solutions by e-beam radiation.....	71
<b>Figure 6.21.</b> Effect of total absorbed dose on the peak mean diameter of PVP nanogels that are synthesized from 2 mg/mL aqueous PVP solutions by e-beam radiation.....	72
<b>Figure 6.22.</b> Normalized chromatograms of unirradiated PVP and PVP nanogels prepared from 1 mg/mL solution of PVP aqueous solutions using e-beam with total absorbed doses of 5, 10 and 20 kGy. ....	73

- Figure 6.23.** Normalized chromatograms of unirradiated PVP and PVP nanogels prepared from 1 mg/mL solution of PVP aqueous solutions using gamma rays with total absorbed doses of 5, 10 and 20 kGy. .... 73
- Figure 6.24.** Height based AFM images of mica surface (A), PVP coated mica surface (B), PVP nanogels deposited on mica surface (C). .... 75
- Figure 6.25.** 3D views of AFM images of mica surface (A), PVP coated mica surface (B), PVP nanogels deposited on mica surface (C). .... 76
- Figure 6.26.** Cross-sectional views of PVP coated mica surface (A), PVP nanogels deposited on mica surface (B). .... 76
- Figure 6.27.** Scanning electron micrographs of PVP nanogels being prepared from 1 mg/mL solution PVP using gamma rays with a total absorbed dose of 15 kGy, with a magnification of 15000x (A), 30000x (B). ..... 78
- Figure 6.28.** Scanning electron micrographs of PVP nanogels being prepared from 1 mg/mL solution PVP using gamma rays with a total absorbed dose of 15 kGy, with a magnification of 60000x (A), 120000x (B). .... 79
- Figure 6.29.** Scanning electron micrographs of PVP nanogels being prepared from 1 mg/mL solution PVP using electron beam with a total absorbed dose of 10 kGy, with a magnification of 30000x (A), 60000x (B). ..... 80

## TABLE INDEX

<b>Table 2.1.</b> Shrinkage ratio (%) of two samples without dye when water temperature increased from about 25 °C to 51.2 or 53.1 °C (Sinha-Ray, 2010). .	28
<b>Table 2.2.</b> Contact angles (deg) upon drop deposition measured at different temperatures (Sinha-Ray, 2010). .....	28
<b>Table 3.1.</b> Radiation chemical yields (G values) for the radiolysis products of water for low LET radiation (Buxton, 2008). .....	32
<b>Table 3.2.</b> Spur reactions in water (Aziz and Rodgers, 1987). .....	33
<b>Table 5.1.</b> The materials that are used in this work and their chemical structures.....	42
<b>Table 6.1.</b> Limiting viscosity numbers, $[\eta]$ (dL/g) for PVP in water and in denaturing agents GC, TU and GS having different concentrations, 0.5, 0.1, 1.5 and 2.0 M. ....	55
<b>Table 6.2.</b> Peak mean diameters, their standard deviations and PDI values for nanogels that are synthesized by e-beam irradiation of 1 mg/mL aqueous PVP solutions with changing guanidinium sulfate concentrations. ....	58
<b>Table 6.3.</b> Peak mean diameters, their standard deviations and PDI values for nanogels that are synthesized by e-beam irradiation of 2 mg/mL aqueous PVP solutions with changing guanidinium sulfate concentrations. ....	59
<b>Table 6.4.</b> Peak mean diameters, their standard deviations and PDI values for nanogels that are synthesized from 2 mg/mL aqueous PVP solutions by using gamma irradiation at the indicated acetone compositions. ....	62

**Table 6.5.** Peak mean diameters, their standard deviations and PDI values for nanogels that are synthesized from 1 mg/mL and 2 mg/mL aqueous PVP solutions by using gamma radiation. .... 70

**Table 6.6.** Peak mean diameters, their standard deviations and PDI values for nanogels that are synthesized from 1 mg/mL and 2 mg/mL aqueous PVP solutions by using e-beam radiation. .... 70

**Table 6.7.** Peak mean diameters, their standard deviations and PDI values for nanogels that are synthesized from 1 mg/mL aqueous solutions of PVP by using e-beam and gamma radiation..... 74

# 1. INTRODUCTION

After the first report of Wichterle and Lim published in Nature in 1960, there has been an exponential increase in the scientific reports on hydrogels. Hydrogels, which consist of hydrophilic polymers having three dimensional network structures, find applications in tissue engineering, molecular recognition and controlled release - drug delivery applications due to their swelling ability and biocompatibility with living tissue. Their nanometric/micrometric counterparts, nanogel and microgels attract a great deal of attention due to their unique properties like fixed shape, different rheological behaviour, higher resistance to degradation and the ability to trap other molecules within their structure (Ulanski and Rosiak, 2004). Therefore, starting from the work of Staudinger in 1935 in which they prepared divinyl benzene microgels, the number of publications/year on this subject is steadily rising. Figure 1.1 shows the exponential increase in the number of publications on nanogels/microgels for the last two decades.

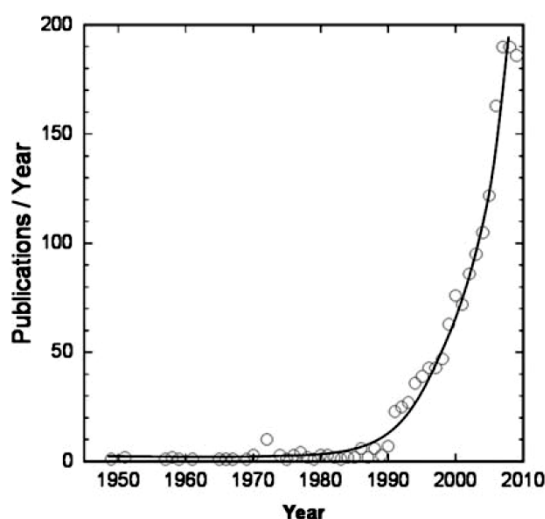


**Figure 1.1.** Evolution of the number of publications on nanogels/microgels since 1950 (Sanson and Rieger, 2010).

Owing to the diversity of synthesis methods, structure and property of reactants, nanogels may find various applications such as chemical and biological sensors, coatings, water purification devices, super absorbents, contrast agents, drug and vaccine carrier systems, nanodevices, nanoreactors, polymeric drugs, etc.

Nanogels are nanoscale dispersions of polymer chains crosslinked in a physical or a chemical way and the methods to prepare these particles can be classified in two groups. The first group covers 'crosslinking polymerization' where the starting materials for the synthesis are monomers or monomer mixtures. For the second group, the reactant is a polymer and nanogel formation is achieved by intramolecular crosslinking. Typical examples of crosslinking polymerization are free-radical polymerization, anionic polymerization and emulsion polymerization. The main problem in these methods is to control the competition between inter- and intramolecular crosslinking during the propagation step, which will result in macrogelation or microgelation, respectively. Furthermore, the use of monomers can be a big problem for biomedical applications due to the possibility of residual monomers. The second method of synthesis covers the so called "monomer-free techniques". Radiation-induced intramolecular crosslinking method stand out from the rest due to its versatility. With respect to other classical methods, radiation induced synthesis is preferable because of the absence of additives (initiator, catalyst, etc.), thus a higher possibility to produce clean materials, the possibility of initiating the reaction at any temperature and to control the degree of crosslinking. In this thesis, e-beam irradiation and gamma irradiation were used to prepare PVP nanogels.

Size of the nanogels play an important role in their biomedical applications. It is known that size of the nanoscaled particles strongly affects the circulation time in blood and bioavailability of the particles within the body by evading RES (Reticulo Endothelial System). It is considered as nanoparticles with a size between 10 and 100 nm will be optimal considering their circulation time in blood. Therefore, nanogels that are designed for drug delivery should mainly meet the particle size criteria.

For the radiation induced synthesis of nanogels different parameters (e.g. total absorbed dose, dose rate, polymer concentration and temperature) (Ulanski et al, 1998, 1999, 2002, An, 2007) have been extensively studied. However, as the nanogels are generally prepared from aqueous systems, an additional approach could be proposed considering polymer solution thermodynamical concepts.

Within the scope of this thesis, an efficient and versatile method is proposed to control the particle sizes of nanogels, that is, controlling the solution thermodynamics of polymer solutions. The underlying principle of this dissertation is to prepare dilute aqueous poly(vinyl pyrrolidone) (PVP) solutions by using denaturing agents, and acetone, as a non-solvent, to have a control on the polymer coil dimensions. The effect of guanidinium sulfate on PVP coils were analysed using viscosimetric measurements whereas the effect of acetone is determined by dynamic light scattering.

Upon the addition of acetone, a decrease is observed in the polymer coils of PVP where this decrease is systematical with the increasing percent of acetone in acetone/water binary mixture. These polymer coils were the precursors of PVP nanogels since the decrease in PVP coil will result in a smaller nanogel after irradiation. The PVP nanogels were produced in a simple and efficient way by simply irradiating them with ionizing radiation.

Additional parameters to control the particle size and particle size distribution were studied in this thesis. Starting from aqueous solutions of PVP, nanogels were synthesized with either e-beam or gamma irradiation, thus the effect of the type of radiation source, subsequently the effect of radiation dose, on the sizes of nanogels were determined. Furthermore, different total absorbed doses were used to prepare PVP nanogels in the range of 5-20 kGy and their effect on the sizes of PVP nanogels were investigated. Moreover the effect of polymer concentration was also studied.

Changes in the hydrodynamic volume of PVP and PVP nanogels were mainly analysed by using dynamic light scattering. Additionally, gel permeation chromatography was used to observe the changes in hydrodynamic volumes of PVP nanogels with respect to pristine PVP both for binary solvent and aqueous systems. PVP nanogels were also characterized by atomic force microscopy and scanning electron microscopy to have a close up view of the prepared nanogels.

## 2. NANOGELS AND MICROGELS

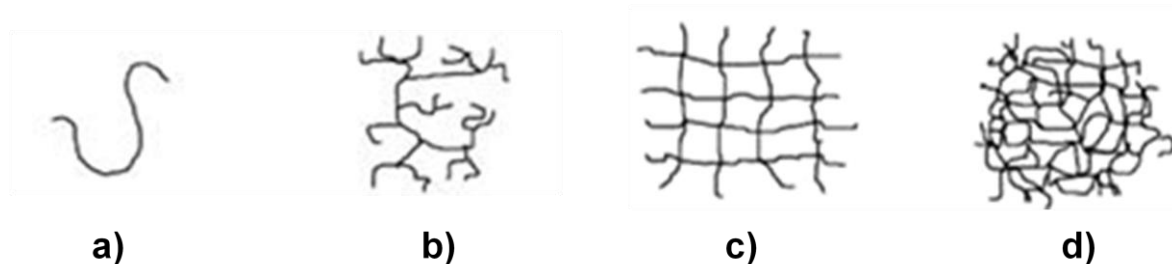
To understand the concept of nano- and microgels, their analogues, macroscopic gels should first be considered. Macroscopic gels are a specific class of polymers that can swell to a large extent in a solvent by maintaining their three-dimensional network structure in the swollen state with the presence of permanent crosslinks. The term “macroscopic (polymeric) gel” is a general definition that covers other situations where their solvents may vary, e.g. water, body fluids. On the other hand, the term ‘hydrogel’ is proposed where the solvent filling the pores of the network structure is water. After the first report on the use of hydrogels for biomedical applications (Wichterle and Lim, 1960) their use has increased tremendously especially in tissue engineering (Drury and Mooney, 2003; Park et al., 2005; Kim et al., 2009; Han et al., 2010; Liu et al., 2010; Desai et al., 2010), molecular recognition (Yoshimura et al., 2004; Koshi et al., 2006; Wada et al., 2009; Ikeda et al., 2010; Zhang and Ji, 2010; Yan et al., 2010) controlled release and drug delivery applications (Lee, 1984; Şen and Yakar 2001; Van Tomme and Sophie, 2007; Ma and Prabhu, 2011; Mi et al., 2010; Li et al., 2011).

In 1935 Staudinger and Husemann introduced a new concept to polymer technology by preparing divinyl benzene microgel particles. However, the term ‘microgel’ was first introduced by Baker in 1949 who worked on emulsions of SBR rubbers and recognized that these crosslinked structures were intramolecularly crosslinked macromolecules which constituted a new form of polymer molecule. In the early literature the term microgel was used for gels within both nano and/or microscopic scale. A general definition can be made as nanogels and microgels are the counterparts of macroscopic gels having dimensions in the nanoscopic or microscopic scale. Accepted definition for these particles is that they are internally crosslinked macromolecules where all the chains of a nanogel or a microgel are linked together (Ulanski and Rosiak, 2004).



Flory made an assertion that only a small part of the reaction gelation process must be intramolecular regarding the unwanted effect of these reactions (Flory, 1941). Recent knowledge show that intramolecular reactions (crosslinkings) are of great importance to end up with either macrogelation (i.e. hydrogel, macroscopic gel) or microgelation. Therefore these reactions gained too much importance in polymer chemistry, pharmacy and materials science because of the diversity of applications of microgels.

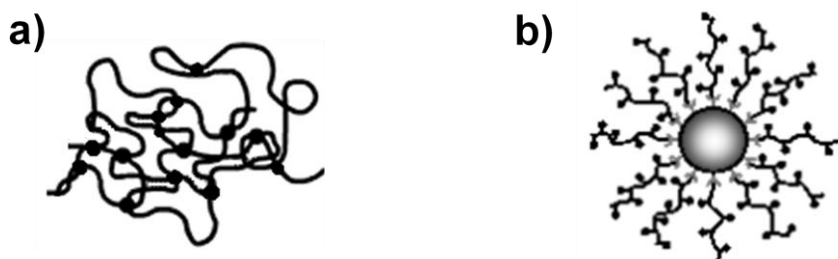
Nano- and microgels are now classified as a specific form of macromolecules among the others (linear, dendrimer, branched, etc.). Figure 2.1 shows some of these different structures schematically. They can be visualised as coiled state of a linear macromolecule where a permanent network, consisting of intramolecular crosslinkages exists. Contrary to linear polymers, new properties arise from the fact that these substances are covalently crosslinked. Like their macroscopic counterparts they have the ability to swell in water, body-fluids, etc.



**Figure 2.1.** Macromolecules of different forms: a) linear, b) branched, c) network, d) microgel (Greenley, 1980).

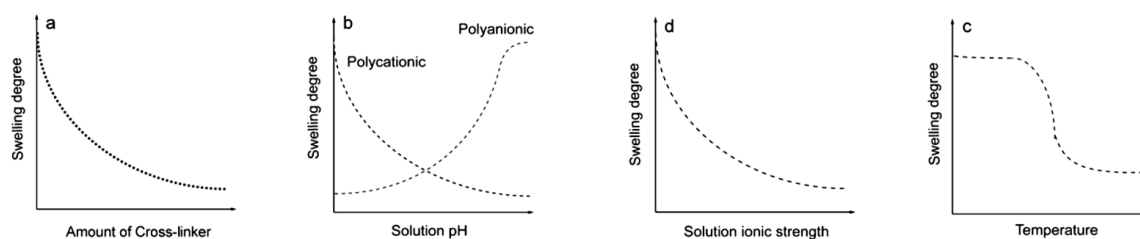
It is first noted by Baker that for their very large size they showed very low solution viscosities and the molecular weight exponent in the Mark-Houwink equation was very low ( $<0.5$ ) and in some instances approached zero. This demonstrated that in 'solution' these microgels behaved more like Einstein spheres than dissolved linear polymer coils and the microgels exhibited much lower than expected solution viscosities (Baker, 1949).

In addition to these distinct properties of nano- and microgels, current interest is to gain more complex morphologies that are able to react to external stimuli. Core-shell structured, anisotropic, multilayered, smart (intelligent) nano- and microgels are some examples from this quest (Sanson and Rieger, 2010). Figure 2.2 represents a classical microgel and a core-shell structured microgel schematically.



**Figure 2.2.** Microgels of different forms: a) random (homogeneous), b) core-shell.

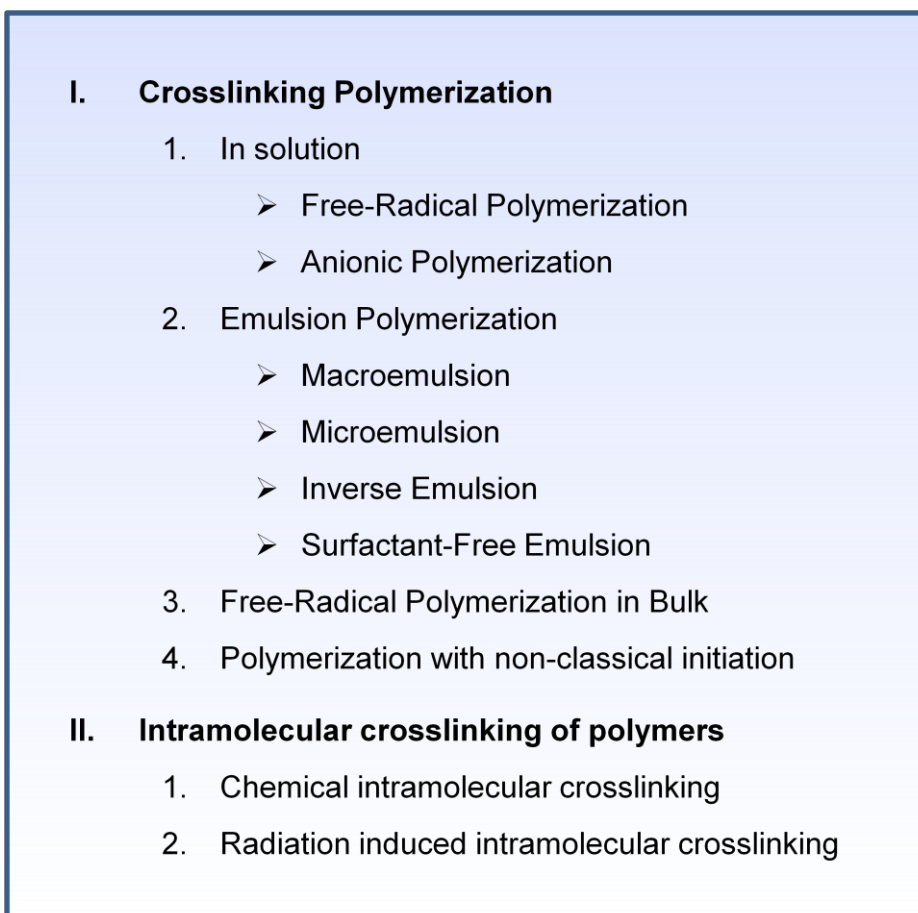
One of the main factors that directly routes the properties of nanogels is their swelling ability. Depending on the chemical compositions, solution pH, temperature and ionic strength and amount of the crosslinker used, swelling degree may change which directly affects the application areas of the nanogels synthesized. Figure 2.3. shows these factors affecting nanogel swelling: a) An increase in the extent of crosslinking decreases the swelling of the nanogels comprised of a hydrophilic polymer. b) An increase in the pH value results in the collapse of a nanogel comprised of weak polybase chains, and the swelling of nanogels comprised of a weak polyacid. c) An increase in the ionic strength decreases the swelling of polyelectrolyte nanogels. d) Nanogels comprised of polymers exhibiting LCST behavior collapse as the temperature increases above the LCST.



**Figure 2.3.** Factors affecting nanogel swelling (Kabanov and Vinogradov, 2009).

## 2.1. Synthesis Methods of Nanogels

An accepted classification for the synthesis methods has been made by Ulanski and Rosiak as shown in Figure 2.4. They separated the proposed techniques into two main groups. The first group covers 'crosslinking polymerization' where the starting materials for the synthesis are monomers or monomer mixtures. For the second group, the substrate is a polymer and nanogel formation is achieved by intramolecular crosslinking.

- 
- I. Crosslinking Polymerization**
    - 1. In solution
      - Free-Radical Polymerization
      - Anionic Polymerization
    - 2. Emulsion Polymerization
      - Macroemulsion
      - Microemulsion
      - Inverse Emulsion
      - Surfactant-Free Emulsion
    - 3. Free-Radical Polymerization in Bulk
    - 4. Polymerization with non-classical initiation
  - II. Intramolecular crosslinking of polymers**
    - 1. Chemical intramolecular crosslinking
    - 2. Radiation induced intramolecular crosslinking

**Figure 2.4.** List of synthesis methods of nano- and microgels (Ulanski and Rosiak, 2004).

### 2.1.1. Crosslinking Polymerization

Crosslinking polymerization techniques are studied intensely over the years to obtain macroscopic networks. Polymerization starts from a monomer or a monomer mixture where the on-going process can be a free radical polymerization or an anionic polymerization. For the propagation step, reactive sites of the propagating chain may react either with a monomer, with a group that is still reactive on its own chain or with a reactive pendant group on another chain. The latter case will cause branching in polymeric chains and after a specific point, gelation begins and eventually a three dimensional network structure will be obtained (intermolecular crosslinking). This leads the system to a macroscopic gel ("wall to wall" gel) where its dimensions are defined in the limits of its reaction vessel. The other possibility, reaction of the propagating chain with a reactive group on its own chain can be classified as an intramolecular crosslinking. The linear chain will become a coil and in an ideal case, where only this process occur, the final product will be a solution containing separate permanent coils that their shape is fixed by high amount of crosslinks. Depending on the synthesis parameters, sizes of these coils may vary and they can be identified as microgels or nanogels. Figure 2.5 illustrates the two routes for a crosslinking polymerization in solution.

In practice, separating these two processes and obtaining only one type of product is a challenge due to the fact that most of the time these two process occur concomitantly.

Since these reactions are generally carried out in solution, we can divide this process into two sections: a) free-radical polymerization in solution, b) anionic polymerization in solution.

### 2.1.1.1. Free-Radical Polymerization

Crosslinking by free-radical polymerization can be preferred because of its simplicity, applicability to different monomers and media and nondependence to surfactants. However there are some drawbacks for this method. Since there is a competition between inter- and intramolecular crosslinking during the propagation step, the synthesis parameters should be carefully controlled especially for free-radical crosslinking. One way to keep this competition under control is to adjust the concentration of substrates, due to the fact that when working in low concentrations, the propagating chains are separated from each other and the probability of a crosslink between a reactive group on a propagating chain with a group on another chain is lowered. Hence, a microgelation process is preferred.

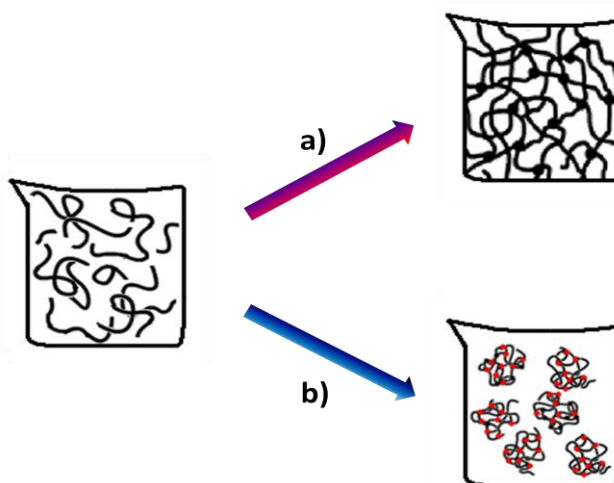


**Figure 2.5.** Types of polymer crosslinking: a) intermolecular crosslinking, final product is a macroscopic gel, b) intramolecular crosslinking (crosslinks are represented by red dots), final product is a microgel (or nanogel).

Delaittre and co-workers synthesized thermoresponsive microgel core and a covalently attached hairy shell via a simple nitroxide-mediated controlled free-radical polymerization in an aqueous dispersion using particular control agents of the nitroxide type and a macroinitiator (Delaittre et al., 2007). In the following year they patented their work that covers the same method with different macroinitiators (Magnet et al., 2008) obtaining different microgels.

Classical radical polymerization is used in various nano- or microgel preparations over the years (Wu et al., 1994; Sun et al., 1997; De Groot et al., 2001; Nolan et al., 2005; Lopez-Leon et al., 2006; Matsumoto et al., 2008). However, to achieve a better control on some issues, i.e. size, homogeneity, PDI, molecular weight, architecture, some specific examples of free-radical polymerization (namely controlled FRP) begin to appear in literature.

Another versatile method to prepare nano- or microgels is atom transfer radical polymerization (ATRP). Yu and co-workers studied the development of networks and structural heterogeneity in the ATRP of dimethacrylates and reported that the ATRP microgels compared to the microgels prepared by conventional free radical polymerization, are more homogeneous, have narrower size distributions. They also found that crosslinking degree and degree of structural heterogeneity of the ATRP products increased with vinyl conversion (Yu et al., 2007). Another ATRP example is the synthesis of star polymers by a new "core-first" method where the sequential polymerization of crosslinker and monomer is achieved using ATRP for homopolymerization of ethylene glycol diacrylate (EGDA) to generate a multifunctional crosslinked core (nanogel) (Gao and Matyjaszewski, 2008).

Oh and co-workers have also supported the advantageous features of ATRP. They concluded that, due to the formation of uniform network, the ATRP-nanogels synthesized have higher swelling ratios, better colloidal stability, and controlled degradation, as compared to nanogels prepared by conventional free-radical polymerization. They used atom transfer radical polymerization (ATRP) in inverse miniemulsion and disulfide-thiol exchange to prepare well-defined biodegradable functional nanogels (ATRP-nanogels) (Oh, 2006; Oh et al., 2009).

A different example is the synthesis of microgel-supported acylating reagent (MGAR) by Activators Re-Generated by Electron Transfer for Atom Transfer Radical Polymerization (ARGET ATRP) of styrene and divinylbenzene using a macroinitiator, a catalyst system and a reducing agent (Li, 2010). Furthermore, Bencherif and co-workers achieved the synthesis of nanostructured hybrid

hydrogels by combining ARGET ATRP and FRP and managed to incorporate nanogels of sizes into a larger three-dimensional (3D) matrix which is developed for drug delivery scaffolds for tissue engineering applications (Bencherif et al., 2009).

#### **2.1.1.2. Anionic Polymerization**

Different from most of the other methods, in anionic polymerization, the reactive species are ions instead of radicals. This situation can sometimes be troublesome, since the carbanions that are participating in chain growth can react rapidly with other species like water, alcohols, etc. Therefore, one has to work in very pure systems to avoid these possibilities. Additionally, to eliminate some side reactions, the polymerization should be performed at low temperatures. Nevertheless the nano- or microgels synthesized by this technique are nearly monodisperse which is a big advantage for some applications (Ulanski and Rosiak, 2004).

#### **2.1.1.3. Emulsion Polymerization**

Classical theory for the mechanism of free-radical emulsion polymerization is proposed by Smith-Ewart-Harkins in 1940s. In emulsion polymerization the system is an emulsion, composed of a monomer and a surfactant. Surfactant is generally required to stabilize the colloidal system; otherwise latex particles nucleated during the early stage of polymerization may experience significant coagulation in order to reduce the interfacial free energy. The most common type of emulsion polymerization is an oil-in-water emulsion, in which droplets of monomer (hydrophobic) are emulsified with surfactant in a continuous phase of water. Emulsion polymerization can be divided into three categories: miniemulsion, microemulsion and classical (conventional) emulsion polymerization which show different particle nucleation and growth mechanisms and kinetics.

In the conventional emulsion polymerization emulsified monomer droplets ( $10^4$  nm based on diameter) are dispersed in the liquid phase as micelles. However they do not contribute to particle nucleation due to their small surface area. Monomer droplet leads the system to form monomer micelles which can be either inactive or active (contain propagating chains). After the consumption of monomers inside the micelle, metastable (kinetically stable) polymer particles are produced via free radical polymerization in the active micelle droplets. Figure 2.6 represents classical emulsion polymerization process with moderate surfactant amount. In miniemulsions, latex particles are typically prepared in the size range of 100 to 500 nm (Daniels and Anderson, 2003).

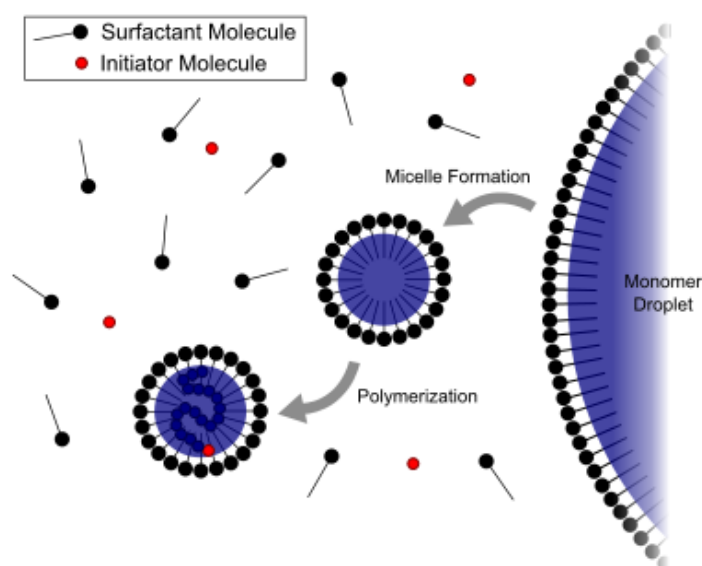


**Figure 2.6.** Classical emulsion polymerization process.

Microemulsions are spontaneously formed from mixtures of water and monomer containing large amount of surfactant (at about 20 percent). This high amount of surfactant induce the system being thermodynamically stable, transparent, one-phase that have micelles less than 100 nm in diameter. These micelles have an extremely large oil-water interfacial area ( $\sim 10^5$  m<sup>2</sup> dm<sup>-3</sup> in diameter). The main advantage of this system is the elimination of polymerization in monomer droplets. Hence, by using this technique, nearly monodisperse nano- or microgels can be synthesized which can not be achieved with other emulsion polymerization techniques. However, the presence of surfactant in higher amounts can be a



serious problem since a complete removal of the surfactant should be made for pure systems. This is a big disadvantage for the particles that are aimed to be used in biomedical field. Surfactant-free emulsion process can be a solution for this problem but this method is limited to only a few monomers.

Inverse emulsion polymerization involves the dispersion and then polymerization of hydrophilic monomers, normally in aqueous solution, in a non-aqueous continuous phase. This method allows to synthesize nano- or microgels from water soluble monomers.

In general, emulsion polymerization sort the microgelation problem out since crosslinking reactions are completed in single micelles that are separated by surfactants. Furthermore, since there are so many parameters (i.e. monomers, comonomers, initiators, surfactants, etc.) it is possible to optimize the polymerization process and have a control over particle size, polydispersity and architecture (Liu et al., 2009-a; Peng et al., 2009; Chai, 2010; Zillessen and Bartsch, 2010) of nano- or microgels proper for desired applications.

The most common works on emulsion polymerization include N-isopropylacrylamide (NIPAM) as a monomer since it has a LCST at about 32°C, allowing the final product (nano- or microgel) to be thermoresponsive. Li and co-workers synthesized stable, temperature-sensitive polymer gels by surfactant-free (soapless) process by using photochemical emulsion polymerization of NIPAM and N,N'-methylenebisacrylamide, and the particle diameters are controlled to <100 nm (Li et al., 2002). Wu and co-workers obtained temperature sensitive nanogels via emulsion polymerization in the size range of 50 to 200 nm (Wu et al., 2007). Quan and co-workers synthesized multifunctional and thermosensitive poly(N-isopropylacrylamide-co-Pr acrylic acid-co-hydroxyethyl methacrylate) (P(NIPAAm-co-PAAc-co-HEMA)) nanogels using miniemulsion polymerization (Quan et al., 2008). Borsos and Gilanyi obtained Poly(N-isopropylacrylamide-co-acrylic acid) copolymer microgel particles by emulsion polymerization method. The prepared microgel particles show narrow size distribution hence the microgel

system can form liquid crystal structure (Borsos and Gilanyi, 2010). In addition to these, in a recent work, a series of cationic poly(N-isopropylacrylamide/4-vinylpyridine) [poly(NIPAM/4-VP)] polyelectrolyte co-polymer microgels are prepared by surfactant-free emulsion polymerization with varying compositions of 4-VP and NIPAM (Nur et al., 2010). As it is mentioned before, this method provides various options for gel architecture. Therefore, Chai and co-workers synthesized Poly(NIPAM-co-DMC) microgels by surfactant-free emulsion polymerization and include silica nanoparticles in shell for drug release application (Chai et al., 2010). Moreover, Li et al. synthesized Poly (N-isopropylacrylamide) /chitosan microgel by surfactant-free emulsion polymerization and found out that the microgel particles presented a microsphere with core-shell morphology (Liu et al., 2009-b). In another work novel core-shell particles with polystyrene (PS) as the shells and thermosensitive poly(N-isopropylacrylamide) (PNIPAM) microgels as the cores were prepared by a seeded emulsion polymerization of styrene using a PNIPAM microgel suspension as the seed latex. Upon dehydration of microgels inside the core-shell particles, hollow PS particles were obtained (Peng et al., 2008). Nur and co-workers synthesized poly(N-isopropylacrylamide) [pNIPAM]-based homo-polymer and co-polymer microgel particles by surfactant-free emulsion polymerization which show useful application in the removal of water from biodiesel prepared from rape seed. Making use of Karl Fischer experiments they showed that microgel particles can be used to reduce the water content in biodiesel to an acceptable level for incorporation into internal combustion engines (Nur et al., 2009).

#### **2.1.1.4. Crosslinking Polymerization in Bulk**

This method is not as applicable as other methods since there is a high tendency for the system to end up with macrogelation. One has to be careful and stop the process before macrogelation begins to obtain microgels.

#### **2.1.1.5. Polymerization with Non-classical Initiation**

Generally, for the synthesis of nano- or microgels chemical initiators are used to initiate chain reactions. Therefore the purity of the system is highly important in some applications and the presence of these initiators in the end-product will be a big problem. Alternative techniques may be a solution for this problem like photopolymerization, ultrasound-induced polymerization or radiation-induced polymerization. Although these methods provide some benefits, there is still another problem to solve, that the system may include residual monomers which can sometimes be even carcinogenic. Consequently, monomer-free techniques should be taken into consideration to obtain highly pure nano- or microgels.

#### **2.1.2. Intramolecular Crosslinking of Polymers**

Different from the other techniques, these methods are starting from a polymer instead of a monomer or a monomer mixture, thus these methods are alternatively called as “monomer-free techniques”. Here, properties of the product can be easily controlled by choosing the right polymer for synthesis of the desired product (proper grade, molecular weight, etc.). On the other hand, for the monomers that don't exist, synthesis step will be impractical or even impossible in some cases. Using polymers as a starting material will also unravel this situation.

##### **2.1.2.1. Chemical Intramolecular Crosslinking**

This method is similar to other classical techniques in the sense of initiation process. Nevertheless the substrate should be a preformed linear or branched polymer that contains reactive pendant groups which can undergo crosslinking reaction by an initiator, or a suitable crosslinking agent should be used to react with bifunctional polymers that will result in intramolecular recombination (Ulanski and Rosiak, 2004).

### 2.1.2.2. Radiation Induced Intramolecular Crosslinking

In this technique the initiation step is induced by ionizing radiation in the form of gamma rays that are emitted from the nucleus of some unstable (radioactive) atoms like cobalt-60 or cesium-137 or fast electrons that are produced by accelerators. The theory behind this method will be discussed in a separate chapter (Section 3) but it should first be pointed out that the only difference from the other methods is the initiation step. One can work in bulk, emulsion or solution; however the method mentioned here is composed of irradiation of a polymer solution where the effect of ionizing radiation on a polymer chain is mainly “indirectly”. That means, radiation energy is exclusively absorbed by solvent molecules and as a result reactive species occur. These species which are generally radicals start the initiation step. In most of the cases, the solvent is water or an aqueous system and in that case, the radicals initiating the crosslinking polymerization are mainly hydroxyl radicals (when the oxidizing conditions are fulfilled). Section 3.1 deals with the concepts of radiation chemistry of aqueous systems in more detail.

As it is discussed before, there is a competition between inter and intramolecular crosslinking in these systems. Figure 2.7 represents these routes during crosslinking reactions.

This versatile method is commonly used in recent works after the first report on radiation formation of polymeric nanogels by Ulanski, Janik and Rosiak in 1998. In their report they highlighted the requirements to avoid macrogelation and obtain purely intramolecularly crosslinked microgels. The conditions are met when the polymer chains are well separated from each other and when high number of radicals are generated on a single chain. The first requirement can be fulfilled when working in very low concentrations. As early as in 1960 Dieu studied crosslinking of poly(vinyl alcohol) solutions by gamma-radiation and found out that intramolecular crosslinking appears to dominate at very low concentrations

whereas at higher concentrations intermolecular crosslinking leads the system to gelation (Dieu, 1960). This phenomena is also supported by some other works (Tomoda and Tsuda, 1962; Sakurada and Ikada, 1963, 1964). On the other hand, high number of radicals per single chain can be maintained by using high-dose rate fast electrons that are generated from a linear accelerator or in general working with high dose rates. After the foundation of these requirements, there has been a growing interest in synthesizing nanogels using radiation-induced crosslinking.

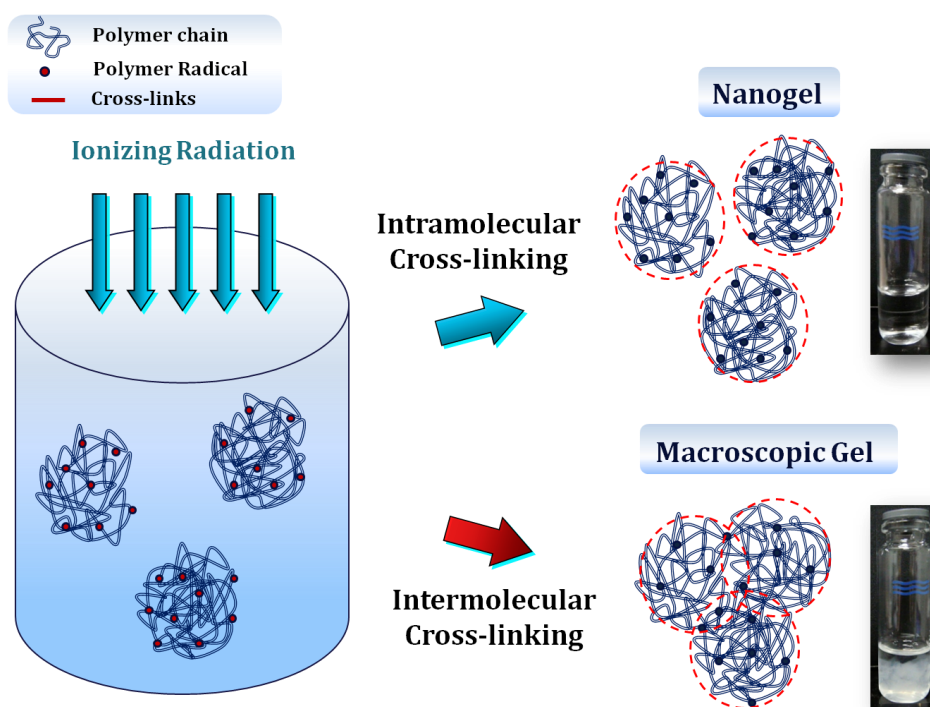


**Figure 2.7.** Reaction path for the radiation induced synthesis of nanogels from polymer solutions, where the system can end up with either a nanogel (via intramolecular crosslinking) or a macroscopic gel (via intermolecular crosslinking).

In the first report about the radiation formation of polymeric nanogels, Ulanski et al. preferred a water-soluble, biocompatible, crosslinking type polymer, poly(vinyl alcohol) (PVA) for the experiments (Ulanski et al., 1998). According to the kinetic studies and the molecular weight, viscosity measurements they concluded that ionizing radiation is a promising technique to synthesize intramolecularly crosslinked nano- or microgels. Figure 2.8 shows the interesting results of

irradiated PVA solutions. As the total absorbed dose increases, intrinsic viscosity, which is a direct function of the size of polymer coils in solution, decreases due to the shrinkage of polymer coils as a result of intramolecular crosslinking. Additionally, there is only a slight decrease in weight average molecular weight that signifies the minor effect of intermolecular crosslinking (Ulanski et al., 1998).

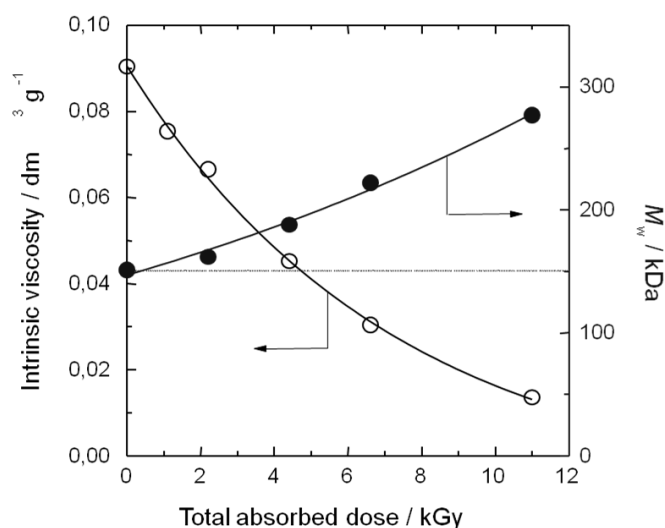


**Figure 2.8.** Change in intrinsic viscosity and weight average molecular weight with the total absorbed dose of PVA solution (Ulanski et al., 1998).

Later on they worked on another water-soluble polymer, poly(vinyl pyrrolidone) (PVP) and supported their previous results. They observed that after the irradiation of dilute PVP solutions, there was a significant decrease in radius of gyration ( $R_g$ ) values of polymer solutions while there was no remarkable change in their average molecular weights. This phenomenon is a clear evidence for the polymer coil shrinkage resulting from intramolecular crosslinking process (Ulanski and Rosiak, 1999).

Following work is done on radiation induced synthesis of poly(vinyl methy ether) (PVME) microgels (Sabharwal et al., 1999; Arndt et al., 2001; Schmidt et al., 2005). As it is shown in Figure 2.9-A, due to the thermosensitive structure of PVME a change in temperature during irradiation results in changes in microgel sizes. Figure 2.9-B shows the SEM image of synthesized PVME nanogel in its swollen state (Arndt et al., 2001).

In a different work, electron beam irradiation of PVME solutions above its LCST resulted in formation of temperature-sensitive PVME microgel (Rosiak, 2007).

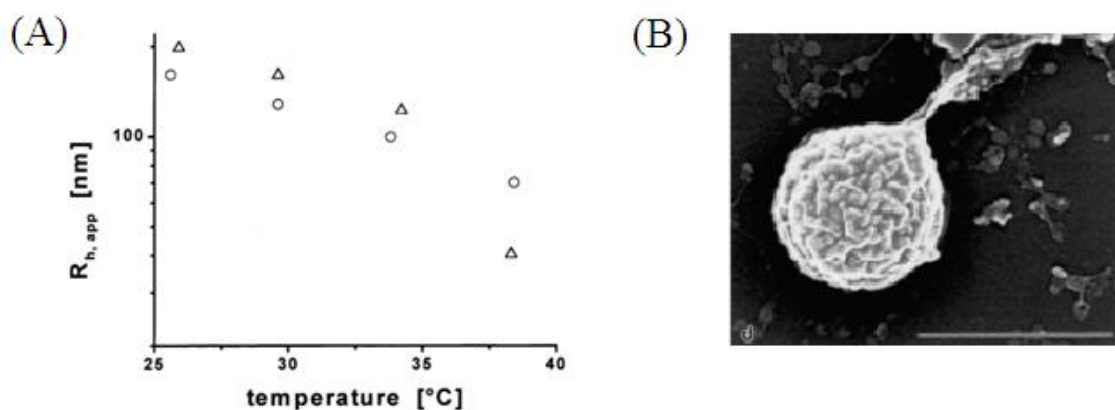


**Figure 2.9.** Apparent hydrodynamic radius ( $R_{h,app}$ ) of PVME microgel vs. temperature [total dose: 20 kGy ( $\Delta$ ), 80 kGy (o)] (A) and the SEM image of PMVE microgel in its swollen state after irradiation with a dose of 80 kGy (B) (Arndt et al., 2001).

Additional work is done on a polyelectrolyte polymer – poly(acrylic acid) (PAA). Ulanski and co-workers obtained PAA nanogels by using pulse radiolysis and discussed the competition of processes during the reaction: intra- and intermolecular crosslinking, intra- and intermolecular disproportionation, and scission. As it is shown in Figure 2.10, the significant decrease in intrinsic viscosity, which is a direct measure of polymer coil size, shows that the major process is intramolecular recombination. The changes in molecular weight is a sign of intermolecular recombination that is of minor importance (Ulanski et al., 2002). Similar work is done by Kadlubowski et al. in which they use pulses of fast electrons to induce intramolecular crosslinking (Kadlubowski et al., 2003).

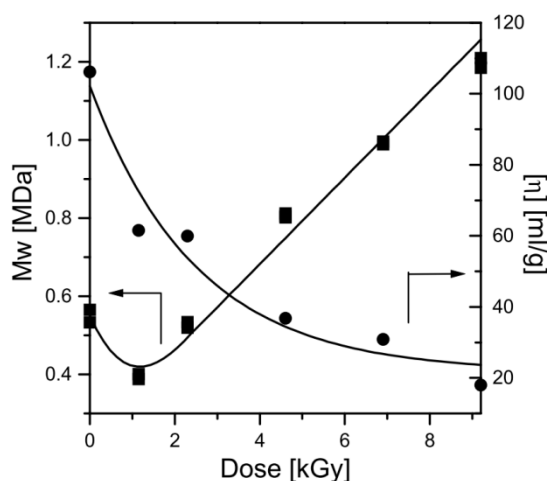


**Figure 2.10.** Weight average molecular weight (■) and intrinsic viscosity,  $[\eta]$  (●) of pulse irradiated PAA solutions as a function of total absorbed dose (Ulanski et al., 2002).

## 2.2. Applications of Nanogels

Nanogels have gained a lot of interest due to their striking properties. Compared to macroscopic gels they have much lower viscosity, very high surface area, rapid thermal response, rapid solution response (i.e. pH sensitivity) that allows them to be used as:

1. Chemical and biological sensors (Peng et al., 2009; Li and Liu, 2010; Wu et al., 2010-a),
2. Coatings (Holtz and Asher, 1997; Rahimi et al., 2009),
3. Water purification devices (Morris et al., 1997; Quevedo et al., 2009),
4. Super absorbents (David et al., 2008; Bueno et al., 2009),
5. Polymeric drug (Oh et al., 2009; Ryu et al., 2010; Kang et al., 2010; Du et al., 2010; Goncalves et al., 2010),
6. Drug and vaccine carrier systems (Kiser et al., 1998; Oishi et al., 2007; Liu and Li, 2008-a; Sun et al., 2009),
7. Nanodevices (van der Linden et al., 2002; Oishi and Nagasaki, 2008),
8. Nanoreactors (Zhang et al., 2004; Li et al., 2009),
9. Contrast agents (Leon et al., 2007; Liu and Li, 2008; Gong et al., 2009),
10. Nanocrystals (Li et al., 2006), where this list can be broadened when very specific examples are taken into consideration.



Recent works for the applications of nano- and microgels are mainly in biomedical field. There is a growing interest in integrating nanotechnology with medicine, creating so-called nanomedicine aiming for disease diagnosis and treatment with unprecedented precision and efficacy (Farokhzad and Langer, 2006). There are a variety of products which can be used as drug delivery systems. The requirements for these systems include small size, biocompatibility, biodegradability, high loading capacity, and prolonged circulation. These products may be classified as, polymer-protein conjugates (Haag, 2004; Duncan, 1992, 2006; Kim et al. 2007), dendrimers (Malik et al., 1999; Svenson and Tomalia, 2005; Lee et al., 2006; Sun and Zhu, 2010), polymeric micelles (Kwon and Kataoka, 1995; Jones and Leroux, 1999; Ge et al., 2002; Matsumura et al., 2004; Nishiyama and Kataoka, 2006), polymeric vesicles (Yu et al., 1996; Discher and Eisenberg, 2002; Photos et al., 2003; Holowka et al., 2006), nanospheres (Govender et al., 1999; Brigger et al., 2002; Otsuka et al., 2003; Panyam and Labhasetwar, 2003) and nanogels (Lemieux et al., 2000; Vinogradov et al., 2002, 2004; Yu et al., 2006, Chen et al., 2009; Hirakura et al., 2010; Galmarini et al., 2010; Patel and Patel, 2010; Nochi et al. 2010). Some of these systems are illustrated in Figure 2.11.

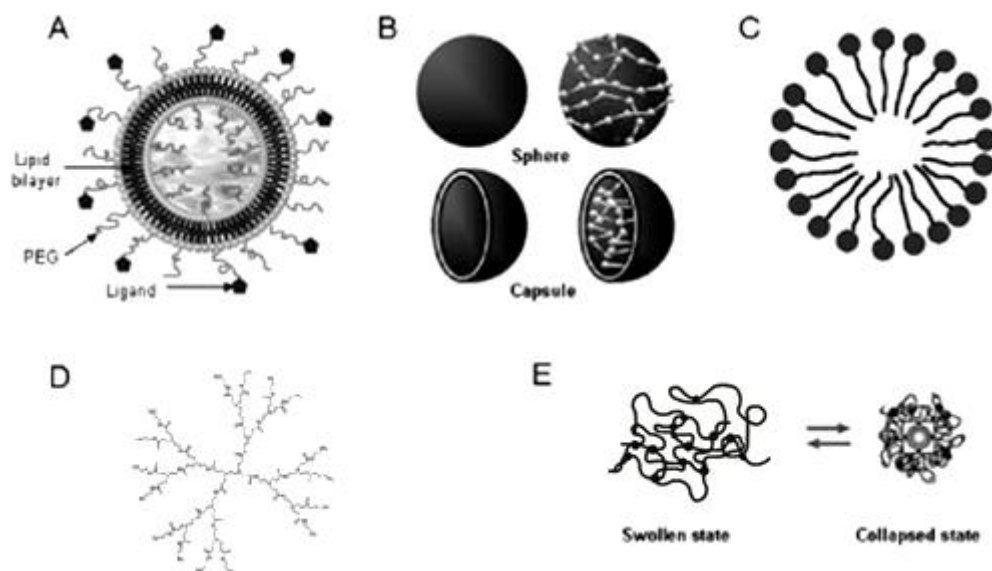


**Figure 2.11.** Different architectures of polymers that are mainly used in biomedical applications: A) Liposome, B) Nanosphere and Nanocapsule, C) Micelle, D) Dendrimer, E) Nanogel.

The physical encapsulation approach controlling drug release from a polymer matrix was originated from the seminal work by Folkman and Long in 1964. They reported that hydrophobic small molecules could diffuse through the wall of silicone tubing at a controlled rate. This approach started an age and the first polymer-based slow release system is synthesized by Langer and Folkman in 1976. So far, almost all the nanoparticle delivery systems which have been approved by the FDA or are currently in clinic trials are based on polymers or liposomes (Qiu and Bae, 2006).

For polymer-protein conjugates 'pegylation' concept is a milestone that was presented by Davis where he introduced poly(ethylene glycol) (PEG) for protein modification (Davis et al., 1978; Wieder et al., 1979). PEG is highly flexible, highly water soluble, non-degradable, non-toxic, and non-immunogenic polymer. The conjugation of PEG to a protein or peptide can shield antigenic epitopes of the polypeptide, resulting in significant reduction of the recognition by reticuloendothelial system (RES). Because of the steric effect, pegylation also reduces protein degradation by proteolytic enzymes. In addition, PEG conjugation increases the molecular weight (MW) and the hydrodynamic volume of proteins, resulting in decreased blood clearance by renal filtration.

Specific targeting using nano-sized polymer-drug conjugates is of specific importance nowadays. There are two methods used for specific targeting. First one is known as passive targeting where nanoparticle accumulation through target is made mainly by its size. When nanoparticles used as drug delivery vehicles for passive tumor targeting they can easily penetrate into the tumor tissue due to the Enhanced Permeability and Retention (EPR) effect (Maeda et al., 2000). Figure 2.12 illustrates this effect that, normal tissue vasculatures are lined by tight endothelial cells, hence preventing nanoparticle drugs from escaping, whereas tumor tissue vasculatures are leaky and hyperpermeable allowing preferential accumulation of nanoparticles in the tumor interstitial space.

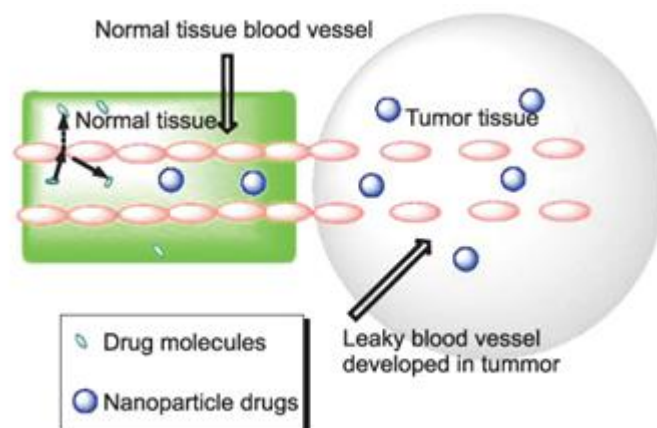


**Figure 2.12.** Schematic illustration of nanoparticle passing through tumor tissue through EPR effect (Wang et al., 2009).

In general, the accumulation of nanoparticles in tumor tissues is dependent on several factors including the size, surface characteristics, and circulation half-life of the nanoparticles and the degree of angiogenesis of the tumor (Allen and Cullis, 2004). It is speculated that nanoparticles with a size between 10 and 100 nm will be optimal for tumor accumulation.

However, careful analysis is required to investigate the independent contributions of passive targeting via the EPR effect, the second route is to use active targeting to tumors via ligand–receptor binding, and stimuli-responsive targeting via extrinsic (e.g., thermal targeting) or intrinsic (e.g., pH) triggers on the overall accumulation and spatial distribution of the drug within tumors, and to reveal the impact of these parameters on the therapeutic efficacy of 'smart', 'stimuli-responsive' macromolecular and nanoparticle drug-delivery vehicles.

A novel and recent example is reported by Wu et al. (Wu et al., 2010-b). They reported a class of core-shell structured multifunctional hybrid nanogels to combine targeting, optical sensing of environmental temperature change, fluorescence imaging of cancer cell, adequate drug loading, and controllable drug release into a single nanoparticle (NP) system. The spherical hybrid nanogel particle is comprised of Ag-Au bimetallic NP as core, thermo-responsive nonlinear

PEG-based hydrogel as shell, and surface hyaluronic acid (HA) chains as targeting ligands, Figure 2.13 illustrates these multifunctional core-shell hybrid nanogels. The Ag-Au bimetallic NP core is designed to emit fluorescent light for optical sensing and cellular imaging on tumor cells, as well as absorb and convert the NIR light to heat for photothermal treatment. The hybrid nanogels can overcome cellular barriers to enter the intracellular region and light up the mouse melanoma B16F10 cells. The hybrid nanogels can serve as excellent drug carriers, which cannot only provide a high loading capacity for a model anticancer drug TMZ, but also offer a thermo-triggered release of the drug molecules in the gel network providing high efficacies, Figure 2.14.

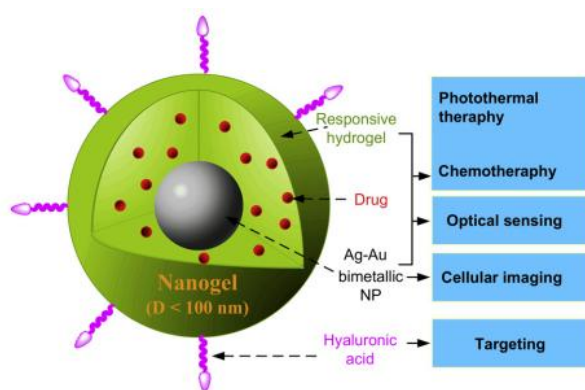


**Figure 2.13.** Schematic illustration of multifunctional core-shell hybrid nanogels (Wu et al., 2010-b).

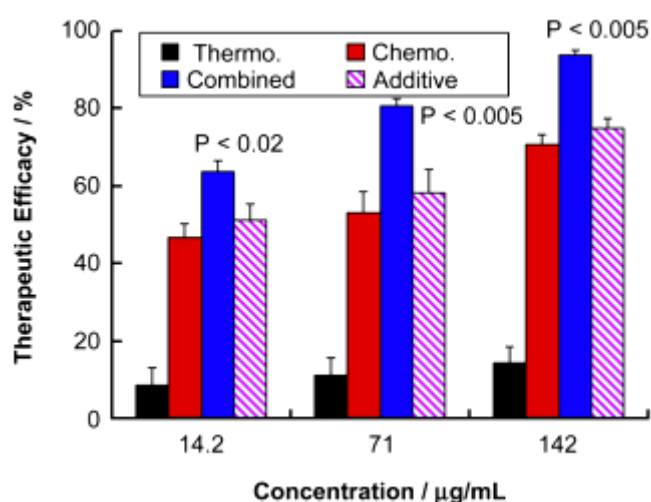


**Figure 2.14.** Therapeutic efficacies of photothermal, chemo, and combined chemo-photo-thermal treatments with AgeAu@PEGeHA hybrid nanogels as drug carriers, respectively (Wu et al., 2010-b).

Another attractive application of nanogels is introduced by Gota and his co-workers (Gota, 2009). They demonstrate for the first time intracellular thermometry with a newly developed fluorescent nanogel thermometer. Since pathological cells are warmer than normal cells because of their enhanced metabolic activity, measuring cellular temperature can contribute to the explanation of intricate biological processes and the development of novel diagnoses. This novel thermometer is practical owing to the fact that with increasing temperature, nanogel in the cytoplasm produces stronger fluorescence, through which a temperature difference of less than 0.5 °C can be distinguished without any interference due to precipitation or interaction with cellular components. The functional temperature range and fluorescence color of the thermometer can be modified by replacing the gel component(s). They reported that this device is superior to its analogues to other candidate thermometers in terms of biocompatibility (i.e., size, sensitivity, and solubility) and negligible interactions with cellular components. Intracellular temperature variations associated with biological processes can be monitored with a temperature resolution of better than 0.5 °C. Figure 2.15 represents the chemical structure, working principle and pH insensitivity of nanogels synthesized. At a lower temperature, nanogel swells by absorbing water into its interior, where the water-sensitive DBD-AA units are quenched by the neighboring water molecules. When heated, it shrinks with the release of water molecules, resulting in fluorescence from the DBD-AA units. They used HCl and KOH for the pH adjustments and they found the fluorescence quantum yield as 0.37 at 40 °C.

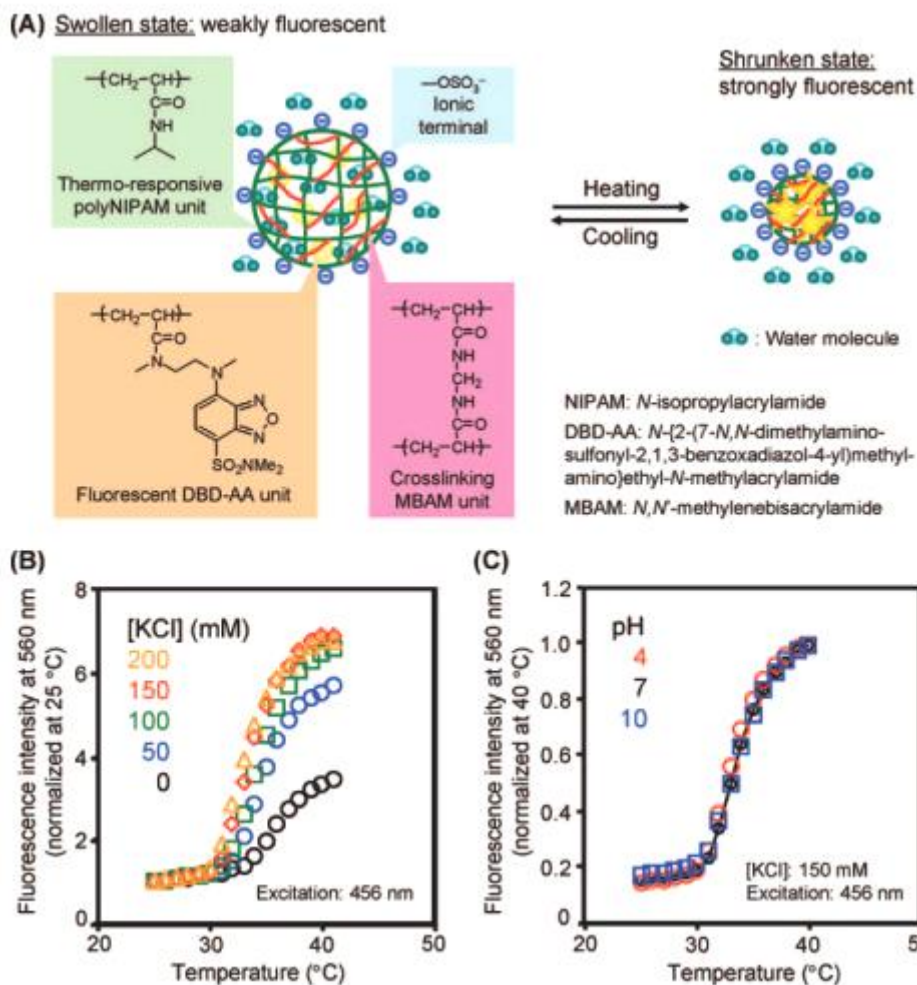


**Figure 2.15.** Fluorescent nanogel thermometer: Schematic diagram and chemical structures of the components (A), Fluorescence pH responses to temperature variation in water and in KCl solutions (B), Insensitivity to pH variation (C) (Gota, 2009).

Chen and co-workers have synthesized a novel hollow core-porous shell structure PAA nanogel by removal of HPC from crosslinked hydroxypropylcellulose-poly(acrylic acid) (HPC-PAA) nanoparticles (Chen, 2010). They found that the nanogels have a hollow structure and are responsive to changes of the environmental pH. The nanogel exhibits a surprisingly high loading ability to both proteins and small molecular drugs which is at least 10 times higher than that of common drug carriers. The PAA nanogels have also shown sustained drug release properties and can cross biological barriers to deliver their payload

inside the cells. Figure 2.16 schematically represents the formation of porous hollow PAA nanogels.

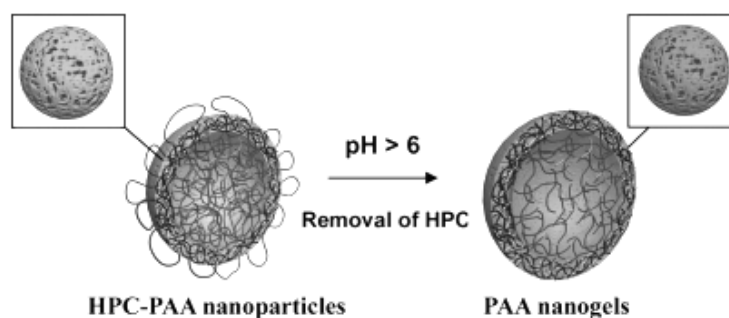


**Figure 2.16.** Schematic illustration of the formation of porous hollow PAA nanogels (Chen, 2010).

Sinha-Ray and his co-workers introduced a new concept: “nanogel raisins”. Shrinkage of individual nanogel “raisins” at elevated temperatures increases nanoporosity via increased exposure of the existing nanopores to water, or formation of new nanopores/nanocracks in the overstretched polymer matrix in the vicinity of shrinking nanogel raisins. In their work they synthesized PAA/PVA/PNIPAM nanofibers by electrospinning technique. They found out that only isolated PNIPAM “raisins” in the fibers behaved as nanogels, whereas the nanofiber mats as a whole did not behave as hydrogels. Table 2.1 represents this behaviour where sample 1 consists of PAA/PVA/PNIPAM nanofibers produced by Sihna-Ray and sample 2 consists of fibers produced from a poly(methyl methacrylate/ N-isopropyl acrylamide) copolymer CP1-1. It can be seen that the fibers in sample 1 do not shrink/swell in water as a whole whereas sample 2 behaves like an hydrogel and show strong shrinkage/swelling. Also SEM images approve this behavior as it is seen in Figure 2.17, since the fibers remain mainly intact and their dimension is not visibly affected after immersion in water for 4 days. PAA/PVA portion of the fibers forms a rigid skeleton, preventing global shrinkage/swelling characteristic of standard PNIPAM-containing composite mats. The absence of the overall swelling/shrinkage of the nanofiber mats prevent them to behave as macroscopic hydrogels. Instead, they describe them as nanogels with isolated PNIPAM “raisins”. Table 2.2 also represents the characteristics of the

fibers synthesized (sample 1) compared to hydrogel-like counterparts (sample 2). Sample 1 is partially wettable below LCST whereas, at temperature higher than LCST, it is nonwetable. On the other hand sample 2 shows no significant change. As a result, the release rate of the embedded dye from the nanofibers increases at elevated temperatures as well as eliminating the formation of nanopores or nanocracks by introducing nanogels to the system.

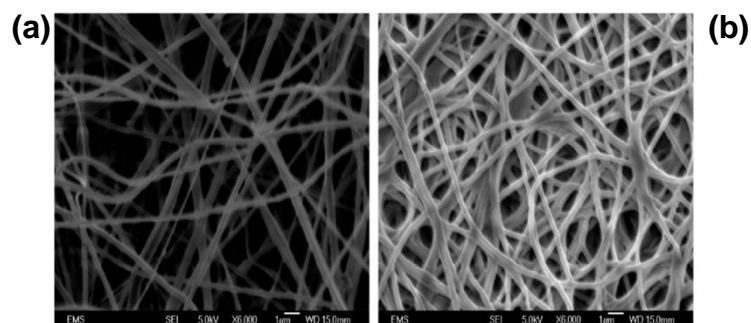


**Figure 2.17.** Crosslinked electrospun nanofibers: (a) fibers with high PNIPAM concentration, (b) fibers with high PNIPAM concentration after immersion in water for 4 days (Sinha-Ray, 2010).

**Table 2.1.** Shrinkage ratio (%) of two samples without dye when water temperature increased from about 25 °C to 51.2 or 53.1 °C (Sinha-Ray, 2010).

sample	51.2°C	53.1°C
1	5.06	5.06
2	32.31	38.46

**Table 2.2.** Contact angles (deg) upon drop deposition measured at different temperatures (Sinha-Ray, 2010).

sample	SCA $\theta$ at 20°C	SCA $\theta$ at 53 °C
1	57.6	116.7
2	116.4	129.1



### **3. RADIATION INDUCED SYNTHESIS OF NANOGELS**

Since nanogel synthesis using ionizing radiation provides a number of advantages and makes an easy control of the final product, it can be taken as the most successful method among the other conventional techniques described above. However, to gain control over the process, the theoretical knowledge on radiation chemical aspects should be reinforced. Since most of the synthesis are carried out in aqueous systems, it is crucial to understand the general concepts of water radiolysis and subsequent effects of reactive species on polymeric solutes.

#### **3.1. Radiation Chemistry of Aqueous Systems**

An important and distinguishing feature of ionizing radiation is that its absorption is in a non-selective way so that molecules are ionized according to their relative abundance in the medium. Therefore, for dilute solutions, the knowledge of the radiation chemistry of the solvent is the centerpiece. Primary reactive species are predominantly formed in the solvent and then induce secondary chemical effects in minor solutes. This phenomenon is called as 'indirect effect'. On the other hand, direct effects are dominant in cases where the reactive radicals cannot move freely (i.e. at solute concentrations above 0.1 M for small solutes or in bulk material) (Spinks, Woods, 1962).

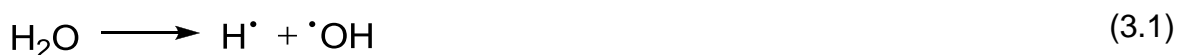
The action of ionizing radiation on water has been the subject of a great deal of experimental and theoretical study. The interest in water arises from its relative simplicity and its biological and ecological importance. The wide variety of aqueous systems are of special interest in radiobiology and nuclear reactor technology.

Historically, the processes taking place when water is subjected to high energy radiation began to occupy scientists only a few years after the first successful

separations of weighable amounts of radium salts. Thus, it was found by Curie and Debierne as early as 1901 that solutions of radium salts continually involve hydrogen and oxygen gases. Additionally, formation of H and OH radicals by irradiation of water was first noted by Debierne in 1914.

The work of Fricke and co-workers, carried out in twenties and thirties described the ferrous sulfate method of dosimetry of ionizing radiations which then formulated the concept of 'indirect effect' of radiation on the dissolved substance (Hart, 1959), established the influence of oxygen on the course of radiolysis of aqueous solutions. In 1960s, free radicals (mainly H<sup>•</sup>, or an equivalent reducing species such as the solvated electron, and <sup>•</sup>OH) are considered the most important intermediates in radiation induced reactions of water and aqueous solutions, though the radiolysis products hydrogen and hydrogen peroxide can also play a part. The development in these ideas up to 1959 has been described by Hart.

According to these theories, it is concluded that the action of ionizing radiation on water results in the formation of atomic hydrogen and OH radicals (Weiss, 1944):



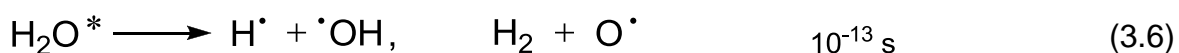
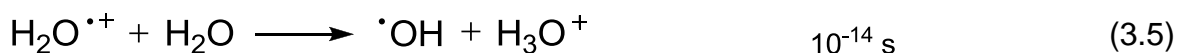
These radicals are produced as follows. The high energy photon passing through the water brings about the ionization of the molecules located close to its path, or track:



The secondary electrons formed have sufficient energy to ionize a few other molecules of water nearby. The clusters of ions thus produced are called 'spurs' (Vereshchinskii and Pikaev, 1964).

After these initial approaches there has been a big progress in radiation chemistry of water and consequently, the radiolysis products, reaction mechanisms and kinetics of reactions in water have been in focus.

The current state of knowledge can be summarized by the following reactions (the time by which event is estimated to be complete is indicated);



Reaction 3.4 represents ionization and electronic excitation of water molecules that occur on the timescale of an electronic transition. The positive radical ion  $H_2O^{\bullet+}$  is believed to form hydroxyl radical and hydronium ion in  $10^{-14}$  s. The electronically excited states  $H_2O^*$  are known to dissociate in the vapour phase in reaction 3.6, and the secondary electron which is released in reaction 3.3 is known to be surrounded with polar water molecules and become hydrated  $e_{aq}^{-}$  within  $10^{-12}$  s. For low LET radiation such as  $^{60}\text{Co}$   $\gamma$ -rays and fast electrons from an accelerator, about  $10^{-12}$  s after the initial ionization event, the species  $e_{aq}^{-}$ , OH and  $H_3O^+$ , together with any dissociation products of  $H_2O^*$  are clustered together in small widely separated spurs, which on average contain 2 to 3 ion pairs (Reactions 3.5 – 3.7). Next, these products begin to diffuse randomly, with the result that a fraction of them encounter one another and react to form molecular and secondary radicalic products, while the remaining escape into the bulk liquid and effectively become homogeneously distributed to react with solutes acting as radical scavengers. These spur reactions are almost complete within  $\sim 10^{-7}$  s (Aziz and Rodgers, 1987). The sequence of events that is initiated by the passage of the ionizing radiation through water is shown in Figure 3.1.

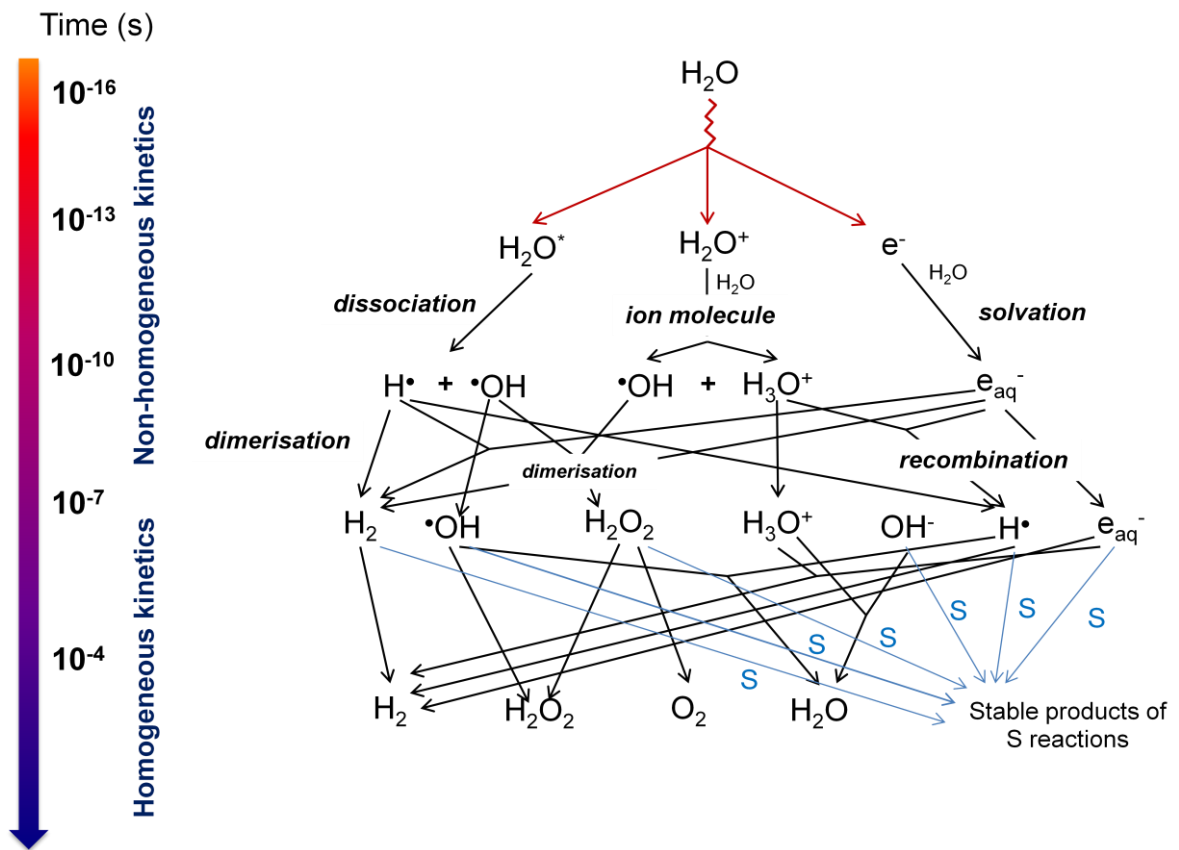


**Figure 3.1.** Scheme of reactions of transient species produced by irradiation in water without or with a diluted S acting as a radical scavenger (Buxton, 2008).

As a consequence, final products from the radiolysis of water for low LET radiation (e.g.  $0.23 \text{ eV nm}^{-1}$ ) can be represented as given below:

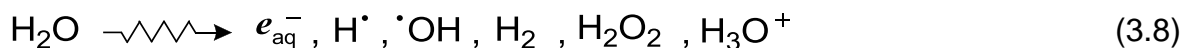


**Table 3.1.** Radiation chemical yields (G values) for the radiolysis products of water for low LET radiation (Buxton, 2008).

G-values ( $\mu\text{mol J}^{-1}$ )	
$e_{\text{aq}}^-$	0.28
$\cdot\text{OH}$	0.28
$\text{H}_3\text{O}^+$	0.28
$\text{H}^\bullet$	0.062
$\text{H}_2$	0.047
$\text{H}_2\text{O}_2$	0.073

Here the radiation chemical yields are expressed in  $\mu\text{mol J}^{-1}$ . Additionally, it can also be quoted as molecules/100 eV. The conversion factor is:

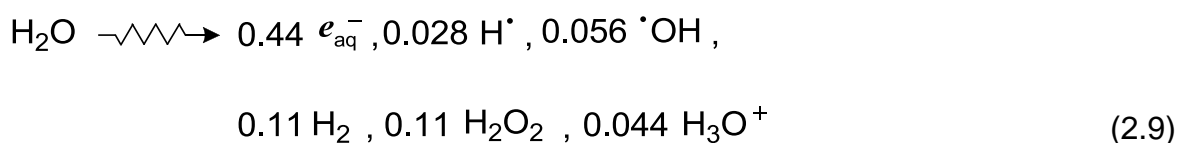
$$1 \text{ molecule}/100 \text{ eV} = 1.036 \times 10^{-7} \text{ mol J}^{-1} \text{ (or } 0.1036 \mu\text{mol J}^{-1}\text{)}$$

The G values in reaction 3.8 are known as primary yields and it is estimated that about 40% of the initial yield ( $G^\circ$ ) produced in reactions (3.5) – (3.7) are consumed by the spur reactions, i.e.  $G^\circ(e_{\text{aq}}^-) \sim 0.5 \mu\text{mol J}^{-1}$ . The spur reactions are listed in Table 3.2.

**Table 3.2.** Spur reactions in water (Aziz and Rodgers, 1987).

Reaction	$k$ ( $10^{10} \text{ dm}^3 \text{ mol}^{-1} \text{ s}^{-1}$ )
$e_{\text{aq}}^- + e_{\text{aq}}^- \longrightarrow \text{H}_2 + 2\text{OH}^-$	0.54
$e_{\text{aq}}^- + \cdot\text{OH} \longrightarrow \text{OH}^-$	3.0
$e_{\text{aq}}^- + \text{H}_3\text{O}^+ \longrightarrow \text{H}^\cdot + \text{H}_2\text{O}$	2.3
$e_{\text{aq}}^- + \text{H}^\cdot \longrightarrow \text{H}_2 + \text{OH}^-$	2.5
$\text{H}^\cdot + \text{H}^\cdot \longrightarrow \text{H}_2$	1.3
$\cdot\text{OH} + \cdot\text{OH} \longrightarrow \text{H}_2\text{O}_2$	0.53
$\cdot\text{OH} + \text{H}^\cdot \longrightarrow \text{H}_2\text{O}$	3.2
$\text{H}_3\text{O}^+ + \text{OH}^- \longrightarrow 2\text{H}_2\text{O}$	14.3

LET effect should also be considered for the primary yields of radiolysis products. For example, for  $\text{LET} = 108 \text{ eV nm}^{-1}$  the primary yields (G-values) become those in reaction 3.9 (Buxton, 2008).



$^{60}\text{Co}$  and electron beam accelerators are frequently used as radiation sources due to their relatively low cost, availability and convenience. Gamma photons from  $^{60}\text{Co}$  and high energy electrons from electron beam accelerators produce secondary electrons when they interact with matter. The average LET of  $^{60}\text{Co}$  gamma photons or high energy electrons are approximately  $0.2 \text{ eV nm}^{-1}$  in aqueous media (Kochanny Jr. et al., 1963).

As shown in Table 3.1, the principal primary radicals are the hydrated electron ( $e_{\text{aq}}^-$ ) which is a powerful reductant (standard reduction potential  $E^\circ = -2.78 \text{ V}$ ) and the hydroxyl radical ( $\cdot\text{OH}$ ) which is a powerful oxidant ( $E^\circ(\cdot\text{OH}/\text{OH}^-) = 1.90 \text{ V}$  in neutral solution, and  $E^\circ(\text{H}^+, \cdot\text{OH}/\text{H}_2\text{O}) = 2.72 \text{ V}$  in acidic solution) (Buxton, 2008). The hydrogen atom ( $\cdot\text{H}$ ) is not an important species in neutral or alkaline solution, but it becomes the major reductant ( $E^\circ(\text{H}^+/\text{H}\cdot) = -2.31 \text{ V}$ ) in acidic solution ( $\text{pH} < 3$ ) through reaction 3.10 (Spinks and Woods, 1962).



Prior to water radiolysis the system produces approximately equal yields of reducing ( $e_{\text{aq}}^- + \text{H}\cdot$ ) and oxidizing ( $\cdot\text{OH}$ ) species, but generally it is desirable to have either totally reducing or totally oxidizing conditions. Choosing the appropriate conditions for generating the species of interest starting with these free radicals is of paramount importance. This can mainly be done by using solutes which alter the proportions of radical products.

Chemical effects due to hydroxyl radicals (oxidizing conditions) may be enhanced by the addition of hydrogen peroxide, which acts as a scavenger for hydrogen atoms (and solvated electrons) and at the same time produces more hydroxyl radicals (Hart EJ, 1951).



Moreover, a very practical and frequently used method of converting  $e_{\text{aq}}^-$  to  $\cdot\text{OH}$  is to saturate the aqueous solution with  $\text{N}_2\text{O}$  ( $[\text{N}_2\text{O}] \sim 25 \text{ mmol dm}^{-3}$ ) (Janata and Schuler, 1982):



Since  $k = 8.7 \times 10^9 \text{ dm}^3 \text{ mol}^{-1} \text{ s}^{-1}$  for reaction 3.12 followed by reaction 3.13, the half-life of  $e_{\text{aq}}^-$  in this system will be  $\sim 3 \text{ ns}$ . Since  $G(\text{H}) \sim 0.1 [G(e_{\text{aq}}^-) + G(\cdot\text{OH})]$ , the contribution of H to any reactions with  $\text{N}_2\text{O}$  may be less important than  $\cdot\text{OH}$  reactions ( $k = 2.1 \times 10^6 \text{ dm}^3 \text{ mol}^{-1} \text{ s}^{-1}$ ) unless the former is kinetically favoured (Wardman, 1978).

### 3.2. Reaction Mechanisms of $e_{\text{aq}}^-$ and $\cdot\text{OH}$ with PVP

It has already been mentioned that for dilute solutions, the radiolytic transformations of the dissolved substance take place as a result of the indirect effects of the radiation, i.e., by the reaction between the solute and the products of the radiolysis of water. Poly (vinyl pyrrolidone) (PVP) belongs to the group of polymers which undergo crosslinking (Davis et al., 1981-a). It is a hydrophilic polymer and used in this thesis as a solute in water or aqueous systems where its concentration was kept very low (1-4 mg/mL) to promote intramolecular crosslinking. Therefore, to make a plausible explanation for the chemical reactions occurring in irradiated aqueous solutions, the reaction mechanism of primary reactive species ( $e_{\text{aq}}^-$  and  $\cdot\text{OH}$ ) with PVP should be considered. Figure 3.2 represents the possible products of hydrogen atom abstraction reactions of  $\cdot\text{OH}$  with the polymer. It was suggested that about 2/3 of radicals are localized on the main chain of PVP as a result of hydrogen atom abstraction at the methyldyne carbon atom (Rosiak et al., 1990, Rosiak and Olejniczak, 1993), Figure 3.2-A, whereas it is shown that hydrogen atom abstraction occurs also at the methylene group adjacent to nitrogen atom, Figure 3.2-B (Davis et al., 1981-b).

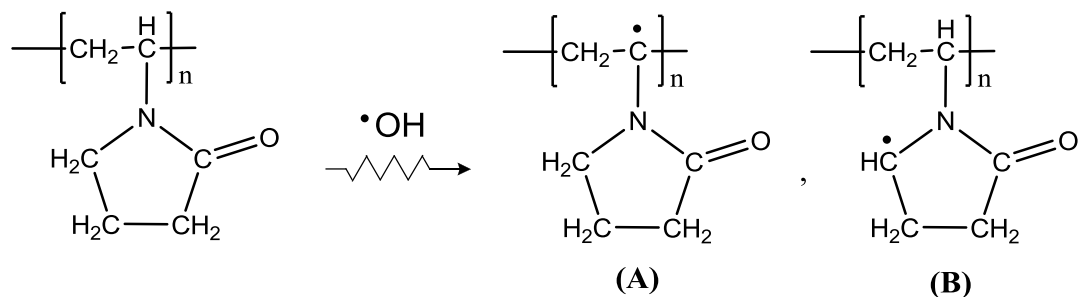


**Figure 3.2.** Reaction of  $\cdot\text{OH}$  with poly(vinyl pyrrolidone) (Rosiak et al., 1990).

In order to obtain oxidizing conditions,  $\cdot\text{OH}$  should be the major species in the reaction with PVP. Therefore, the reducing effect of  $e_{\text{aq}}^-$  can easily be eliminated by saturating the solution with nitrous oxide according to reactions 3.12 and 3.13. Figure 3.3 represents the reaction mechanism of  $e_{\text{aq}}^-$  with PVP which is insignificant due to the reasons explained above.

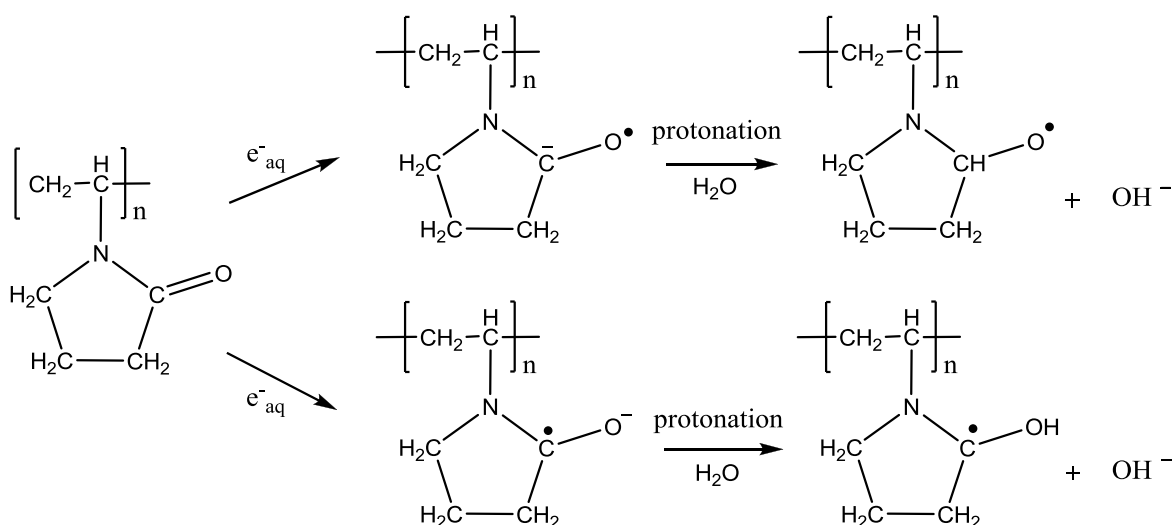


**Figure 3.3.** Reaction of  $e_{\text{aq}}^-$  with poly(vinyl pyrrolidone) (An, 2007).

The PVP carbon-centered free radicals can also face with recombination, disproportionation, hydrogen transfer or scission reactions. Among these, the most important type is radical recombination which directly effects the gelation process. As it has already been mentioned, the type of the reaction is of prime importance.

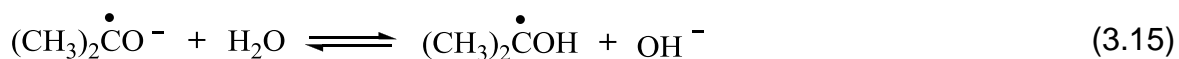
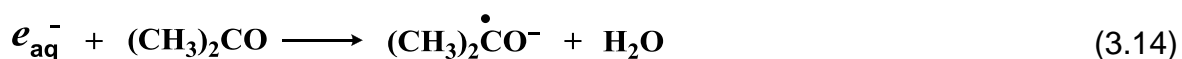


The requirements should be met (concentration, radiation dose, etc.) for the system to choose either intramolecular or intermolecular crosslinking.

### 3.3. Effect of Acetone

This thesis covers the use of acetone/water mixtures as a non-solvent for PVP. Its effect on thermodynamical concepts for PVP solution will be discussed in Section 6.3. However its radiolysis products and their reactions should also be considered since its volume fractions in the binary acetone/water mixtures are in a considerable range (0.60-0.66).

In 1965 Riesz identified the radiolysis products of aqueous air-free acetone solutions as 2,5-hexanedione, isopropyl alcohol, hydroxyacetone, hydrogen peroxide and hydrogen where their quantities are not higher than  $\mu\text{mol/L}$  (Riesz, 1965). In a previous work, the determination of rate constants by pulse radiolysis is maintained and the results confirmed that acetone is an excellent scavenger for hydrated electrons as it is seen in equation 3.14. The reaction constant for this equation was found as  $5.9 \times 10^9 \text{ M}^{-1} \text{ sec}^{-1}$  (Hart et al., 1964). This phenomenon is also advantageous since the crosslinking reactions are carried out in oxidizing conditions where the reducing species, mainly  $e_{\text{aq}}^-$ , should be eliminated from the system. After the reaction of acetone with hydrated electron,  $\alpha$ -hydroxyalkyl radical anions are formed. These radical anions can react to form alkoxy radicals depending on the pH of solution.



## 4. POLYMER SOLUTION THERMODYNAMICS

Since the synthesis of nanogels in this thesis has been achieved by irradiating dilute aqueous polymer solutions not only the knowledge of radiation chemistry of aqueous systems, but also the basic principles about the thermodynamics of polymer-solvent interactions should be well explored. However, the dissolution of a polymer is a bit complex.

When a polymer dissolves in a solvent, the first step is a slow swelling process called solvation. Solvation is related to cohesive energy density (CED), which is the molar energy of vaporization per unit volume. Linear or branched polymers will eventually dissolve after the swelling process, however polymer networks will stay in their swollen state because of their permanent crosslinks. For a dissolution process, intermolecular attractions of both solvent and solute must be overcome. Since the strength of the intermolecular forces between the polymer molecules is equal to CED, these values can be used to predict solubility.

When a polymer is mixed with a pure solvent at a given temperature and pressure, the free energy of mixing will be given by Gibbs free energy equation as it is seen in Equation 4.1:

$$\Delta G = \Delta H - T\Delta S \quad (4.1)$$

Where G is the free energy, which is the driving force in the solution process and  $\Delta H$  and  $\Delta S$  are the changes in enthalpy and entropy of mixing respectively. Here, the free energy G, should decrease in order for solution to take place.

Generally, the van Laar model of solvent mixtures is used to express the thermodynamics of low molecular weight mixtures with approximately same molecular weights. However, this model fails to give realistic predictions of the thermodynamic properties of polymer solutions. In 1942, Flory-Huggins lattice

theory is proposed that takes into account the large differences in size between polymer and solvent molecules and also intermolecular interactions. According to this theory, polymer molecules should be considered to be chains of segments where each segment being equal in size to a solvent molecule. They obtained an expression for the partial molar Gibbs free energy of dilution, that includes Flory-Huggins interaction parameter,  $\chi = Z\Delta H/RT$ , in which  $Z$  is a lattice coordination number. The Flory-Huggins interaction parameter  $\chi$  can be used to express solvent power and it is of enthalpic origin. The value of  $\chi$  for poor solvent is 0.5 and decreases for good solvents. According to this theory, the second virial coefficient,  $A_2$  is given by equation 4.2 where  $V_1$  is the molar volume of solvent and  $v_2$  is the specific volume of solute:

$$A_2 = \left(\frac{1}{2} - \chi\right) v_2^2 / V_1 \quad (4.2)$$

Later on Flory and Krigbaum overcame the limitations of this theory. They recognized that the  $\chi$  term should also have an entropic component, due to the fact that molecular contacts may change the contribution of individual molecules to entropy. A modification of the theory introduced new terms,  $\psi$  for the entropic term and  $\kappa$  for the enthalpic term (Flory, 1953). Since the enthalpic term must be inversely proportional to temperature,  $\kappa$  is replaced by  $\psi\theta/T$ , where  $\theta$  is a new parameter with the dimension of temperature. Thus the  $\left(\frac{1}{2} - \chi\right)$  is replaced by  $(\psi - \kappa)$  and we obtain equation 4.3:

$$\frac{1}{2} - \chi = \psi - \kappa = \psi \left(1 - \frac{\theta}{T}\right) \quad (4.3)$$

Then the second virial coefficient can be expressed as in equation 4.4:

$$A_2 = \psi \left(1 - \frac{\theta}{T}\right) v_2^2 / V_1 \quad (4.4)$$

Thus, at a special temperature  $T = \theta$  (Flory theta temperature),  $A_2$  becomes equal to zero and the solution therefore becomes pseudoideal where the effects of the excluded volume are eliminated and the polymer molecule is in an unperturbed conformation in a dilute solution (the polymer neither expands nor contracts in the solvent). The second virial coefficient is positive at temperatures higher than  $\theta$  and negative at lower temperatures. A solvent, or mixture of solvents, that can also achieve this conformation in a certain temperature is a theta solvent for the particular polymer. These solutions are also called theta solutions.

Theta condition may have a paramount importance in controlling the polymer coil sizes since we are working with dilute polymer solutions for radiation induced synthesis of nanogels. If one can control the thermodynamic parameters, the size of polymer coils in solution, prior to irradiation can also be controlled. This attitude can be a starting point to control also the size of nanogels.

Within the scope of this thesis, solvent/non-solvent pairs will be used to control the sizes of PVP. Acetone was chosen as a non-solvent since it is a theta solvent for PVP when its volume fraction in water is 0.668 (Meza and Gargallo, 1977).

Polymer scientists have been working on polymer thermodynamics over the decades to control the properties of polymers and reactions thereof. The routes to control polymer solution thermodynamics can be achieved by the use of denaturing agents (denaturants) (Güven and Eltan E, 1980), as well as the use of non-solvents or by changing temperature of the solution. The first two will be elaborated in this thesis in order to obtain nanogels having different sizes.

The effect of temperature on polymer coil size of PVP is studied by An et al. in which they observed a change in the size of PVP coils above 50°C, starting from 23 to 15.6 nm, which is a result of more contracted structure due to the disruption of water-polymer hydrogen bonds. The results for unirradiated PVP as a function of temperature is shown in Figure 4.1. Furthermore they prepared nanogels by

using pulsed electron beam irradiation at high repetition rates operating at different temperatures. They observed a decrease in the sizes of PVP nanogels with increasing temperature as seen in Figure 4.2 (An, 2010).

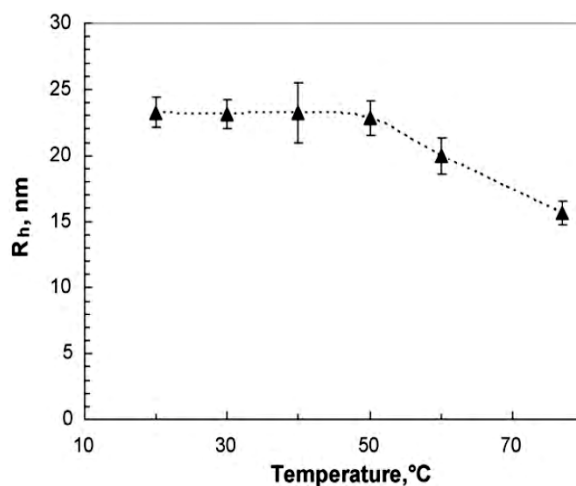


**Figure 4.1.** R<sub>h</sub> of PVP polymer chains as a function of temperature (An, 2010).

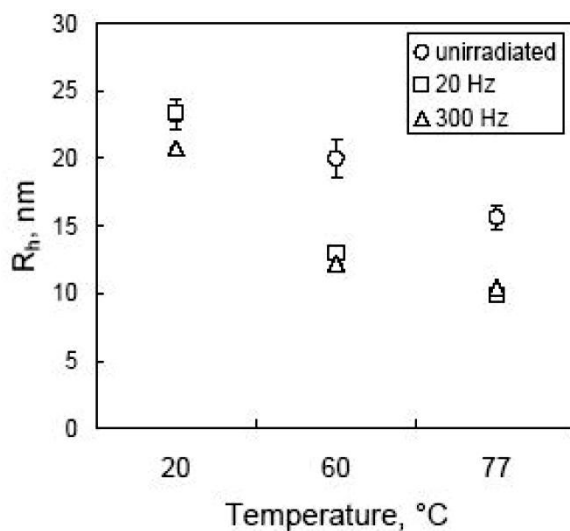


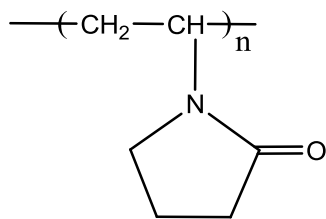
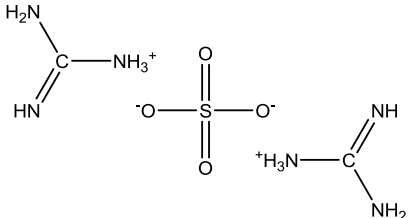
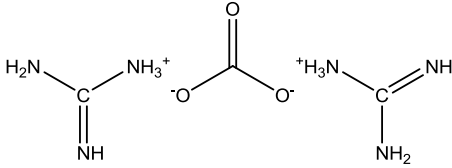
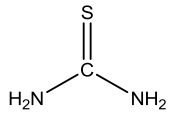
**Figure 4.2.** Change of R<sub>h</sub> of the synthesized PVP nanohydrogels, using e-beam with a total absorbed dose, 5kGy, as a function of irradiation temperature at different pulse repetition rates (An, 2010).

## 5. EXPERIMENTAL

### 5.1. Materials

Poly (vinyl pyrrolidone) (BASF,  $M_w = (1.278 \pm 0.023) \times 10^6 \text{ g mol}^{-1}$  determined by static light scattering) was used as received without further purification. The denaturing agents, guanidinium sulfate, guanidinium carbonate, and thiourea were purchased from Merck, BDH and Fisher Scientific Company respectively. Acetone (Sigma-Aldrich, Chromasolve® for HPLC, 99.9%) is used without further purification and all the solutions were prepared with deionized water with a max conductivity of  $0.01 \mu\text{S}$  and filtered through  $0.2\text{-}\mu\text{m}$ -pore-size Durapore filters (Millipore Corp.) prior to experiments.

**Table 5.1.** The materials that are used in this work and their chemical structures.

Name of Compound	Chemical Structure of Compound
Poly (vinyl pyrrolidone) (PVP)	
Guanidinium Sulfate (GS)	
Guanidinium Carbonate (GC)	
Thiourea (TU)	

## 5.2. Method

Poly(vinyl pyrrolidone) nanogels were synthesized via radiation induced crosslinking method either in the presence of guanidinium sulfate (as a denaturing agent) or acetone in the aqueous solutions of PVP. All solutions were prepared freshly and in glass vials sealed with rubber septa and saturated with prior to irradiation  $N_2O$  for 10 min to simultaneously remove dissolved oxygen. Deionized water and HPLC grade solvents were used for sample preparation and analysis.

Viscosity experiments were carried out for PVP solutions to investigate the effect of denaturing agents guanidinium sulfate, guanidinium carbonate or thiourea on polymer coil sizes. Guanidinium sulfate (GS) was observed to be the most effective denaturing agent and therefore only PVP aqueous solutions with GS are prepared for irradiation. The concentration for GS used in the experiments were 0.1 M, 1.0 M, 1.5 M and 2.0 M. The salt solutions were filtered through a filter paper before preparing polymer solutions.

To achieve theta condition acetone was used as a non-solvent for PVP. Due to the fact that theta solvent for PVP is 66.8% acetone/water mixture (V/V), aqueous mixtures with acetone volume fractions of 0.60, 0.62, 0.64 and 0.66 are prepared for irradiation.

Two types of radiation sources are used in the synthesis. Gamma irradiations were carried out at Sarayköy Nuclear Research and Training Center by placing the samples inside the irradiation chamber of a Gamma Cell (Tenex-Issledovatel) at ambient temperature. A  $^{60}Co$  source with an average dose rate of 1.34 kGy/h was used for the irradiation and the samples. Samples were taken from the chamber at different time intervals to adjust the total absorbed dose as 5, 10 and 15 kGy. Additionally, some of the nanogels are synthesized with high dose, pulsed electron irradiation using a Varian<sup>®</sup> electron beam linear accelerator (LINAC) at the University of Maryland, College Park at ambient temperature. The electron energy was tuned to 7 MeV with maximum beam current of 200 mA within the pulse. The range of total absorbed dose used was 5–20 kGy.

### **5.3. Preliminary Studies**

#### **5.3.1. Static Light Scattering**

Brookhaven BI-MwA model static light scattering system was used to determine the weight-average molecular weight of PVP. This method also allows the user to obtain second virial coefficient and radius of gyration ( $R_g$ ) and these values are determined by constructing the Zimm plot. Calibration of the system was done just before the experiments. PVP K-30 is used for calibration. 7 fixed angles and 5 concentrations (1 to 5 mg/mL) were used to draw the Zimm plot. The refractive indices of aqueous PVP solutions at concentrations of 1.0–5.0 mg/mL were measured by using a Brookhaven differential refractometer at a wavelength of 620 nm to determine the refractive index increment ( $dn/dc$ ).

#### **5.3.2. Viscosity measurements**

Viscosity measurements were carried out to determine the effects of denaturing agents on PVP coil size. A cone and plate viscometer (Brookhaven) with CP-40 spindle was used and the experiments were performed at 25°C. The viscosities of samples were measured under different shear rates and results were expressed as the average of three shear rates where the solution behaves Newtonian.

### **5.4. Characterization of PVP nanogels**

#### **5.4.1. Dynamic Light Scattering (DLS) Analysis**

In order to obtain the hydrodynamic volume of PVP coils or PVP nanogels in a solution, Zetasizer Nano ZS (Malvern Instruments Ltd., UK) equipment available in National Nanotechnology Research Center, UNAM at Bilkent University was used. The instrument uses a 4 mW He-Ne laser (633 nm wavelength) and non-invasive



back-scatter (NIBS) optics that allows to detect the scattering information at 173° which is known as backscatter detection. The software of the instrument gives also a width parameter known as polydispersity or polydispersity index (PDI), which is a number indicative for particle size distribution. Accuracy of the instrument was frequently checked using the standard sample provided by Malvern. Particle size and size distribution were also randomly checked through repeated testing over the same sample. All the experiments were carried out at constant temperature, 25°C. Dispersants' refractive index is measured by Abbe refractometer and viscosity determination was done by cone and plate viscometer (Brookfield).

All the size distribution results are expressed as intensity based distributions and the hydrodynamic diameter values are taken from peak 1 mean diameter which is 100,0 % in intensity in most cases. The system is adjusted to record three successive results in a set and the results are expressed as the average values of at least three sets. Many successive measurements were made to keep standard deviations for the results low. Figure 5.1 shows successive results taken for a single sample to express the average peak mean diameter values.

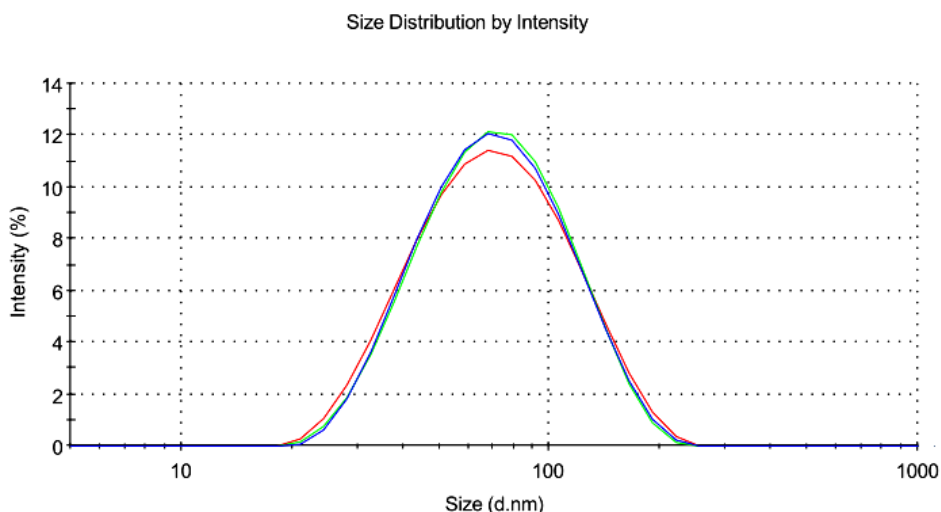


**Figure 5.1.** Successive DLS analyses for a single sample (1 mg/mL PVP in water, 15 kGy).

#### **5.4.2. Gel Permeation Chromatography (GPC) Analysis**

Gel permeation chromatography, namely size exclusion chromatography is used to determine the changes in hydrodynamic volume of PVP nanogels with respect to PVP coils in solution. Since the viscosity of nanogel solution is lower than that of its linear polymer due to the intramolecular crosslinks viscosity based measurements do not yield reliable molecular weight values. Additionally Mark-Houwink constants for nanogels should first be determined to measure molecular weights of nanogels. Because of these drawbacks, GPC chromatograms obtained in this thesis are used to estimate sizes of nanogels based on the GPC chromatograms of linear PVP.

The system used for GPC analysis consists of Waters 1525 binary HPLC pump, AF degasser system, Waters 2414 refractive index detector and a column heating system. The mobile phase was chosen as 0.1 M NaNO<sub>3</sub> to eliminate the possible interactions between PVP and packing material. The gel permeation column used was Ultrahydrogel 2000 (pore size 200 nm), with a diameter of 7.8 and 300 mm of length. A guard column (Ultrahydrogel Guard Column, Waters) was used before the column bank. The temperature was kept as 30°C.

#### **5.4.3. Atomic Force Microscopy (AFM) Analysis**

Veeco Multimode™ V scanning probe microscope (Veeco Metrology LLC, Santa Barbara, CA) with Nanoscope® IV controller was used to obtain AFM images of nanogels. The analysis was performed with 1-10 ohm-cm phosphorus (n) doped Si tips (Veeco, MPP-11100-140) with  $f_0$  values between 70-92 kHz in tapping mode and at room temperature. Force modulation probe is used which is more useful for detecting soft and stiff areas on substrates which exhibit overall uniform topography.

Samples were prepared by casting the solutions on a mica surface. 20  $\mu\text{L}$  solution is allowed to dry at room temperature before analysis. Several regions of the sample have been scanned for a reliable interpretation.

#### **5.4.4. Scanning Electron Microscopy (SEM) Analysis**

The nanogel solutions were cast on silicone surface and the samples were sputter-coated before imaging using a precision etching coating system (PECS, 682, Gatan Inc, Pleasanton, CA) with 8 nm thick gold/palladium. The size and shape of the nanogels were observed using a scanning electron microscope (ESEM, FEI Quanta 200 FEG, FEI Company). The analyses were made in high vacuum and relatively at low acceleration voltages (5 kV) using back-scattered electron technique.

## 6. RESULTS and DISCUSSION

The interest in PVP hydrogels using ionizing radiation generally focuses on intermolecularly crosslinked macroscopic gels (Rosiak and Olejniczak, 1993; Da Silveira, 1993; Aji et al., 2005; Hill et al., 2011). The first proposal about the synthesis of PVP nanogels is made by Ulanski and Rosiak in 1999. As it is clearly seen in Figure 6.1 after irradiation of dilute PVP solutions, there is a significant decrease in radius of gyration ( $R_g$ ) values of polymer solutions while there is no remarkable change in weight average molecular weights of solutions. This phenomena is a clear evidence for the polymer coil shrinkage resulting from intramolecular crosslinking process (Ulanski and Rosiak, 1999).

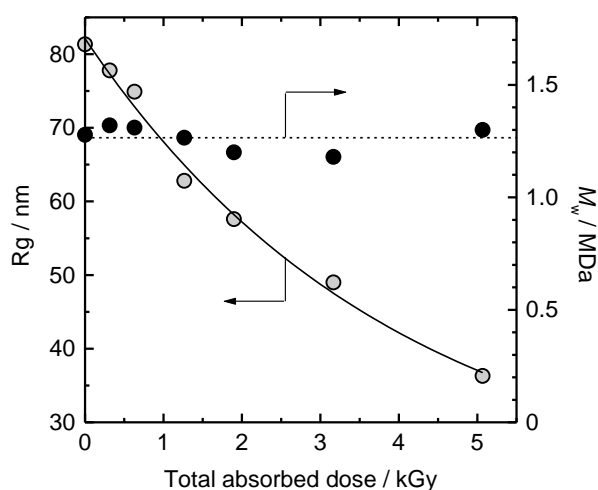


**Figure 6.1.** Change in radius of gyration and weight average molecular weight with the total absorbed dose of PVP solution (Ulanski and Rosiak, 1999).

In this thesis, polymer nanogels were prepared from dilute aqueous solutions of poly(vinyl pyrrolidone) (PVP) by either pulsed electron beam or steady-state  $\gamma$ -ray irradiation. PVP was chosen for the experiments since it has a low cytotoxicity and an excellent biocompatibility with living tissue, and it is a non-carcinogenic and non-antigenic polymer (Robinson et al., 1990). Therefore, it has been used as plasma extender (Ravin and Seligman, 1952), drug carrier of some hydrophilic or hydrophobic drugs (Brunius et al., 2002, Lopes and Felisberti, 2003), and to encapsulate DNA (Saxena, 2006) and it has been extensively applied in

pharmaceutics, biomedical sciences, food, cosmetics, etc. (Bharali et al., 2003; Zelikin et al., 2007).

PVP is a hydrophilic polymer and thus it is highly water soluble. It provides a very good site for hydrogen bonding. The high electronegativity of the oxygen atom on the pyrrolidone ring attracts the hydrogen atoms of water molecules. Dimerization, trimerization or oligomerization of water molecules, hydrogen bonded to one PVP chain finally may act as a bridge connecting two PVP chains together. Solvation of PVP by water was substantiated by the work of Jellinek and Fox where they observed that water bound by PVP has a structure very close to that of ice. An ice-like structure of water attached to PVP chains confirms the view that the extent of hydrogen bonding is quite high. This structure of water around the PVP chains is also established by the IR studies of Klotz on PVP solutions (Klotz, 1959). So we may assume that in aqueous PVP solutions, PVP molecules are linked together through water molecules, hydrogen bonds being responsive for this linkage. If this is true, then breaking of these hydrogen bonds will result in the collapse of a pseudo-network structure displayed by this polymer in aqueous solutions.

It has already been mentioned that nanogels may find various applications in biomedical field. They can be used as matrices for the intravenously controlled release of drugs. However, one should first have a control on the size of the gel which strongly affects the circulation time in blood and so the bioavailability of the particles within the body by evading RES (Reticulo Endothelial System) (Desai et al. 1997). Figure 6.2 emphasizes this event where particles having very small diameters can be easily removed from the body on the other hand particles having diameters more than 200 nm are simply filtered by spleen which will naturally decrease circulation time of the particle (An, 2007). Moreover, it should be noted that particle size plays an important role in the responsiveness to external stimuli since the response rate towards change of stimuli is inversely proportional to the square of the size of the gel (Tanaka and Fillmore, 1979).

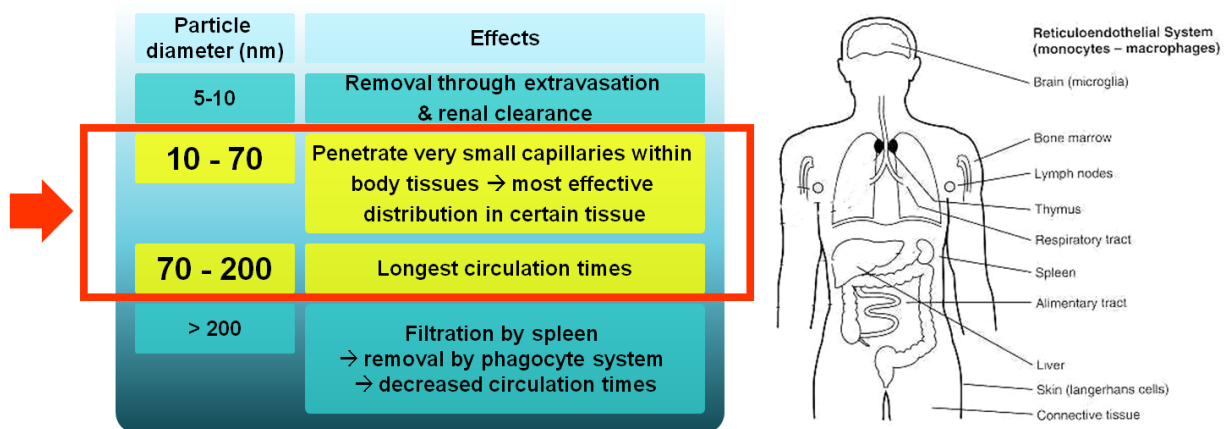


**Figure 6.2.** Particle size effects on bioavailability and circulation time (An, 2007).

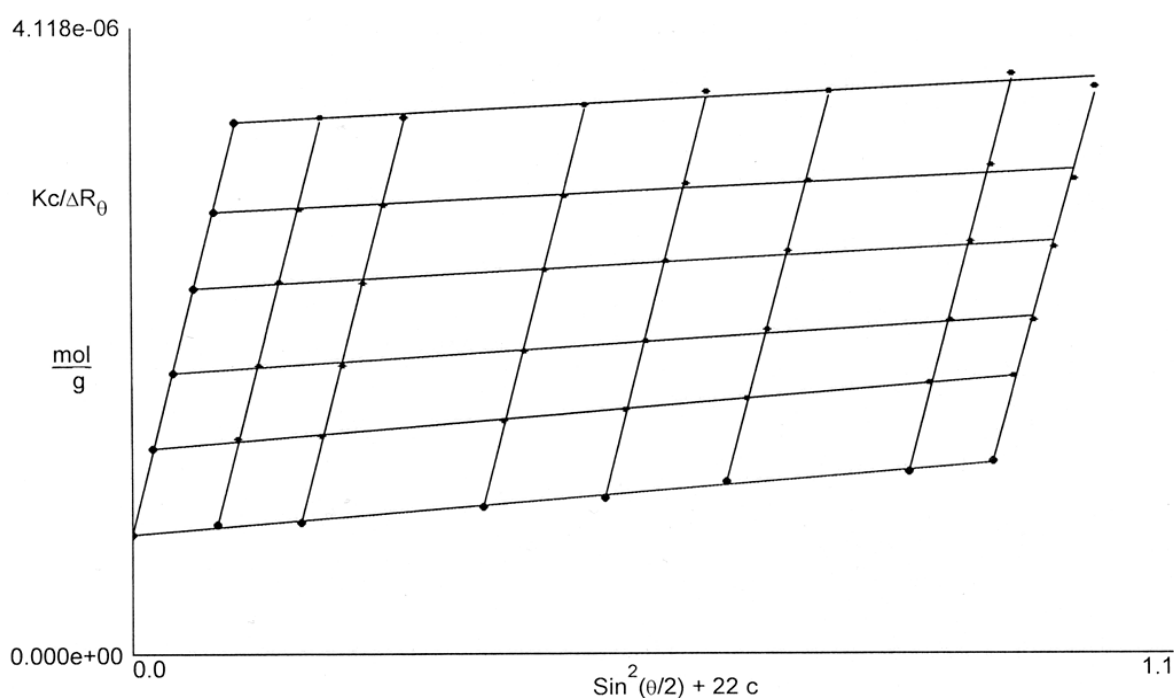
Furthermore, cellular uptake pathway of nanogels, their elimination by the mononuclear phagocyte (MPS) system and their accumulation in cancer cells (via the enhanced permeation and retention effect, EPR effect) are mainly governed by their morphology and size as it is discussed before (Tong and Cheng, 2007). Therefore, nanogels that are designed for drug delivery should mainly meet the particle size criteria.

A novel approach to control the particle size of PVP nanogels, which is of great importance due to the reasons explained above, is proposed in this thesis. Controlling the solution thermodynamics of aqueous PVP solutions is a way to control the polymer coil which will be the precursor of corresponding gels. In order to have a control on polymeric coils in solution, guanidinium sulfate as a denaturing agent, and acetone as a non-solvent was used in the present work. The nanogels were produced in a simple and efficient way by using ionizing radiation.

In the following preliminary studies the weight average molecular weight is determined by using static light scattering. Besides, the effects of denaturing agents on PVP coil sizes are analysed by using viscosimetry.

## 6.1. Determination of Weight Average Molecular Weight of PVP by Static Light Scattering

Static light scattering method is a very efficient technique since it is a primary method and allows the user to obtain weight average molecular weight, radius of gyration and second virial coefficient at the same time by constructing the Zimm plot. Light scattering theory is related with the symmetrical scattering envelope of the scattering particle. However, for high molecular weight species, i.e. polymers, an extrapolation to zero angle should be made to eliminate the destructive interference of the light that is scattered from different regions of the molecule which is generally asymmetrical. Additionally, as the theory is based on ideality, extrapolation to zero concentration is another requirement for this technique.



Extrapolation to zero angle:

Mol. Wt.,  $M_w = (1.278 \pm 0.023)e+06$  g/mol    RMS Error: 1.86e-08

Radius of Gyration,  $R_g = (53.3 \pm 1.7)$  nm

Extrapolation to zero concentration:

Mol. Wt.  $M_w = (1.278 \pm 0.044)e+06$  g/mol    RMS Error: 2.71e-08

2<sup>nd</sup> Virial Coefficient,  $A_2 = (2.698 \pm 0.037)e-04$  cm<sup>3</sup> mol/g<sup>2</sup>

**Figure 6.3.** Static light scattering result for poly(vinyl pyrrolidone) in water by constructing the Zimm plot.

Figure 6.3 shows the Zimm plot of aqueous PVP in solution. The molecular weight of PVP is determined from the intercept of these two extrapolations. It has been found as  $(1.278 \pm 0.023) \times 10^6 \text{ g mol}^{-1}$  which is very close to the value reported by the supplier,  $1.300 \times 10^6 \text{ g mol}^{-1}$ . This high molecular weight was chosen to enable. Additionally, the slope of the zero angle extrapolation gives the average radius of gyration value which is found as  $53.3 \pm 1.7 \text{ nm}$  for PVP coils in water. From the slope of zero concentration extrapolation, second virial coefficient ( $A_2$ ) can be determined which is important for investigating polymer-polymer and polymer-solvent interactions. It is determined as  $2.698 \pm 0.037 \times 10^4 \text{ cm}^3 \text{ mol/g}^3$ . The specific refractive index ( $dn/dc$ ) of PVP in water is found as  $0.1533 \pm 5.5 \times 10^{-3} \text{ mL/g}$  by using a Brookhaven differential refractometer at a wavelength of 620 nm. This high molecular weight for PVP was chosen intentionally in order to start from larger polymer coils and observe a pronounced decrease in nanogel sizes with the changes in polymer solution thermodynamics.

## 6.2. Effect of Denaturing Agents

The interest in effects of denaturing agents (denaturants) is mainly based on denaturation of enzymes or proteins (Sundaram and Venkatesh, 1998; Heegaard and Boas, 2004; Godawat et al, 2010). The effects of denaturing agents on polymer solutions have also been studied and expressed by means of viscosity measurements to investigate the association of PVP in its dilute solutions (Güven and Eltan, 1980). In aqueous solutions of PVP, hydrogen bonding is one of the major type of forces causing association. In order to overcome the forces responsible for association, denaturing agents were used since they can rapture the bridges formed by water molecules. Figure 6.4-A illustrates this effect where PVP molecule in aqueous solution is associated through hydrogen bonding with water molecules and Figure 6.4-B shows blocking of the hydrogen bonding sites of a PVP molecule by a thiourea molecule, thus eliminating the possibility of linking two or more PVP chains.

Denaturing agents that are used to decrease the degree of association are thiourea, guanidinium chloride and guanidinium sulfate. Their effects are investigated by viscosity measurements.

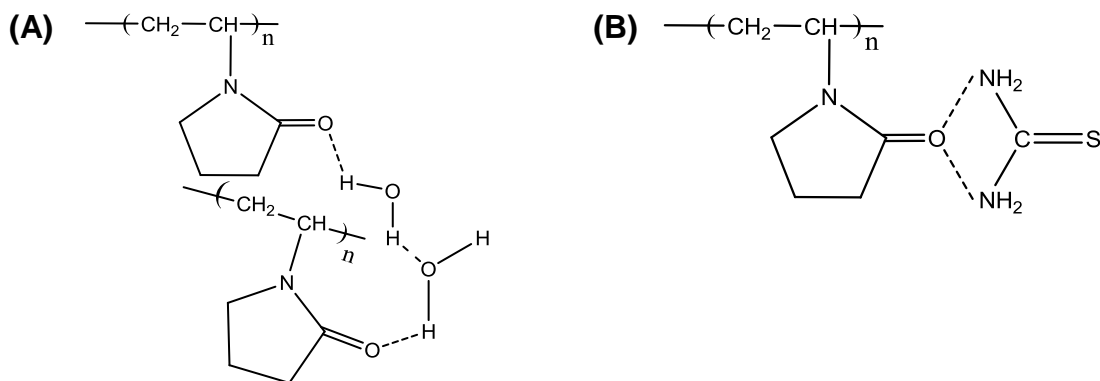


## Viscosity Measurements

In dilute solutions the change of the reduced viscosity with concentration is expressed according to the Huggins equation given below:

$$\eta_{sp}/c = [\eta] + k_H [\eta]^2 c \quad (6.1)$$

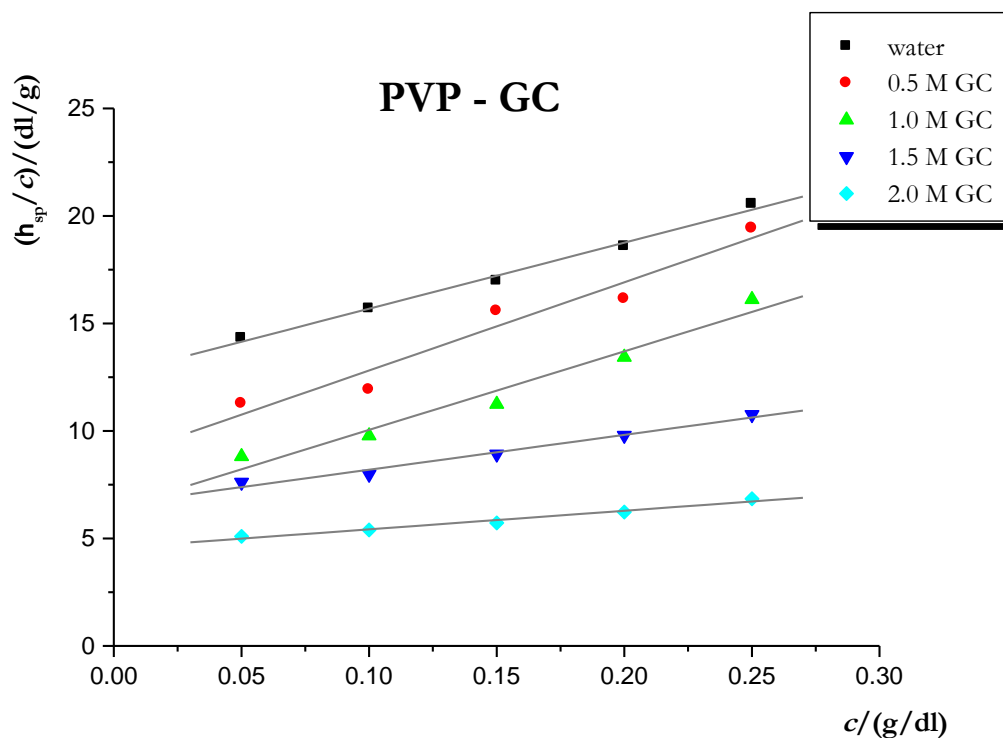
where  $k_H$  is known as Huggins constant which is a measure of the interactions among polymer molecules and  $[\eta]$  is the limiting viscosity number which is a measure of the size and shape of the individual polymer molecules.



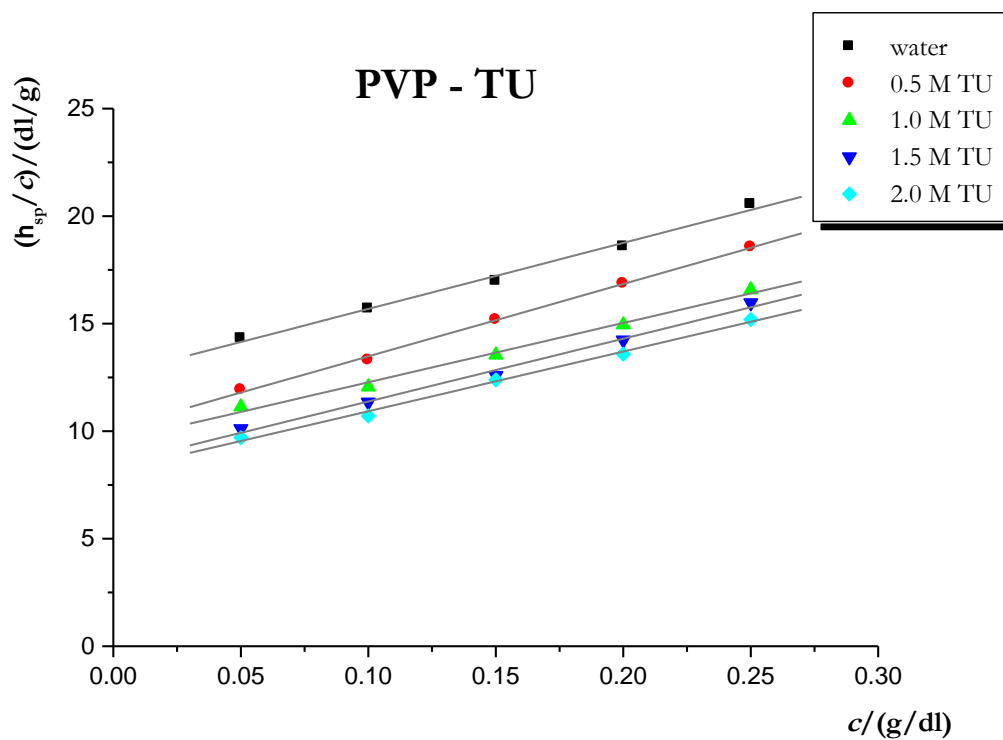
**Figure 6.4.** PVP molecule in aqueous solution (A), and PVP molecule in thiourea solution (B).

Figure 6.5-6.7 shows the change of reduced viscosity,  $\eta_{sp}/c$  of aqueous PVP solutions with concentration,  $c$  for different denaturing agents. Table 6.1 shows the limiting viscosity numbers,  $[\eta]$  (dL/g) for PVP in water and in denaturing agents GC, TU and GS having different concentrations. The results show that guanidinium sulfate is more effective than other denaturants since the decrease in the limiting viscosity number,  $[\eta]$  is very large as compared to guanidinium carbonate and thiourea, for GS it is from 12.61 to 2.87 dL/g. Together with these large decreases in the  $[\eta]$  values, the slopes of the curves also show a continuous decrease. It should be pointed out as the slopes are decreased the system is approaching to theta condition in which the polymer coils act like compact spheres obeying the viscosity law of Einstein as it is given in equation 6.2.

$$[\eta] = \eta_{sp}/c = 2.5/\rho_{eq}. \quad (6.2)$$



**Figure 6.5.** Change of reduced viscosity,  $\eta_{sp}/c$  of aqueous PVP solutions with concentration,  $c$ , for different guanidinium carbonate concentrations at 25°C.



**Figure 6.6.** Change of reduced viscosity,  $\eta_{sp}/c$  of aqueous PVP solutions with concentration,  $c$ , for different thiourea concentrations at 25°C.

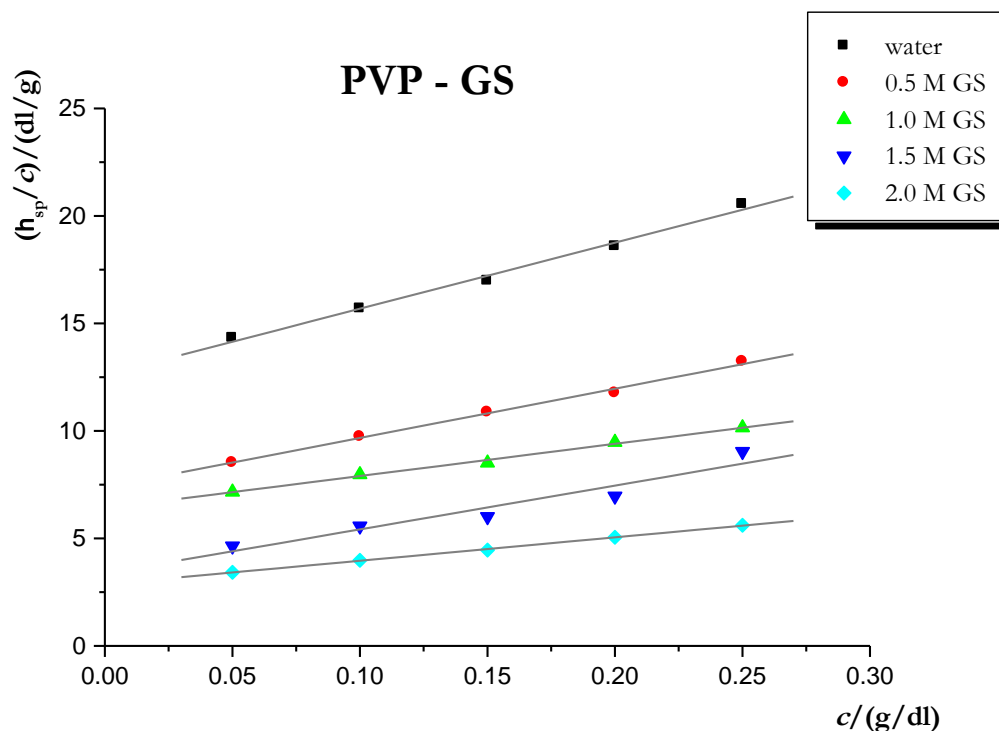


**Figure 6.7.** Change of reduced viscosity,  $\eta_{sp}/c$  of aqueous PVP solutions with concentration,  $c$ , for different guanidinium sulfate concentrations at 25°C.

**Table 6.1.** Limiting viscosity numbers,  $[\eta]$  (dL/g) for PVP in water and in denaturing agents GC, TU and GS having different concentrations, 0.5, 0.1, 1.5 and 2.0 M.

	0.0 M	0.5 M	1.0 M	1.5 M	2.0 M
GC	12.61 ± 0.26	8.71 ± 0.94	6.39 ± 0.67	6.58 ± 0.21	4.56 ± 0.14
TU	12.61 ± 0.26	10.11 ± 0.13	9.52 ± 0.23	8.46 ± 0.23	8.15 ± 0.19
GS	12.61 ± 0.26	7.38 ± 0.15	6.40 ± 0.10	3.38 ± 0.55	2.87 ± 0.03

After these viscosity measurements, guanidinium sulfate was chosen as the denaturing agent to control the sizes of polymer coils in aqueous solution because of its high effectiveness. Three concentrations of PVP were selected for the radiation synthesis of nanogels (1, 2 and 4 mg/mL) in the presence of 0.5, 1.0, 1.5

and 2.0 M guanidinium sulfate (GS) and the syntheses were carried out using pulsed electron beam linear accelerator at ambient temperature. The total absorbed dose for the synthesis was chosen as 5, 10 and 20 kGy.

### ***Dynamic Light Scattering Analysis***

Characterization of PVP nanogels was made by dynamic light scattering. Figures 6.8 and 6.9 summarize the results for the peak mean diameters of nanogels that are synthesized from 1 mg/mL and 2 mg/mL aqueous PVP solutions respectively with changing guanidinium sulfate concentrations by using e-beam irradiation. The concentration of 4 mg/mL was observed to be too high for the formation of nanogels since mostly intermolecularly crosslinked gels were observed. The sizes of nanogels are collectively shown in more detail in Tables 6.1 and 6.2 where standard deviations for peak mean diameters and PDI values (polydispersity index, based on size distribution by intensity) are also given.

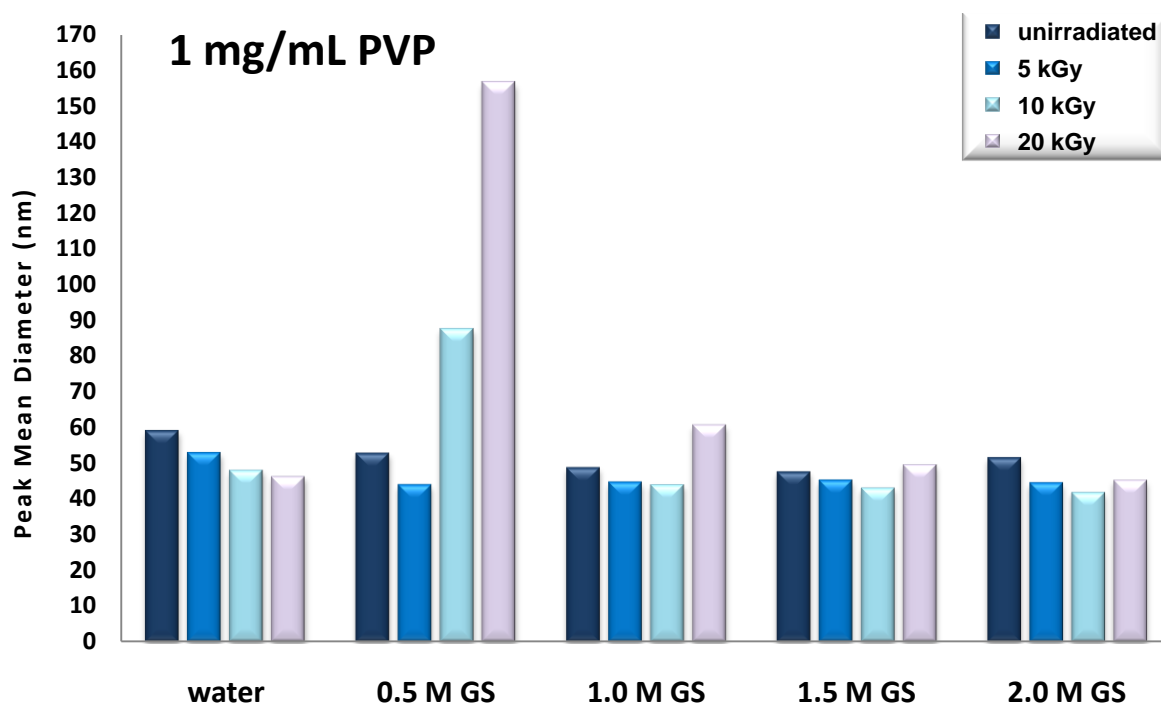


**Figure 6.8.** Effect of denaturing agent concentration and total absorbed dose on the peak mean diameters of PVP nanogels that are synthesized from 1 mg/mL aqueous PVP solutions by e-beam irradiation.

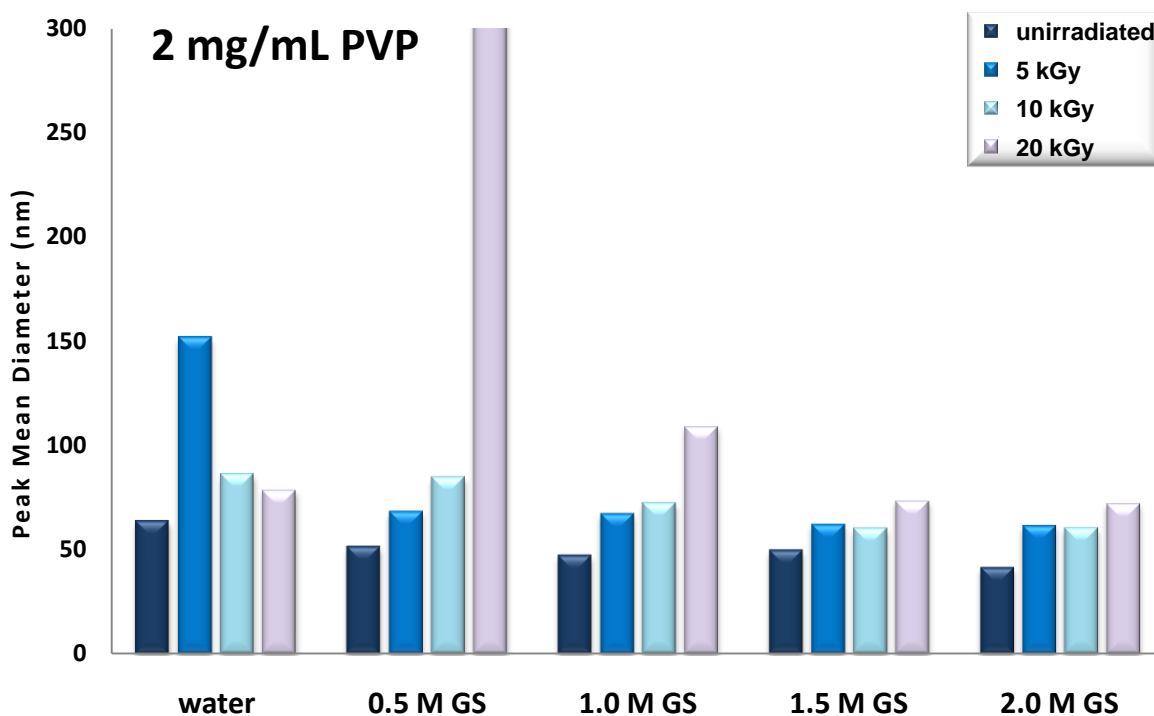


**Figure 6.9.** Effect of denaturing agent concentration and total absorbed dose on the peak mean diameters of PVP nanogels that are synthesized from 2 mg/mL aqueous PVP solutions by e-beam irradiation.

The effect of concentration is clearly seen from Figure 6.8 and 6.9. When the polymer concentration was increased from 1 mg/mL to 2 mg/mL larger PVP nanogels are obtained after e-beam irradiation, which is a typical result of intermolecular crosslinking.

Table 6.2 and 6.3 indicate that there is no systematic decrease in PVP nanogel sizes with the increasing concentrations of GS, although the trend in the results for 1 mg/mL and 2 mg/mL is nearly identical. The sulfate group in GS is assumed to take part in intermolecular crosslinking mechanism during irradiation but this phenomenon needs further investigation and verification.

**Table 6.2.** Peak mean diameters, their standard deviations and PDI values for nanogels that are synthesized by e-beam irradiation of 1 mg/mL aqueous PVP solutions with changing guanidinium sulfate concentrations.

1 mg/mL	unirradiated			5 kGy			10 kGy			20 kGy		
	d (nm)	std dev.	PDI	d (nm)	std dev.	PDI	d (nm)	std dev.	PDI	d (nm)	std dev.	PDI
water	58.93	0.75	0.25	52.70	1.54	0.24	48.04	0.38	0.17	46.35	0.72	0.17
0.5 M GS	52.65	1.34	0.28	43.77	1.07	0.27	87.50	1.48	0.19	156.60	2.69	0.22
1.0 M GS	48.61	0.98	0.24	44.55	1.38	0.26	43.98	0.81	0.21	60.74	0.98	0.17
1.5 M GS	47.46	0.43	0.38	45.02	0.87	0.32	43.13	0.48	0.26	49.66	0.51	0.21
2.0 M GS	51.40	0.43	0.53	44.35	0.45	0.51	41.87	0.71	0.31	45.29	0.49	0.25

**Table 6.3.** Peak mean diameters, their standard deviations and PDI values for nanogels that are synthesized by e-beam irradiation of 2 mg/mL aqueous PVP solutions with changing guanidinium sulfate concentrations.

<b>2 mg/mL</b>	<b>unirradiated</b>			<b>5 kGy</b>			<b>10 kGy</b>			<b>20 kGy</b>		
	<b>d (nm)</b>	<b>std dev.</b>	<b>PDI</b>	<b>d (nm)</b>	<b>std dev.</b>	<b>PDI</b>	<b>d (nm)</b>	<b>std dev.</b>	<b>PDI</b>	<b>d (nm)</b>	<b>std dev.</b>	<b>PDI</b>
<b>water</b>	63.30	0.37	0.42	151.50	1.41	0.42	85.86	1.52	0.21	78.64	0.59	0.23
<b>0.5 M GS</b>	51.17	0.71	0.23	68.19	1.22	0.23	84.41	0.70	0.20	309.00	9.48	0.46
<b>1.0 M GS</b>	46.96	0.61	0.25	67.18	0.15	0.25	72.10	1.23	0.21	109.20	0.60	0.20
<b>1.5 M GS</b>	49.43	1.92	0.26	62.13	0.60	0.26	60.02	1.26	0.26	73.42	0.21	0.19
<b>2.0 M GS</b>	41.24	1.21	0.27	61.47	0.61	0.27	60.25	0.57	0.26	72.20	0.96	0.18

### **6.3. Effect of a Non-solvent, Acetone**

An extensive work on flexibility and hydrodynamic properties of PVP has been done by Abdelazim et al. by determining the unperturbed dimensions of PVP through performing viscosity measurements in cosolvent systems (Abdelazim et al., 1992). Mainly they studied the effect of water/acetone binary mixtures to determine the theta condition for PVP. They showed that the theta composition of water/acetone for PVP at room temperature is  $\Phi$  (acetone) = 0.668 which is in good agreement with the previous studies (Elias, 1961, 1962; Meza and Gargallo, 1977) at 25°C. This behaviour was tried to be explained by referring to preferential solvation of polymer in binary solvents (Gargallo and Radic, 1982).

The effect of a non-solvent, acetone has been investigated to control the size of PVP coils in the solution. The high hydrophilicity of PVP may be a problem in its aqueous solutions since some of its chains are associated with hydrogen bonds which may result in enlarged polymer coils due to dimer, trimer formations. If such solutions are irradiated, intermolecular crosslinking and thus micro- or even macrogelation may take place. To avoid this unwanted situation and also to control the resultant size of nanogel a non-solvent can be introduced to the system to reduce the coil sizes by approaching theta condition. Thus polymer-polymer interactions will be enhanced instead of polymer-solvent interactions and as a result, the increase in amount of acetone will result in a shrinkage in polymer coils as the system reaches theta condition. The hydrophobic interaction of the PVP chains increase with the increasing amount of acetone since the H-bonding formed between "C=O" group of acetone and "N-H" group of PVP is considered to be more stable than that of between the "OH" group of water and "N-H" group of PVP.

#### ***Dynamic Light Scattering Analysis***

In order to observe a clear difference in polymer coil sizes, volume fractions of acetone were chosen as 0.60, 0.62, 0.64 and 0.66 which are very near to theta solvent composition, 0.668. The concentration was chosen as 2 mg/mL to better



follow the decrease in coil size due to the effect of acetone. Table 6.4 shows the dynamic light scattering results of unirradiated PVP in acetone/water solutions and corresponding PVP nanogels synthesized via gamma irradiation. The results show that unirradiated PVP solutions show a clear shrinkage in polymer coils with increasing amount of acetone in the binary mixture which is a direct support of the results obtained in this topic before (Abdelazim 1992). Figure 6.10 shows these results clearly, that a shrinkage from 63 nm (water) to 51 nm (%66 Ac/w) is observed with the introduction of acetone to the system. After irradiating the samples with gamma radiation, an interesting situation has been observed. For PVP concentration of 2 mg/mL, we end up with a blurry solution after the irradiation of PVP aqueous solution, independent of the total absorbed dose. This phenomenon is pointing a microgelation problem since the particle diameters around 200 nm supports this assumption. However, all the samples prepared in acetone/water mixtures ended up with nanogelation. As the acetone is introduced to the system transparent solutions were obtained containing nanogels having diameters between 56 and 44 nm. Figure 6.11 simply shows this result which is the same for all doses (5, 10 and 20 kGy).

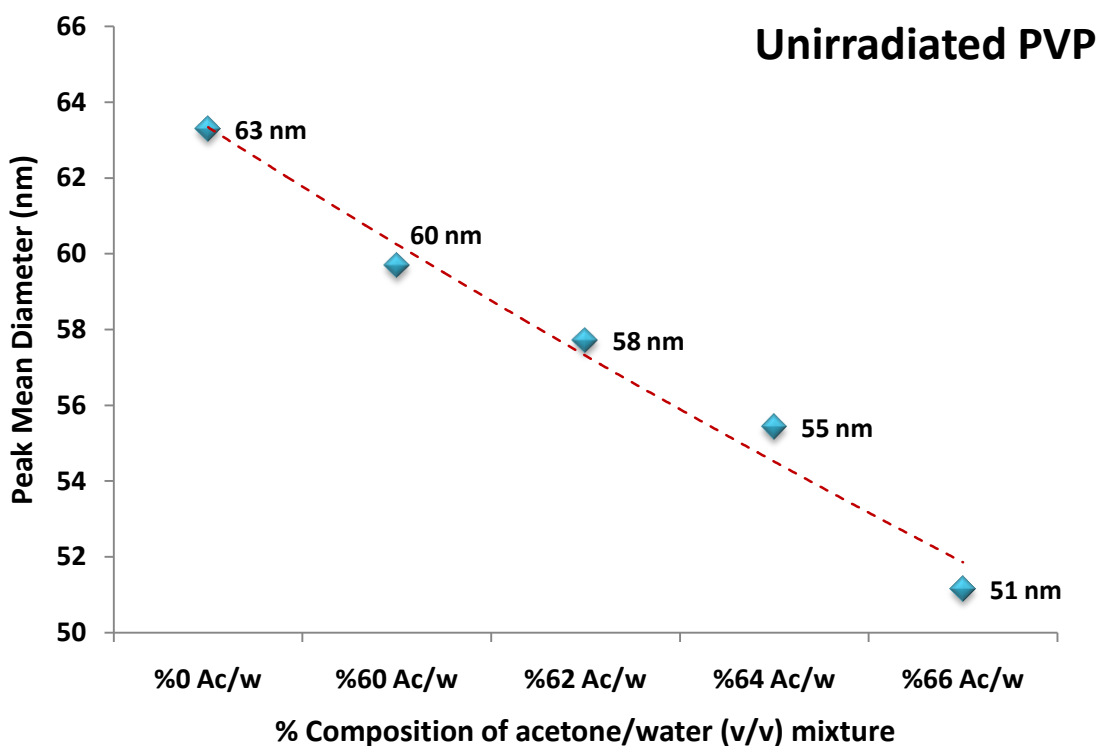


**Figure 6.10.** Effect of acetone amount in the acetone/water binary mixture on the peak mean diameter of unirradiated PVP.

**Table 6.4.** Peak mean diameters, their standard deviations and PDI values for nanogels that are synthesized from 2 mg/mL aqueous PVP solutions by using gamma irradiation at the indicated acetone compositions.

<b>gamma</b>	<b>unirradiated</b>			<b>5 kGy</b>			<b>10 kGy</b>			<b>15 kGy</b>		
<b>2 mg/mL</b>	<b>d (nm)</b>	<b>std dev.</b>	<b>PDI</b>	<b>d (nm)</b>	<b>std dev.</b>	<b>PDI</b>	<b>d (nm)</b>	<b>std dev.</b>	<b>PDI</b>	<b>d (nm)</b>	<b>std dev.</b>	<b>PDI</b>
<b>water</b>	63.29	0.37	0.26	206.60	4.78	0.35	247.90	5.66	0.38	236.4	1.06	0.31
<b>% 60 Ac</b>	59.69	0.58	0.32	56.42	0.30	0.20	55.94	0.43	0.23	56.28	0.58	0.22
<b>% 62 Ac</b>	57.72	0.81	0.28	53.13	0.18	0.23	51.49	0.12	0.23	51.63	0.32	0.23
<b>% 64 Ac</b>	55.43	0.39	0.26	48.20	0.21	0.22	48.85	0.13	0.22	47.80	0.28	0.21
<b>% 66 Ac</b>	51.15	0.73	0.32	45.51	0.39	0.21	45.17	0.54	0.22	44.06	0.46	0.21

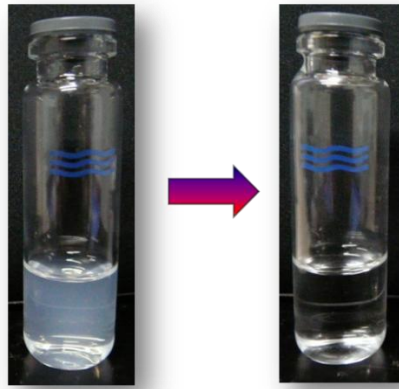


**Figure 6.11.** Irradiated PVP in water - a blurry solution, and a transparent solution that consists of PVP nanogels synthesized in acetone/water mixture.

Additionally, the PDI values in Table 6.4 show that the size distributions are narrower for PVP nanogels prepared in binary mixtures than those of prepared in water. The PDI values are between 0.20 and 0.23 for PVP nanogels prepared from binary mixtures, between 0.31 and 0.38 for the nanogels prepared in water.

Figure 6.12 shows the particle mean diameters of PVP nanogels obtained from 2 mg/mL acetone/water mixtures by means of gamma irradiation. As the amount of non-solvent increases polymer-polymer interactions are increased and the contraction of coils help the system prefer intramolecular crosslinking due to shorter inter-radical distances on the same PVP backbone. Additionally, Figure 6.13 also expresses these results in comparison with pristine PVP. A decrease from 236 nm to 44 nm is a clear evidence that this is an efficient and useful approach to control the size of PVP nanogels.

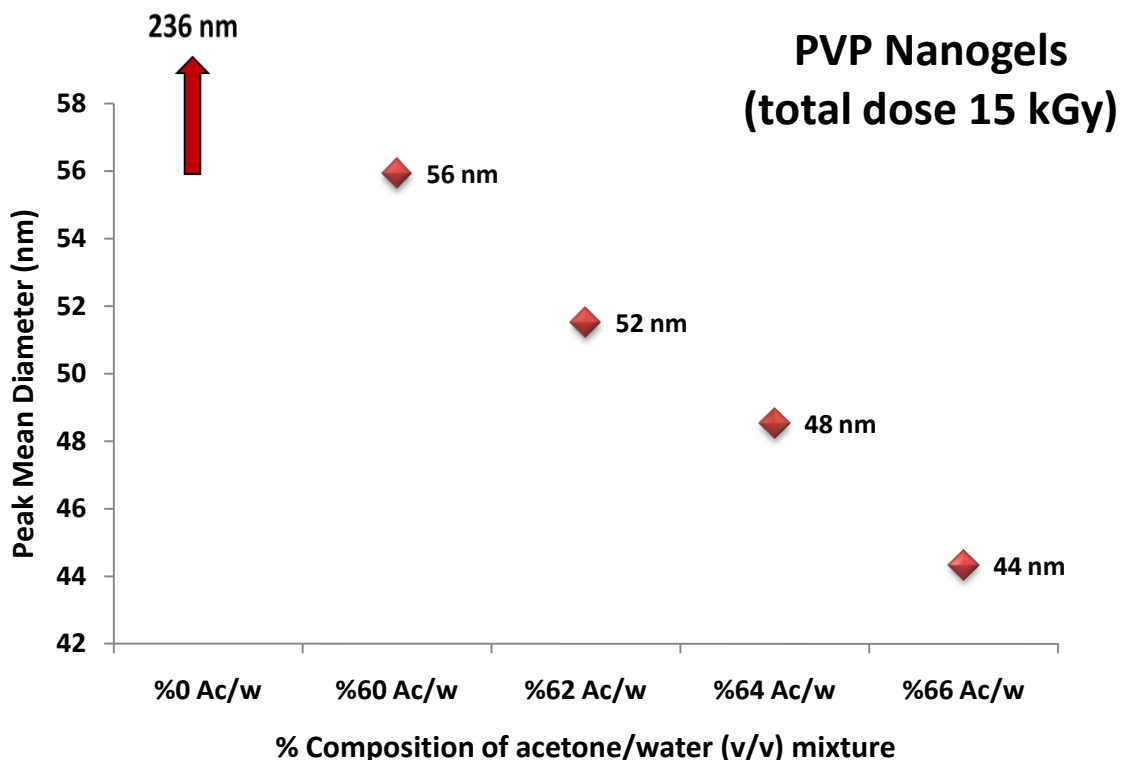


**Figure 6.12.** Effect of acetone amount in the acetone/water binary mixture on the peak mean diameter of PVP nanogels that are synthesized from 2 mg/mL PVP solutions by gamma radiation with a total absorbed dose of 15 kGy.

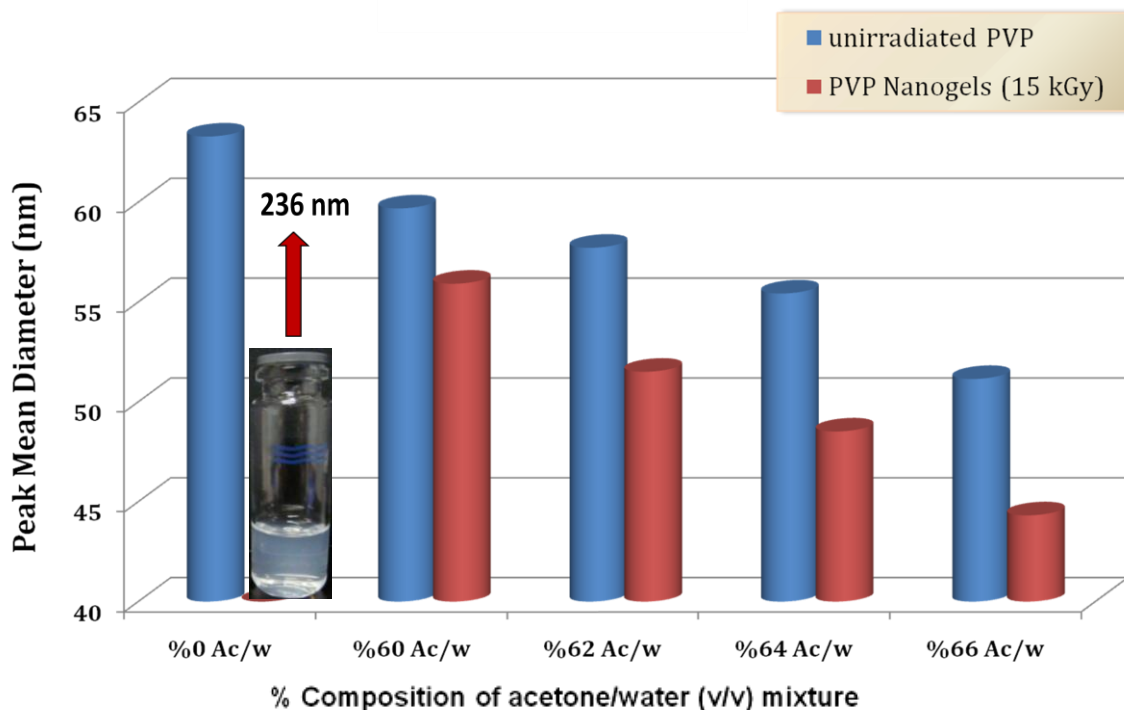


**Figure 6.13.** Effect of acetone amount in the acetone/water binary mixture on the peak mean diameter of PVP nanogels, as compared to unirradiated PVP coil sizes.

The nanogels are known to be intramolecularly crosslinked single polymer coils which are depicted by a clear reduction in their particle size which can be characterized by viscometry, static or dynamic light scattering, etc. However, additional information in proof of their formation should be considered to make more reliable predictions. The nanogels with increasing crosslink densities should show a decrease in the radius of gyration ( $R_g$ ) while maintaining their weight-average molecular weight ( $M_w$ ) almost the same.

### ***Gel Permeation Chromatography (GPC) Analysis***

Gel permeation chromatography (GPC) is known to be a versatile technique in analysing the molecular size distributions of polymers. GPC can therefore be a simple and an efficient tool to control the relative changes in the molecular sizes of nanogels. One can predict the sizes of nanogels from retention times since separation is based on hydrodynamic volume differences. Smaller species will appear in the eluent at higher retention times, and inversely, larger particles will leave the system earlier. Figure 6.14 shows the successive GPC chromatograms for unirradiated PVP and PVP nanogels prepared in acetone/water mixtures with acetone ratios of 0.60, 0.62, 0.64 and 0.66 from 2 mg/mL solution of PVP using gamma rays with a total absorbed dose of 15 kGy. The GPC chromatograms for other total absorbed doses, 5 and 10 kGy, are not represented here, since there is only a minor effect of the total dose on particle size and polydispersity of nanogels. The GPC results are also consistent with those of DLS where the results are also expressed as size distribution by intensity. It can be clearly seen that, with the increase in acetone amount of the mixture from 0.60 to 0.66 nanogels are eluted at higher retention times, thus, their sizes are decreasing with the increasing amount of acetone in acetone/water mixture. Additionally, the peak widths can be used to predict the polydispersities for PVP polymer and nanogels and it is observed that the peak widths of nanogels are nearly the same and PVP polymer peak is broader than that of nanogels (Figure 6.15). This result is also consistent with DLS results where average PDI value for PVP nanogels is 0.21 (0.20-0.23) but for PVP polymer it is 0.35 (0.31-0.38).

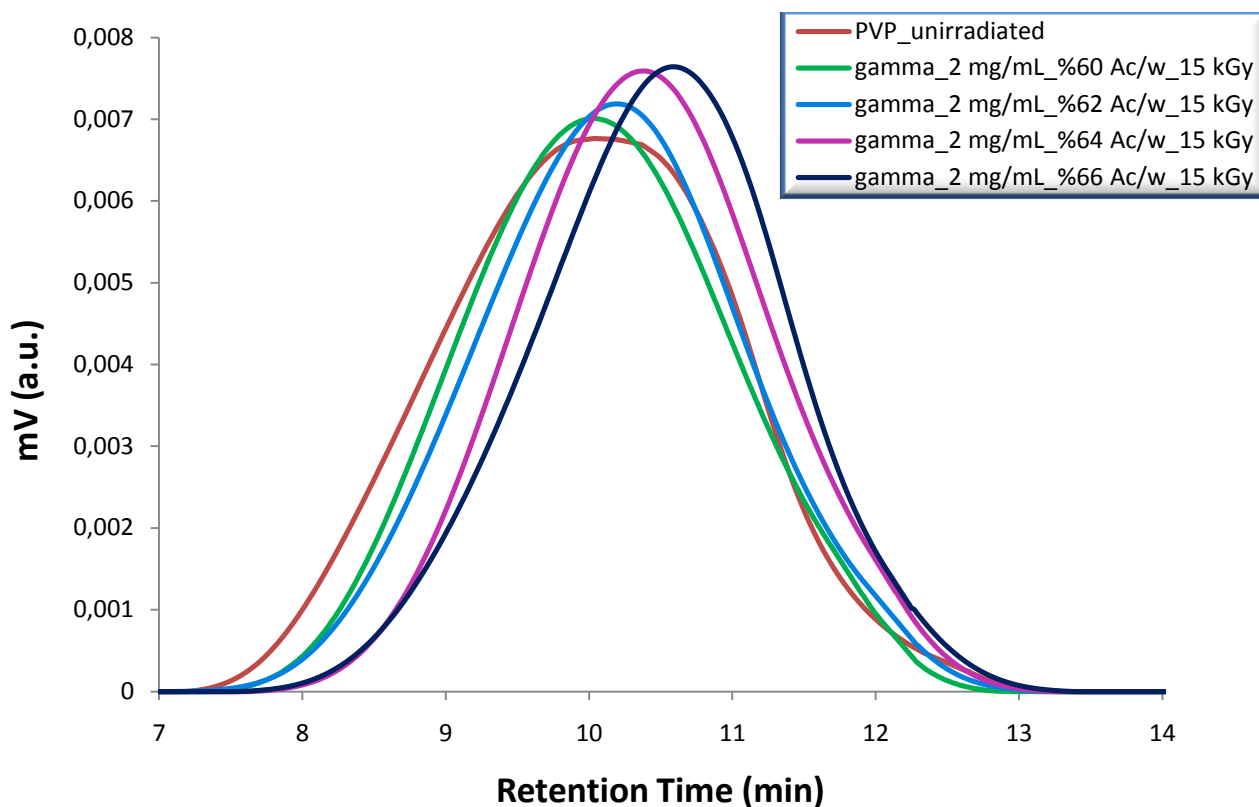


**Figure 6.14.** Normalized chromatograms of unirradiated PVP and PVP nanogels prepared in acetone/water mixtures with acetone ratios 0.60, 0.62, 0.64 and 0.66 from 2 mg/mL PVP solution using gamma rays with a total absorbed dose of 15 kGy.

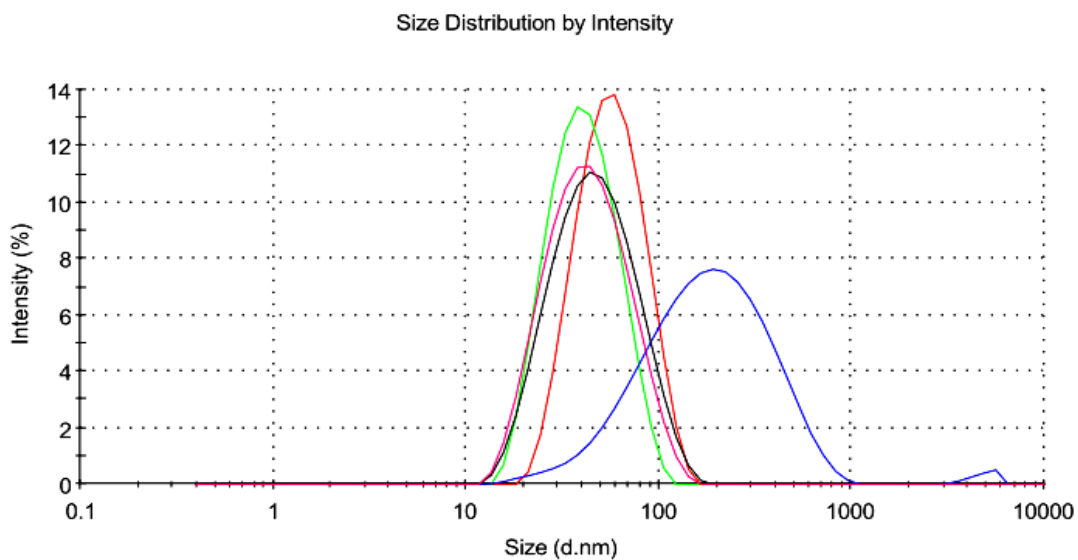


**Figure 6.15.** Size distribution graph based on scattered light intensities of unirradiated PVP (blue) and PVP nanogels prepared in acetone/water mixtures with acetone ratios 0.60 (red), 0.62 (black), 0.64 (pink) and 0.66 (green) from 2 mg/mL PVP solutions using gamma rays with a total absorbed dose of 15 kGy.

### Scanning Electron Microscopy (SEM) Analysis

The synthesized nanogels were characterized by scanning electron microscope. Figure 6.16 shows SEM images of PVP nanogels prepared in 0.66 acetone/water mixture from 2 mg/mL solution of PVP using gamma rays with a total absorbed dose of 15 kGy, with a magnification of 13000x (A) and 50000x (B). It is obviously seen that the particles are mostly homogeneous and spherical in shape.

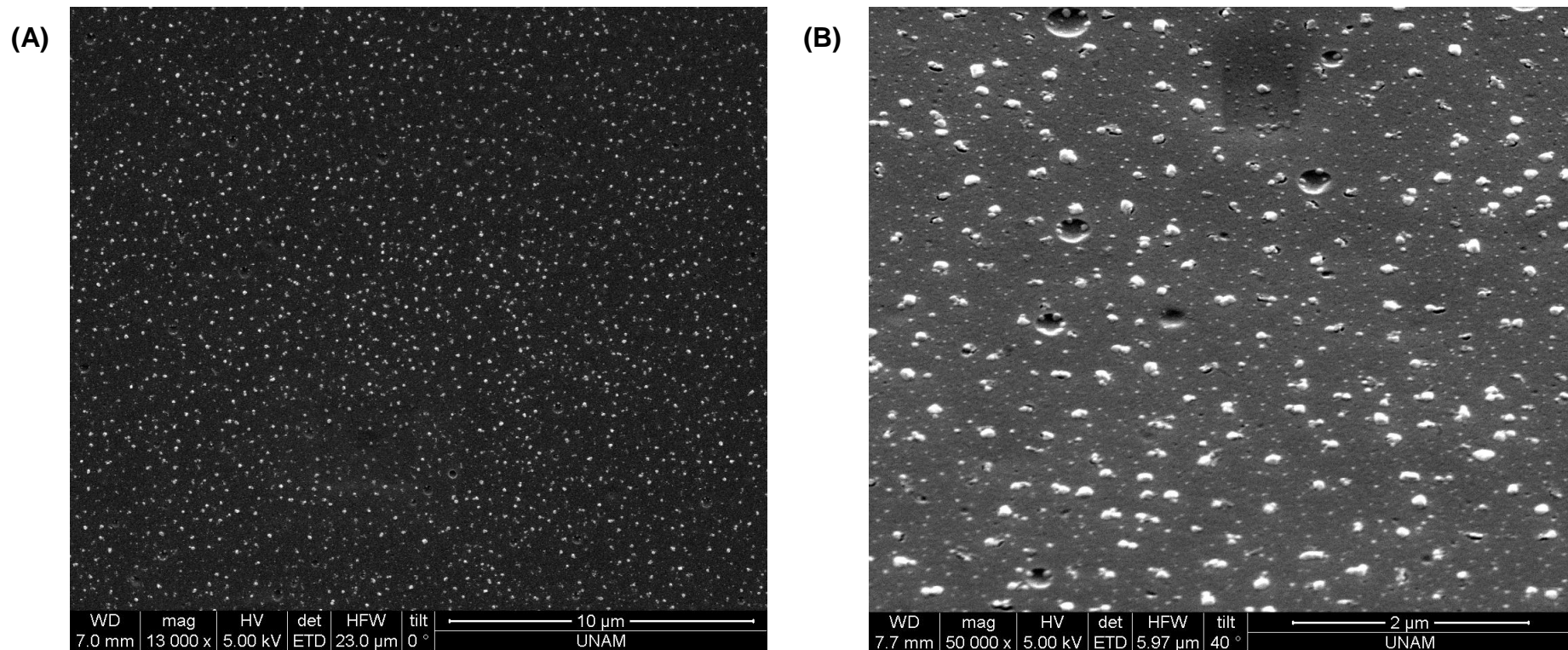


**Figure 6.16.** Scanning electron micrographs of PVP nanogels prepared in 0.66 acetone/water mixture from 2 mg/mL solution PVP using gamma rays with a total absorbed dose of 15 kGy, with a magnification of 13000x (A) and 50000x (B).

#### 6.4. PVP Nanogels Prepared in Water: Effect of Total Absorbed Dose, Polymer Concentration and Type of Radiation Source

The requirements for the preparation of PVP nanogels by radiation-induced crosslinking method were studied intensively by Ulanski and Rosiak. They explained the experimental conditions that should be achieved in order to promote intramolecular recombination which leads the system to microgelation. Intramolecular recombination is mainly based on the high probability of a radical to combine with another on the same chain. In order to achieve this situation the polymer coils should be well separated from each other and the number of radicals that are being produced on each chain should be high. These requirements are fulfilled when low concentrations and high dose rates are chosen for experiments. Figure 6.17 shows the course of the reaction from macrogelation to nanogelation and the requirements to promote this path. We offer an additional way of control as it has already been explained in detail. Approaching theta condition can also promote intramolecular recombination resulting from the shrinkage of polymer coils since the chain segments are getting closer and the recombination of radicals on a single chain is enhanced.



- ✓ **High dose rate**
- ✓ **Low concentration**
- ✓ **Approaching theta conditions**

**Figure 6.17.** Factors promoting intramolecular crosslinking.



## Dynamic Light Scattering Analysis

Table 6.5 shows the peak mean diameters, their standard deviations and PDI values for nanogels that are synthesized from 1 mg/mL and 2 mg/mL aqueous PVP solutions by using gamma radiation whereas Table 6.6 shows the mentioned values for 1 mg/mL and 2 mg/mL aqueous PVP solutions which are synthesized by electron beam irradiation. It can be clearly seen that 2 mg/mL concentration is high for this synthesis parameters both for gamma and e-beam irradiations. Especially for gamma, there is a high increase in particle size due to the formation of intermolecular crosslinks. The diameters as high as 248 nm and high PDI values support this approach where the size broadening may be a result of the combination of these two processes intra- and intermolecular crosslinking occur concomitantly. Additionally, the results were found to be very striking that for 1 mg/mL gamma irradiated samples show no sensitivity to total absorbed dose which was also the same for the samples prepared in acetone/water mixtures. On the other hand e-beam irradiated samples show a substantial decrease starting from 59 to 46 nm as the total absorbed dose is increased. These tabulated results are also collected in Figure 6.18 and 6.19 for the samples prepared by gamma radiation and in Figures 6.20 and 6.21 for e-beam irradiated samples.

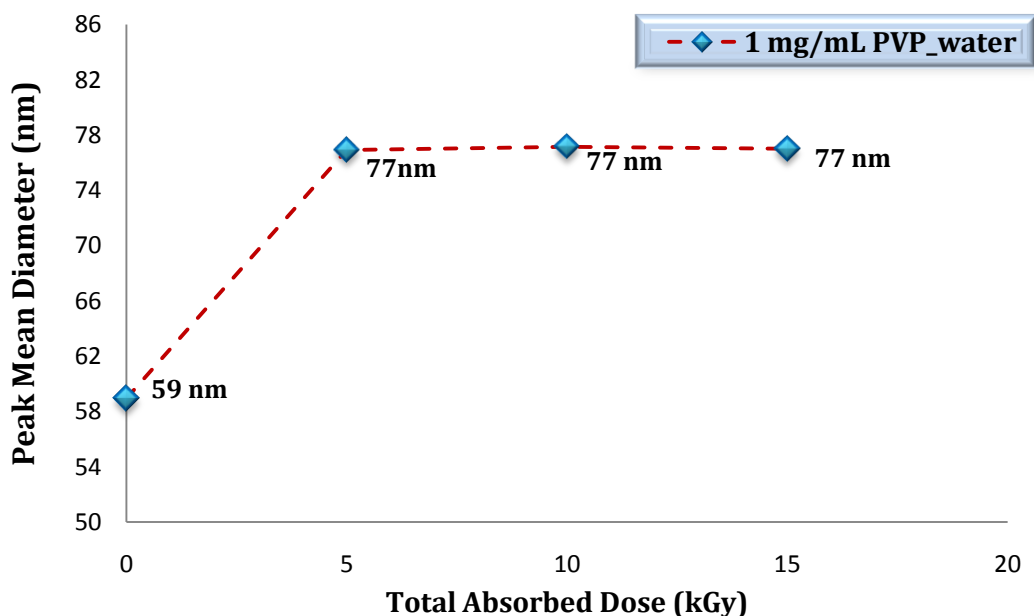


**Figure 6.18.** Effect of total absorbed dose on the peak mean diameter of PVP nanogels that are synthesized from 1 mg/mL aqueous PVP solutions by gamma radiation.

**Table 6.5.** Peak mean diameters, their standard deviations and PDI values for nanogels that are synthesized from 1 mg/mL and 2 mg/mL aqueous PVP solutions by using gamma radiation.

gamma	unirradiated			5 kGy			10 kGy			15 kGy		
water	d (nm)	std dev.	PDI	d (nm)	std dev.	PDI	d (nm)	std dev.	PDI	d (nm)	std dev.	PDI
1 mg/mL	58.93	0.75	0.25	76.84	0.42	0.18	77.16	0.26	0.18	77.00	0.90	0.18
2 mg/mL	63.29	0.37	0.26	206.60	4.78	0.34	247.90	5.66	0.38	236.40	1.06	0.31

**Table 6.6.** Peak mean diameters, their standard deviations and PDI values for nanogels that are synthesized from 1 mg/mL and 2 mg/mL aqueous PVP solutions by using e-beam radiation.

e-beam	unirradiated			5 kGy			10 kGy			20 kGy		
water	d (nm)	std dev.	PDI	d (nm)	std dev.	PDI	d (nm)	std dev.	PDI	d (nm)	std dev.	PDI
1 mg/mL	58.93	0.75	0.25	52.70	1.54	0.24	48.04	0.38	0.17	46.35	0.72	0.17
2 mg/mL	63.29	0.37	0.26	151.50	1.41	0.42	85.86	1.52	0.21	78.64	0.59	0.23

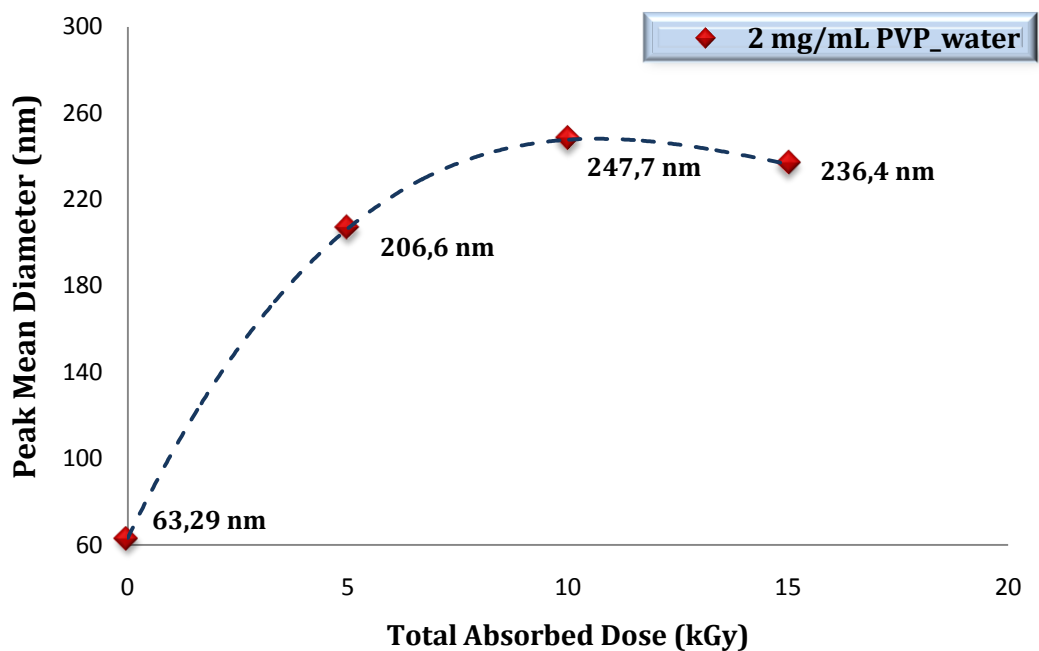


**Figure 6.19.** Effect of total absorbed dose on the peak mean diameter of PVP nanogels that are synthesized from 2 mg/mL aqueous PVP solutions by gamma radiation.

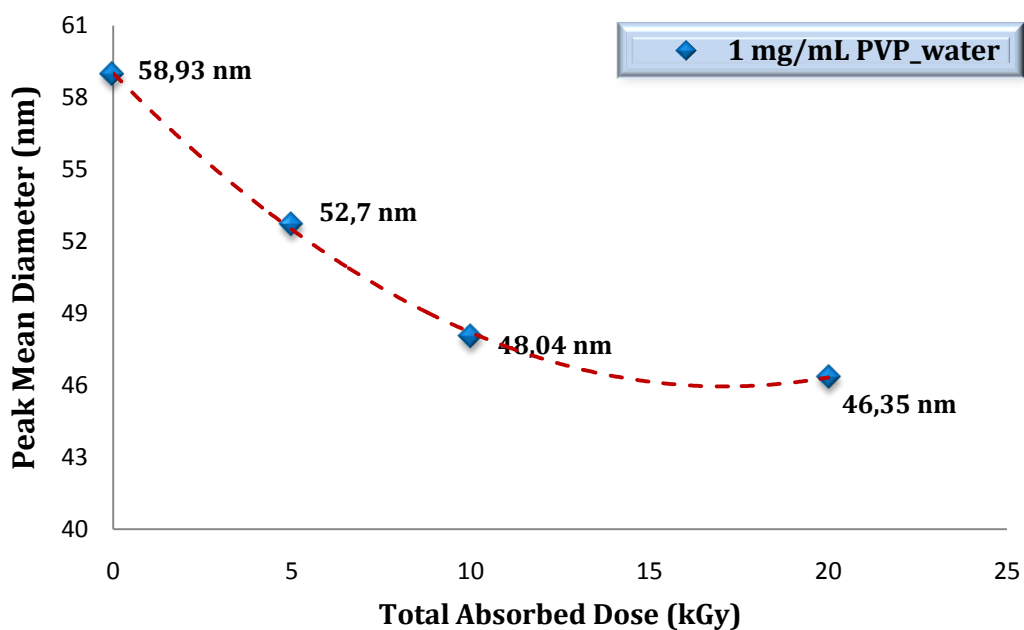


**Figure 6.20.** Effect of total absorbed dose on the peak mean diameter of PVP nanogels that are synthesized from 1 mg/mL aqueous PVP solutions by e-beam radiation.

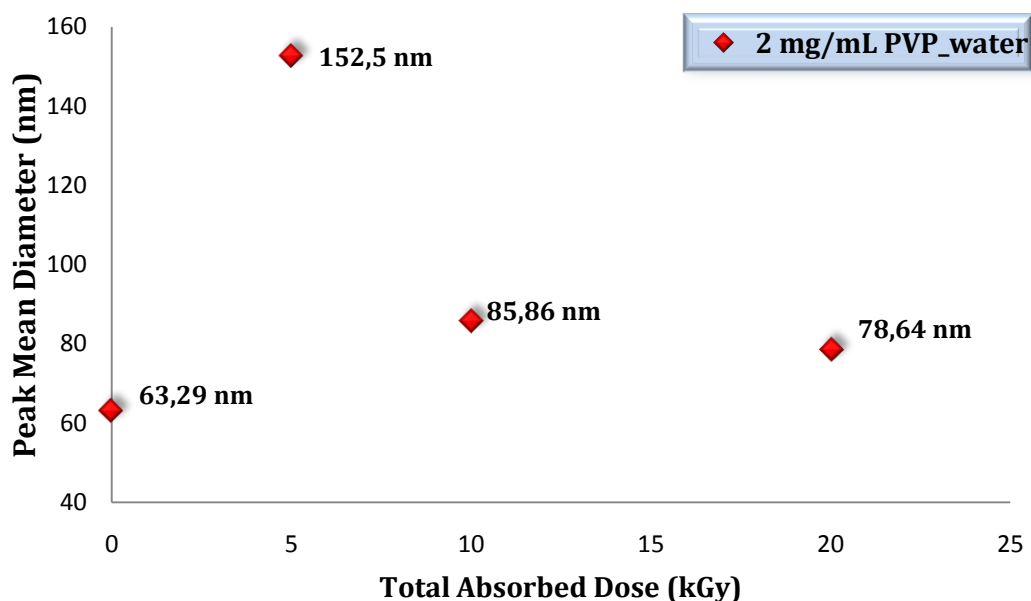


**Figure 6.21.** Effect of total absorbed dose on the peak mean diameter of PVP nanogels that are synthesized from 2 mg/mL aqueous PVP solutions by e-beam radiation.

### ***Gel Permeation Chromatography (GPC) Analysis***

Similar to previous results, again GPC results perfectly fit with experimental data taken from DLS analysis. Figure 6.22 shows the size distribution of PVP nanogels and pristine PVP which are very similar results expressed in Figure 6.20. It should be stressed that, a significant decrease in PDI values is observed after the samples were irradiated with either e-beam or gamma. Therefore, more symmetrical and narrower peaks are observed for irradiated samples. For e-beam irradiated samples, the PDI value for 10 and 20 kGy is lower than the value for 5 kGy which is seen in both DLS results, Table 6.6 and GPC results (Figure 6.22).

Figure 6.23. again supports the mentioned phenomenon which is shown in Figure 6.18, the insensitivity of particle size to total absorbed dose when nanogels are prepared by gamma irradiation. The retention times and polydispersities are nearly identical and this result is in good agreement with the values given in Table 6.4.

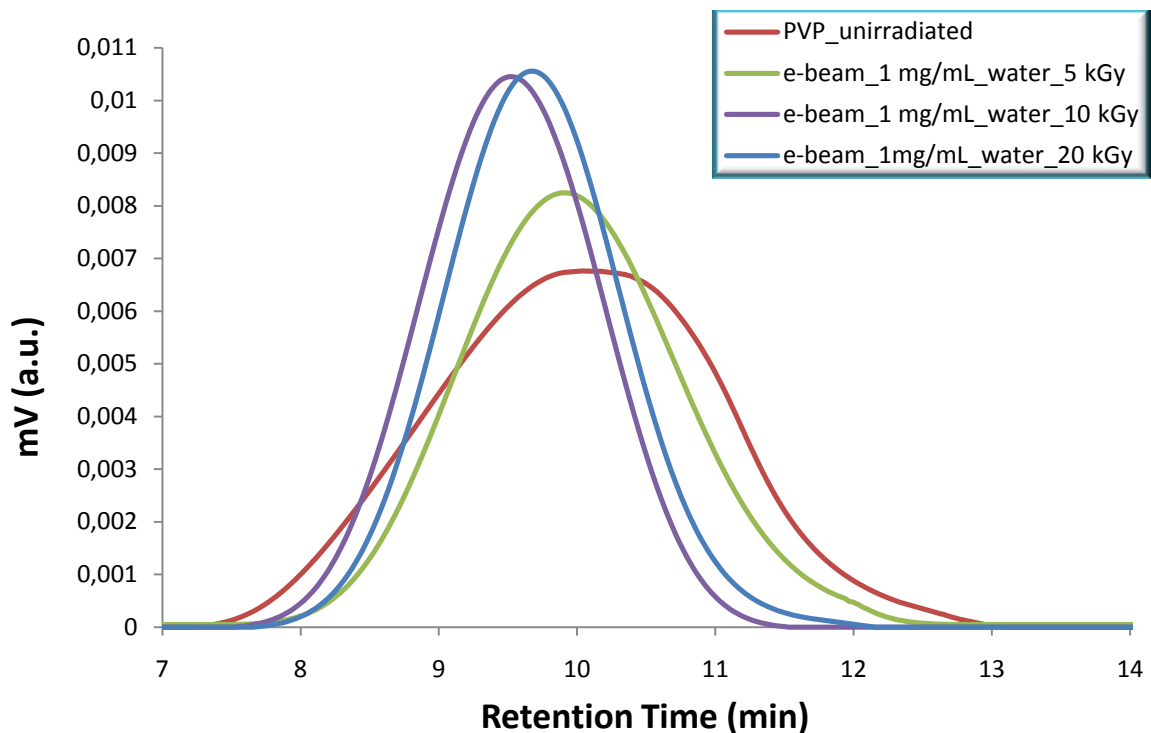


**Figure 6.22.** Normalized chromatograms of unirradiated PVP and PVP nanogels prepared from 1 mg/mL solution of PVP aqueous solutions using e-beam with total absorbed doses of 5, 10 and 20 kGy.

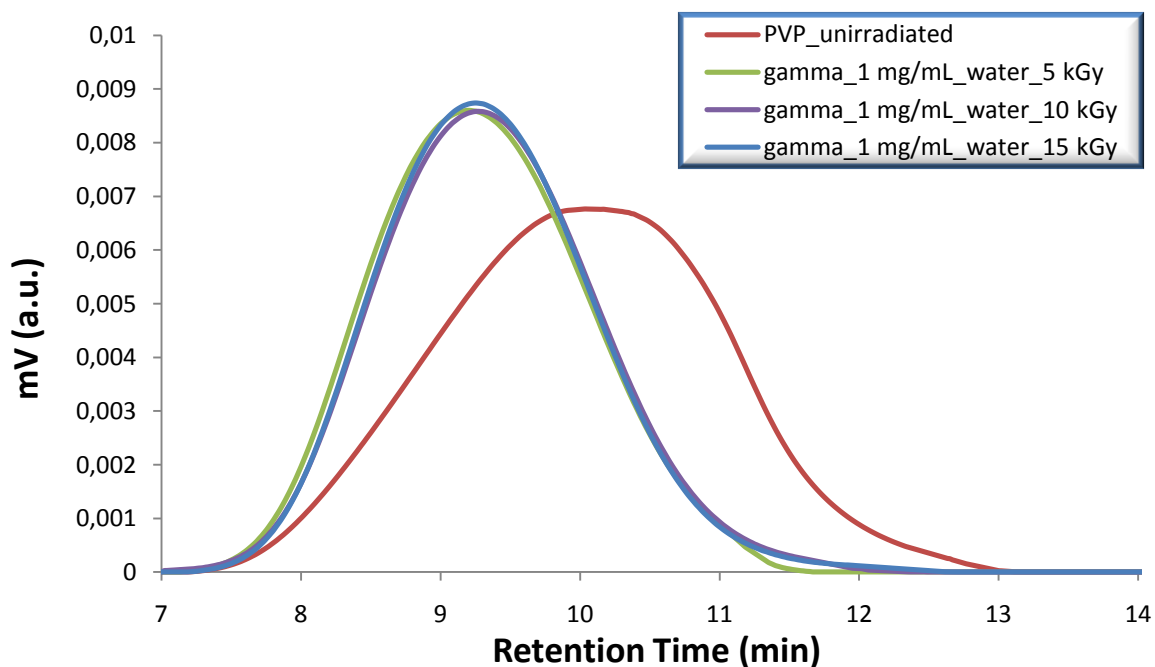


**Figure 6.23.** Normalized chromatograms of unirradiated PVP and PVP nanogels prepared from 1 mg/mL solution of PVP aqueous solutions using gamma rays with total absorbed doses of 5, 10 and 20 kGy.

The GPC chromatograms also provided the information about type of crosslinking. A slight decrease of retention times may point the intermolecular crosslinking. However, as the peaks are within the limits of PVP polymer peak the change in molecular weight should not be very significant. The shift can rather be related to the presence of crosslinkings which are expected to increase the molecular weight slightly. It is assumed that only a minor contribution of intermolecular recombination was present.

**Table 6.7.** Peak mean diameters, their standard deviations and PDI values for nanogels that are synthesized from 1 mg/mL aqueous solutions of PVP by using e-beam and gamma radiation.

1 mg/mL	5 kGy			10 kGy			15 kGy			20 kGy		
water	d (nm)	std dev.	PDI	d (nm)	std dev.	PDI	d (nm)	std dev.	PDI	d (nm)	std dev.	PDI
gamma	76.84	0.42	0.18	77.16	0.26	0.18	77	0.91	0.18	-	-	-
e-beam	52.70	1.54	0.24	48.04	0.38	0.17	-	-	-	46.35	0.72	0.17

Table 6.7 summarizes the effect of type of radiation. The sizes of PVP nanogels are not dependent on total absorbed dose when they are prepared with gamma irradiation. When electron beam is used as the radiation source the hydrodynamic volumes of nanogels are decreased with increasing dose that the sample absorbs. This decrease in the sizes of nanogels with an increase in the total absorbed dose is also consistent with previous works (Ulanski and Rosiak 1998, 1999; Nurkeeva, 2004; Henke et al., 2005).

### **Atomic Force Microscopy (AFM) Analysis**

Atomic force microscopy analysis was performed to investigate the sizes and the size distributions of PVP nanogels topographically. Figure 6.24 shows the height based AFM images of mica surface (A), PVP coated mica surface (B) and PVP nanogels deposited on mica surface (C). Mica surface was chosen as the support material since it has very homogeneous profile as it is seen from Figure 6.24-A. The solutions were cast on mica surface which result for linear PVP as it is seen in Figure 6.24-B. PVP coated the surface as a film and changed the surface profile of mica. The latter image belongs to the PVP nanogels deposited on mica surface where the nanogels are clearly seen and identified from the rest of the sample by their heights that appear as white spots.

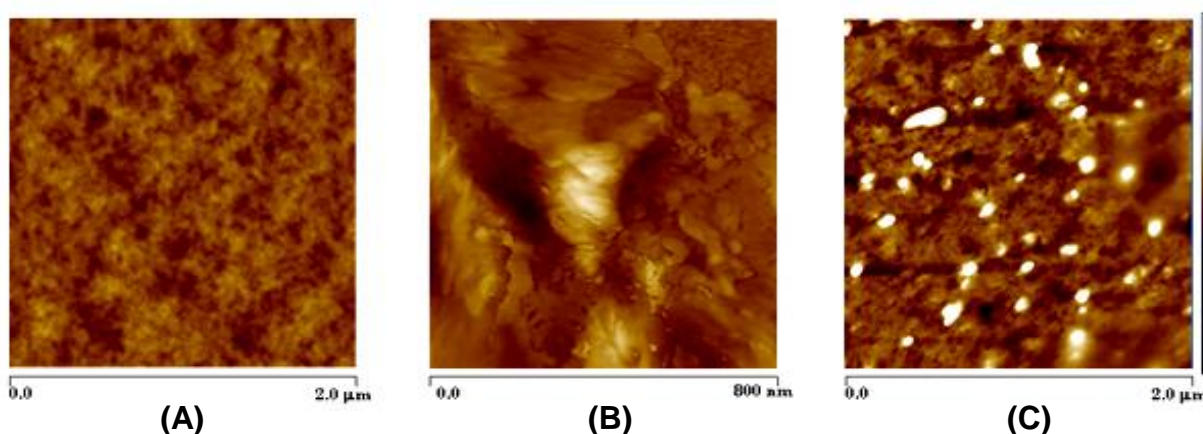


**Figure 6.24.** Height based AFM images of mica surface (A), PVP coated mica surface (B), PVP nanogels deposited on mica surface (C).

Figure 6.25 shows the 3D views of the AFM images given in Figure 6.24. The change in the surface profile after the deposition of linear PVP is clearly seen where linear PVP chains coated the surface as a film. However, the background surface of mica in Figure 6.25-A and PVP deposited mica in Figure 6.25-C remains to be unchanged which is a proof of the presence of crosslinking. For 6.25-C small spikes arising from the deposited nanogels are clearly seen. The roughness values are 5.63 nm for mica surface, 4.91 nm for PVP coated mica surface and 12.6 nm for PVP nanogels deposited on mica surface. For better identification of PVP nanogels, cross-sectional views were taken from previous AFM images. Figure 6.26-A shows that for PVP film, the surface became flat as a result of linear chains which coated the mica surface. On the other hand, the profile in Figure 6.26-B show that nanogels deposited on mica surface are of equal size and dimensions, with approximate diameters of 80 nm.

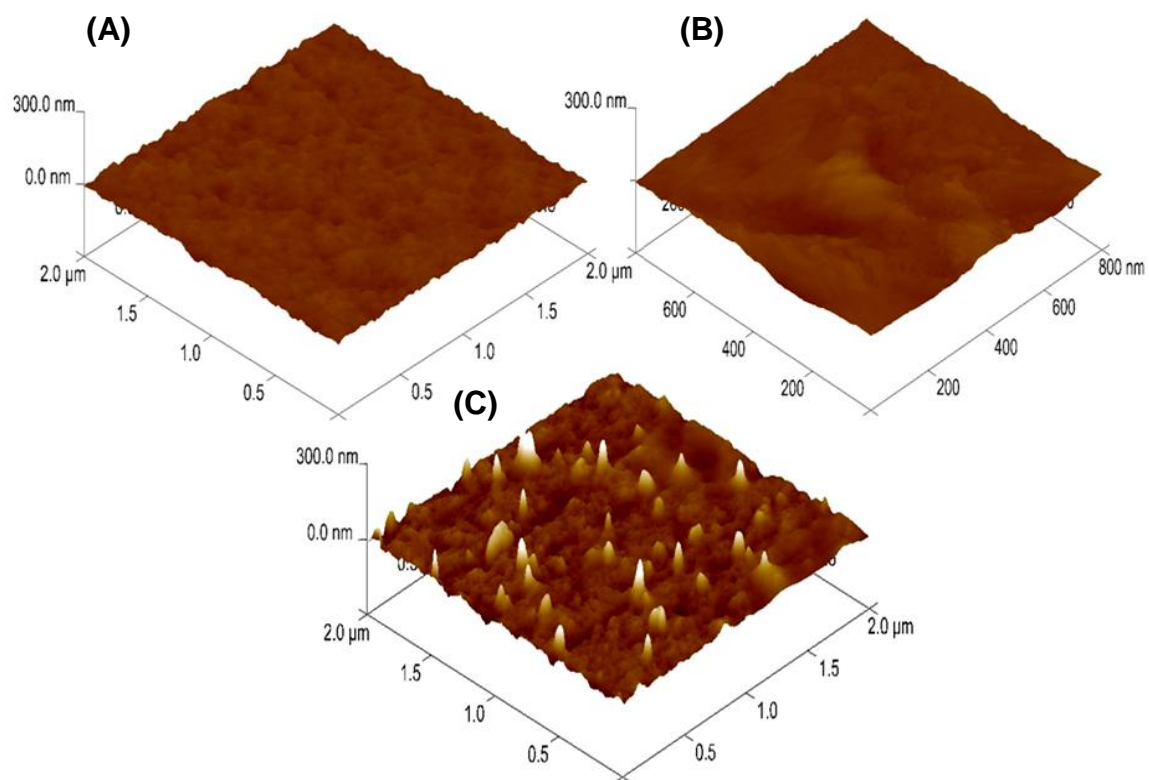


**Figure 6.25.** 3D views of AFM images of mica surface (A), PVP coated mica surface (B), PVP nanogels deposited on mica surface (C).

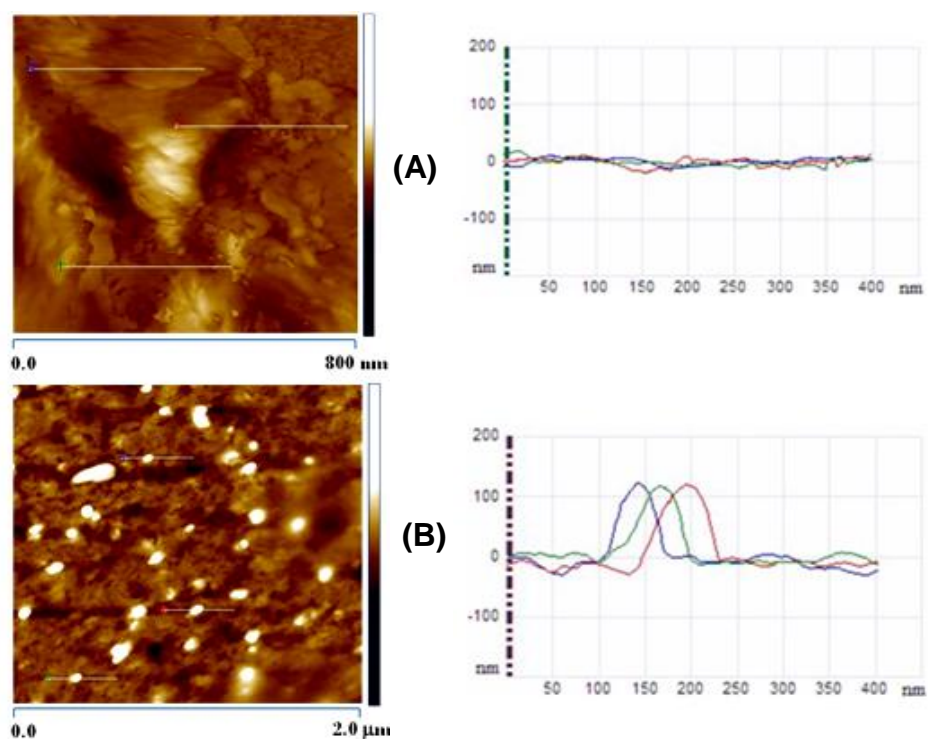


**Figure 6.26.** Cross-sectional views of PVP coated mica surface (A), PVP nanogels deposited on mica surface (B).

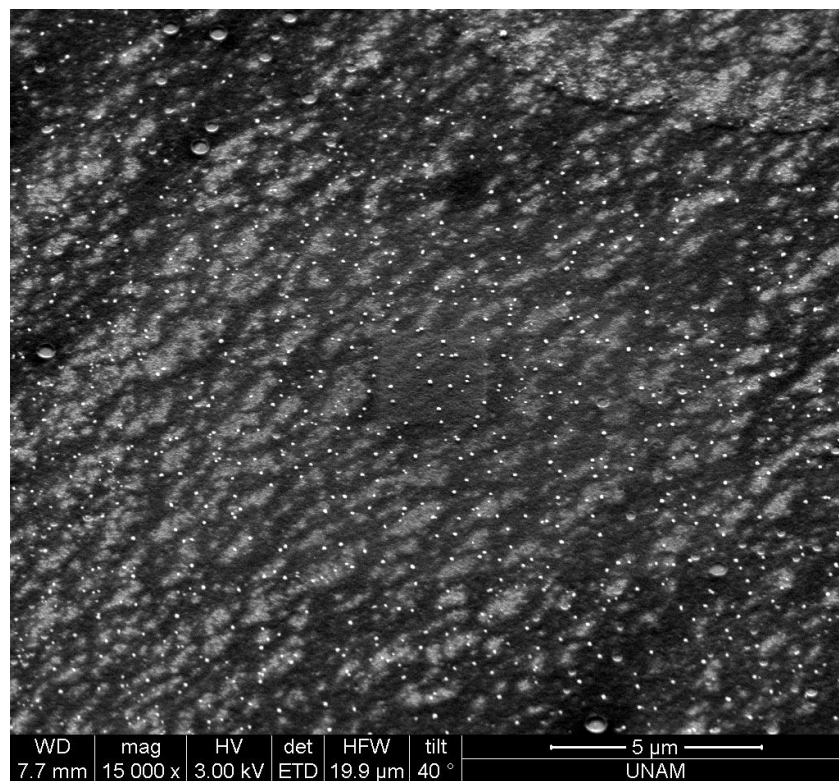


### ***Scanning Electron Microscopy (SEM) Analysis***

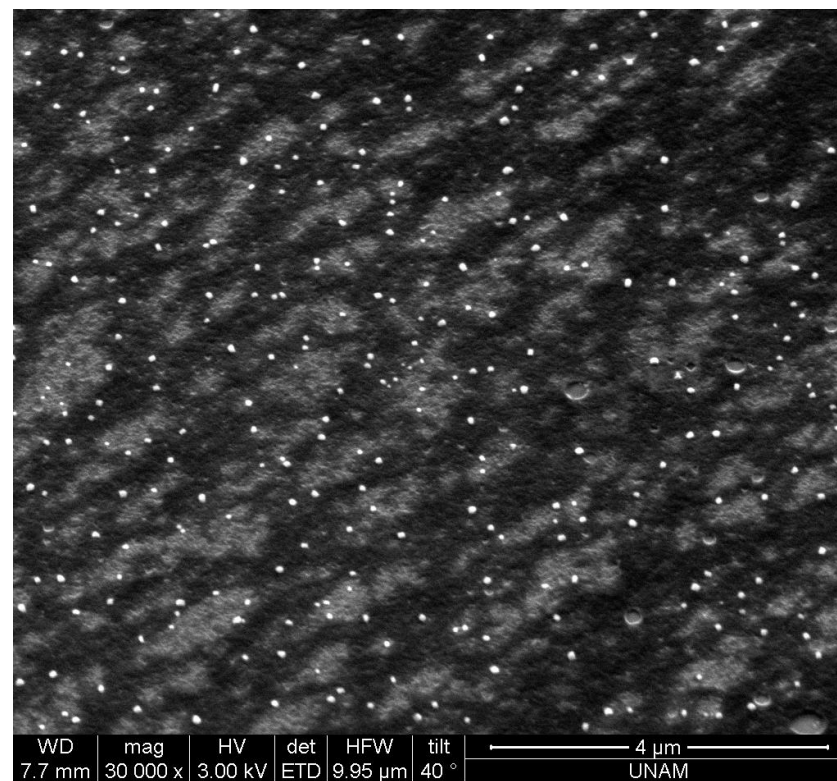
To support these results, scanning electron microscopy technique was used to investigate the nanogels obtained from both e-beam irradiated and gamma irradiated aqueous PVP solutions. Figure 6.27-A clearly shows that gamma irradiated nanogels are very homogeneous. Images with different magnifications are given to estimate the real structure of nanogels.

Figure 6.28-B shows the SEM picture of PVP nanogels where their structures are obviously seen. They are mostly spherical, symmetrical and nanogel particles have nearly the same size. This result is also consistent with the AFM measurements and PDI values taken from DLS analysis.

Figure 6.29 shows the SEM images of nanogels prepared by e-beam irradiation. From Figure 6.29-B, one can easily identify that nanogels are similar in size but mostly appearing in agglomerated forms.

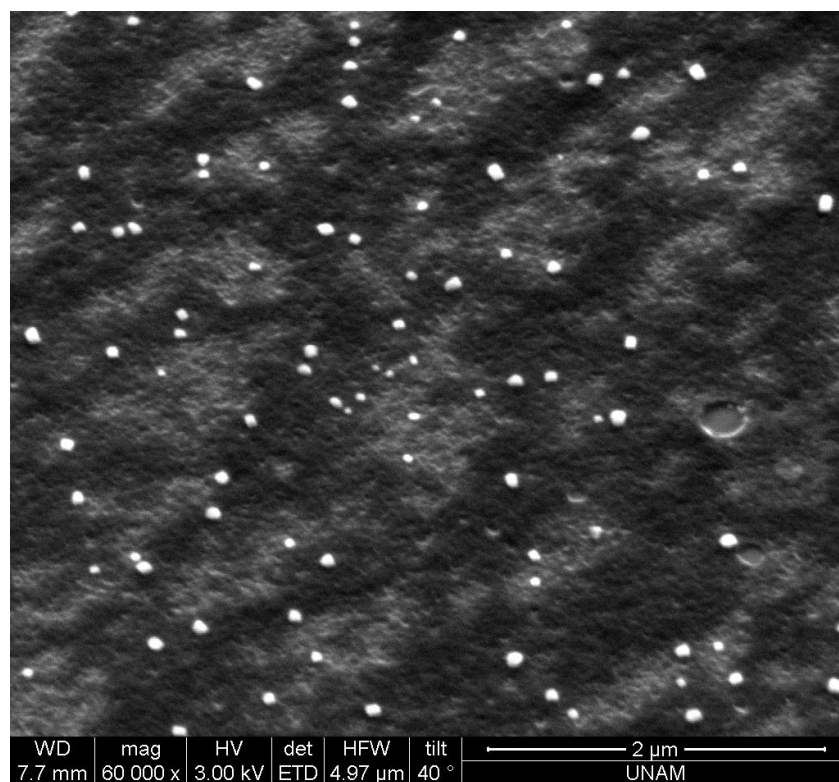


(A)

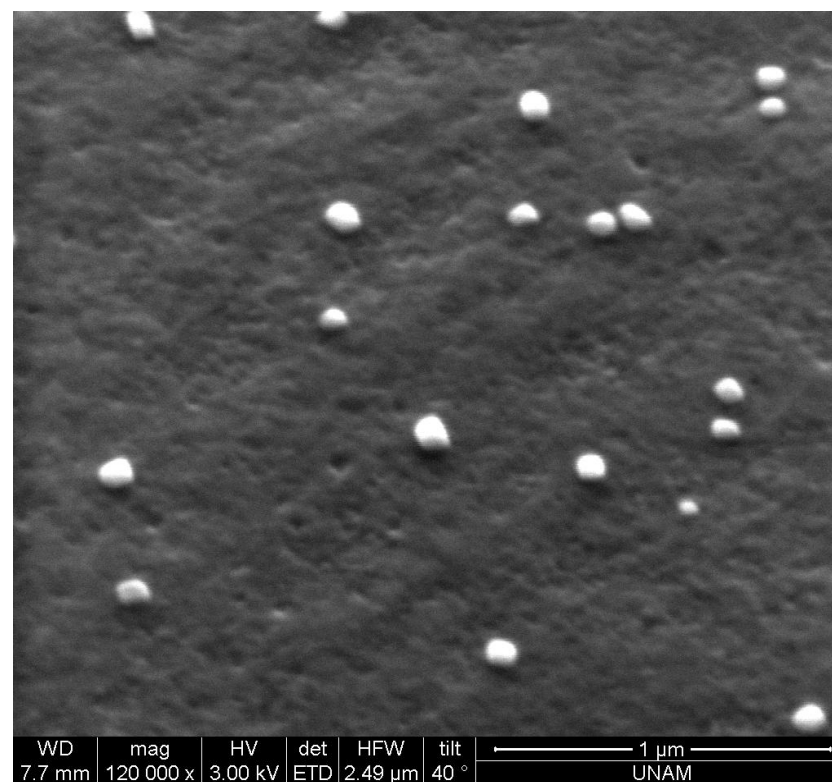


(B)

**Figure 6.27.** Scanning electron micrographs of PVP nanogels being prepared from 1 mg/mL solution PVP using gamma rays with a total absorbed dose of 15 kGy, with a magnification of 15000x (A), 30000x (B).

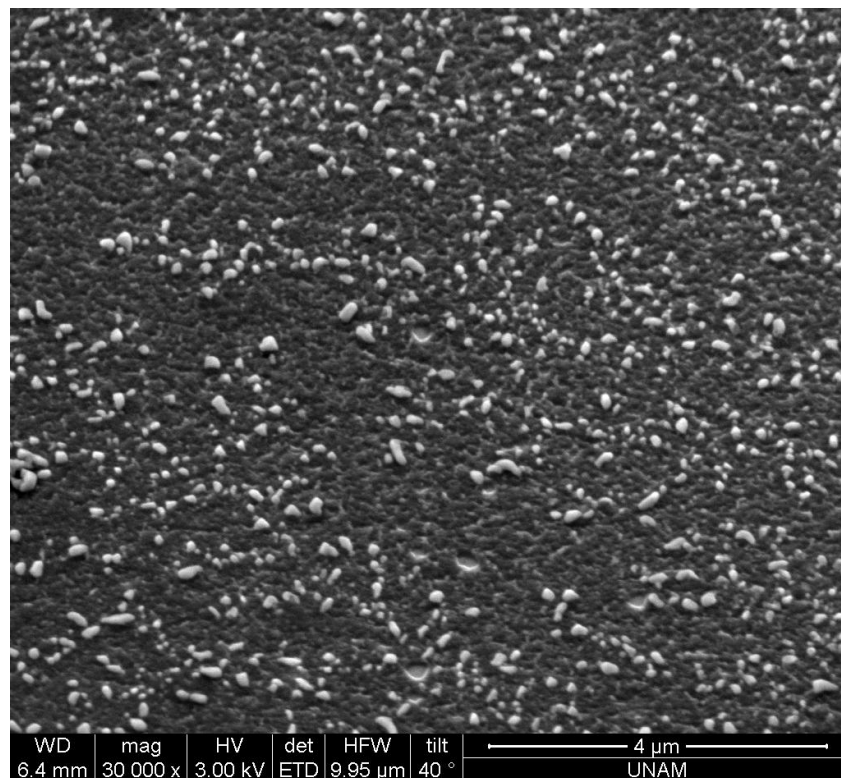


(A)

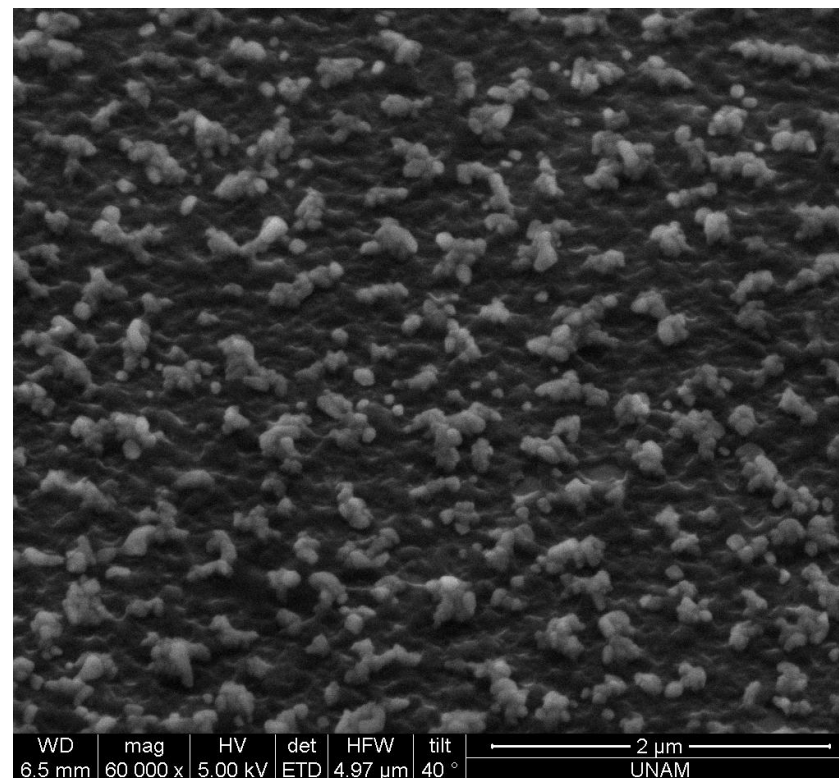


(B)

**Figure 6.28.** Scanning electron micrographs of PVP nanogels being prepared from 1 mg/mL solution PVP using gamma rays with a total absorbed dose of 15 kGy, with a magnification of 60000x (A), 120000x (B).



(A)



(B)

**Figure 6.29.** Scanning electron micrographs of PVP nanogels being prepared from 1 mg/mL solution PVP using electron beam with a total absorbed dose of 10 kGy, with a magnification of 30000x (A), 60000x (B).

## 7. CONCLUSIONS

Radiation-induced intramolecular crosslinking method was applied to prepare polymer nanogels from dilute aqueous solutions of poly (vinyl pyrrolidone) (PVP) using either e-beam or gamma irradiation. The effects of radiation synthesis parameters, i.e. total absorbed dose, dose rate, together with physical parameters, i.e. polymer concentration, effect of a denaturing agent, guanidinium sulfate and effect of a non-solvent, acetone on the properties of nanogels were investigated (e.g. size, polydispersity by size, shape, etc.). These investigations were made by using dynamic light scattering, gel permeation chromatography, atomic force microscopy and scanning electron microscopy analyses.

In the first part of the thesis, various denaturing agents were used to control the shrinkage of PVP coils in solution. Viscosity measurements were performed to investigate the effect of guanidinium carbonate, guanidinium sulfate and thiourea for different denaturing agent concentrations, 0.5 M, 1.0 M, 1.5 M and 2.0 M. Guanidinium sulfate (GS) was chosen for further experiments since it reduced the intrinsic viscosity to its lowest value, 2.87 for 2.0 M GS, therefore acting as the most effective denaturant among others. Afterwards, PVP nanogels were prepared by e-beam irradiation of aqueous solutions with various concentrations of GS. It was observed that there was no systematical change in the hydrodynamic volumes of PVP nanogels and the trend for the results of 1 mg/mL and 2 mg/mL solutions were nearly identical. This phenomena needs further investigation and verification.

In the second part, the effect of a non-solvent, acetone was investigated. Dynamic light scattering of unirradiated PVP solutions showed a clear shrinkage in polymer coils with increasing amount of acetone in the binary acetone/water systems containing several volume fractions of acetone, 0.60, 0.62, 0.64 and 0.66. A shrinkage from 63 nm (water) to 51 nm (0.66 Ac/w) was observed with the introduction of acetone to the system. Afterwards, PVP nanogels were prepared from their diluted aqueous solutions containing corresponding acetone volume

fractions. For 2 mg/mL PVP in water, microgelation was observed after gamma irradiation that the peak mean diameters were 247.9, 206.6 and 236.4 nm for 5, 10 and 15 kGy's respectively. The diameters of irradiated samples showed no sensitivity to total absorbed dose. Upon the introduction of acetone to the system only nanogelation was observed and nanogels having diameters between 56 and 44 nm were obtained. As the amount of non-solvent increases polymer-polymer interactions are increased and the contraction of coils help the system prefer intramolecular crosslinking due to shorter inter-radical distances on the same PVP backbone. A decrease from 236 nm (water) to 44 nm (0.66 Ac/w) is a clear evidence that this is an efficient and useful approach to control the size of PVP nanogels. Moreover, this method can also be used for the other hydrophilic polymers. Gel permeation chromatography results were consistent with dynamic light scattering results that with the increase in acetone amount of the mixture from 0.60 to 0.66, nanogels were eluted at higher retention times, thus, their sizes are decreasing with the increasing amount of acetone in acetone/water mixture. Additionally, from GPC results it was observed that size based polydispersities of nanogels were smaller than that of pristine PVP where average for PVP nanogels is 0.21 (0.20-0.23) but for PVP polymer it is 0.35. Prepared nanogels were also characterized by using scanning electron microscopy.

In the last part of this dissertation, effect of total absorbed dose, type of radiation source and effect of concentration were elaborated for the nanogels prepared from aqueous solutions of PVP. It is concluded that 2 mg/mL concentration is high both for gamma and e-beam where the intermolecular crosslinking becomes more effective. This unwanted situation is more dominant for the samples prepared by gamma irradiation. For 1 mg/mL e-beam irradiated samples, the hydrodynamic volumes of nanogels showed a substantial decrease from 59 to 46 nm with increasing dose from 5 to 15 kGy. However, 1 mg/mL gamma irradiated samples showed no sensitivity to the total absorbed dose. GPC results fit with the experimental data taken from DLS analysis that the polydispersities become lower after irradiation of PVP samples and therefore, GPC peaks were narrower and symmetrical for PVP nanogels than those of unirradiated PVP. Prepared nanogels were characterized by using atomic force microscopy (AFM) and scanning

electron microscopy (SEM). Both AFM and SEM images are believed to be good examples for nanogels when they are compared with those seen in literature. AFM and SEM analysis show that spherical and very homogeneous particles were obtained, especially for gamma irradiated samples, with diameters of approximately 80 nm. These results also support the DLS data.

The unique features of this study can be highlighted as,

- A first thermodynamical approach about solvent/non-solvent pairs to control polymer coil size and thus, size of nanogels.
- The first comparative study between e-beam and gamma irradiation for the synthesis of PVP nanogels.
- For the first time the development of nanogels were followed by gel permeation chromatography (GPC).

## 8. REFERENCES

- Abdelazim A. A.; Tengu H.; Maerta J.; Sundholm F., **1992**, Flexibility and hydrodynamic properties of poly (vinylpyrrolidone) in non-ideal solvents, *Polym. Bull.*, 29, 461–467.
- Ajji, Z.; Othman, I.; Rosiak, J. M., **2005**, Production of hydrogel wound dressings using gamma radiation, *Nucl. Instrum. Methods Phys. Res., Sect. B*, 229, 375–380.
- Allen T. M.; Cullis P. R.; **2004**, Drug delivery systems: entering the mainstream, *Science*, 303, 1818–1822.
- An, J.-C., **2007**, Synthesis, characterization, and kinetic studies of ionizing radiation-induced intra- and inter-crosslinked poly(vinyl pyrrolidone) nanohydrogels, Ph.D., Univ. of Maryland, College Park, 3297324, 166.
- An, J.-C., **2010**, Synthesis of the combined inter- and intra-crosslinked nanohydrogels by e-beam ionizing radiation, *J. Ind. Eng. Chem.*, 16, 657–661.
- Arndt, K.-F.; Schmidt, T.; Reichelt, R., **2001**, Thermo-sensitive poly(methyl vinyl ether) micro-gel formed by high energy radiation, *Polymer*, 42, 6785–6791.
- Aziz F.; Rodgers M. A. J., **1987**, Editors, *Radiation Chemistry Principles and Applications*, VCH, New York, 201–235.
- Baker W.O., **1949**, Microgel, A relation to sol and gel new macromolecule as structural elements of synthetic rubber, *Ind. Eng. Chem.*, 41, 511.



- Bencherif, S. A.; Siegwart, D. J.; Srinivasan, A.; Horkay, F.; Hollinger, J. O.; Washburn, N. R.; Matyjaszewski, K, **2009**, Nanostructured hybrid hydrogels prepared by a combination of atom transfer radical polymerization and free radical polymerization, *Biomaterials*, 30, 5270–5278.
- Bharali, D. J., Sahoo, S. K., Mozumdar, S., and Maitra, A., **2003**, Cross-linked polyvinylpyrrolidone nanoparticles: a potential carrier for hydrophilic drugs, *J. Colloid Interface Sci.*, 258, 415–423.
- Brigger, I.; Dubernet, C.; Couvreur, P., **2002**, Nanoparticles in cancer therapy and diagnosis, *Adv. Drug Deliv. Rev.*, 54, 631–651.
- Brunius C.F.; Ulrica E.; Ann-Christine A., **2002**, Synthesis and in vitro degradation of poly(N-vinyl-2-pyrrolidone)-based graft copolymers for biomedical applications, *J. Polym. Sci., Part A: Polym. Chem.*, 40, 3652–3661.
- Bueno, V. B.; Cuccovia, I. M.; Chaimovich, H.; Catalani, L. H., **2009**, PVP superabsorbent nanogels, *Colloid Polym. Sci.*, 287, 705–713.
- Buxton G. V., **2008**, An overview of the radiation chemistry of liquids, *Radiation Chemistry From Basics to Applications in Material and Life Sciences*, Editors, Spothem-Maurizot M., Mostafavi M., Douki T., Belloni J., EDP Sciences, France, 3–16.
- Chai, S.; Zhang, J.; Yang, T.; Yuan, J.; Cheng, S., **2010**, Thermoresponsive microgel decorated with silica nanoparticles in shell: Biomimetic synthesis and drug release application, *Colloids Surf., A.*, 356, 32–39.
- Chandran, S.; Nan, A.; Ghandehari, H.; Denmeade, S. R., **2005**, An HPMA-prodrug conjugate as a novel strategy for treatment of prostate cancer, *Clin. Cancer Res.*, 11, 9004.

- Chen, J.; Zhao, P.; Ma, L.; Huang, J.; Zheng, H., **2009**, Preparation of photocrosslinked hydroxypropyl chitosan nanogel and its drug releasing properties, *Wuhan Daxue Xuebao, Lixueban*, 55, 549–554.
- Chen, Y.; Zheng, X.; Qian, H.; Mao, Z.; Ding, D.; Jiang, X., **2010**, Hollow core-porous shell structure poly(acrylic acid) nanogels with a superhigh capacity of drug loading, *ACS Appl. Mater. Interfaces*, 2, 3532–3538.
- Da Silveira, B. I., **1993**, Diffusion in poly(vinylpyrrolidone) hydrogels prepared by radiation technique, *Eur. Polym. J.*, 29, 1095–1098.
- David G.; Simionescu B.C.; Albertsson A.C., **2008**, Rapid deswelling response of poly(N-isopropylacrylamide)/poly(2-alkyl-2-oxazoline)/poly(2-hydroxyethyl methacrylate) hydrogels, *Biomacromolecules*, 9, 1678–1683.
- Davis, F. F.; Abuchowski, A.; Van Es, T.; Palczuk, N. C.; Chen, R.; Savoca, K.; Wieder, K., **1978**, Enzyme-polyethylene glycol adducts: modified enzymes with unique properties, *Enzyme Eng.*, 4, 169–173.
- Davis J. E.; Senogles E., **1981-a**,  $\gamma$ -Irradiation of N-vinylpyrrolidin-2-one and its homopolymer, *Aust. J. Chem.*, 34, 1413–1421.
- Davis J. E.; Sangster D. F.; Senogles E., **1981-b**, Pulse radiolysis of aqueous solutions of N-Vinylpyrrolidin-2-one and Poly(N-vinylpyrrolidin-2-one), *Aust. J. Chem.*, 34, 1423–1431.
- De Groot, J. H.; Zurutuza, A.; Moran, C. R.; Graham, N. B.; Hodd, K. A.; Norrby, S., **2001**, Water-soluble microgels made by radical polymerization in solution, *Colloid Polym. Sci.*, 279, 1219–1224.
- Delaittre, G.; Save, M.; Charleux, B., **2007**, Nitroxide-mediated aqueous dispersion polymerization: from water-soluble macroalkoxyamine to thermosensitive nanogels, *Macromol. Rapid Commun.*, 28, 1528–1533.

- Desai M.P.; Labhasetwar V.; Walter E.; Levy R.J.; Amidon G.L., **1997**, The mechanism of uptake of biodegradable microparticles in Caco-2 cells is size dependent, *Pharm. Res.*, 14, 1568–1573.
- Desai, P. N.; Yuan, Q.; Yang, H., **2010**, Synthesis and characterization of photocurable polyamidoamine dendrimer hydrogels as a versatile platform for tissue engineering and drug delivery, *Biomacromolecules*, 11, 666–673.
- Dieu, H. A.; Desreux, V., **1960**, Cross-linking of poly(vinyl alcohol) by  $\gamma$ -radiation, *Large Radiation Sources in Industry. Intern. Atomic Energy Agency, Vienna*, 1, 341–346.
- Discher, D. E.; Eisenberg, A., **2002**, Polymer vesicles, *Science*, 297, 967–973.
- Drury J. L.; Mooney D. J., **2003**, Hydrogels for tissue engineering: scaffold design variables and applications, *Biomaterials*, 24, 4337–4351.
- Du, J. Z.; Sun, T.; Song, W. J.; Wu, J.; Wang, J., **2010**, A tumor-acidity-activated charge-conversional nanogel as an intelligent vehicle for promoted tumoral-cell uptake and drug delivery, *Angew. Chem. Int. Ed.*, 49, 3621–3626.
- Duncan, R., **1992**, Drug-polymer conjugates: potential for improved chemotherapy, *Anticancer Drugs*, 3, 175–210.
- Duncan, R., **2006**, Polymer conjugates as anticancer nanomedicines, *Nat. Rev. Cancer*, 6, 688–701.
- Elias H-G., **1961**, *Makromol. Chem.*, 50, 1.
- Elias H-G., **1962**, *Makromol. Chem.*, 54, 78.

- Farokhzad, O. C.; Langer, R, **2006**, Nanomedicine: Developing smarter therapeutic and diagnostic modalities, *Adv. Drug Deliv. Rev.*, 58, 1456–1459.
- Flory P. J., **1941**, Molecular size distribution in three dimensional polymers I. Gelation, *J. Am. Chem. Soc.*, 63, 3091.
- Flory P.J., **1953**, Principles of Polymer Chemistry, Cornell University Press, Ithaca.
- Folkman, J.; Long, D. M., **1964**, The use of silicone rubber as a carrier for prolonged drug therapy, *J. Surg. Res.*, 4, 139–142.
- Galmarini, C. M.; Warren, G.; Senanayake, M. T.; Vinogradov, S. V., **2010**, Efficient overcoming of drug resistance to anticancer nucleoside analogs by nanodelivery of active phosphorylated drugs, *International J. of Pharmaceutics*, 395, 281–289.
- Gargallo L; Radic D, **1982**, Preferential adsorption of vinyl polymers in binary solvents, *Adv. Colloid Interface Sci.*, 21, 1–53.
- Gao, H.; Matyjaszewski, K., **2008**, Synthesis of star polymers by a new "core-first" method: sequential polymerization of cross-linker and monomer, *Macromolecules*, 41, 1118–1125.
- Ge, H. X.; Hu, Y.; Jiang, X. Q.; Cheng, D. M.; Yuan, Y. Y.; Bi, H.; Yang, C. Z., **2002**, Preparation, characterization, and drug release behaviors of drug nimodipine-loaded poly(epsilon-caprolactone)-poly(ethylene oxide)-poly(epsilon-caprolactone) amphiphilic triblock copolymer micelles, *J. Pharm. Sci.*, 91, 1463–1473.
- Godawat R.; Jamadagni S. N.; Garde S., **2010**, Unfolding of hydrophobic polymers in guanidinium chloride solutions, *J. Phys. Chem. B*, 114, 2246–54.

- Gong, Y.; Fan, M.; Gao, F.; Hong, J.; Liu, S.; Luo, S.; Yu, J.; Huang, J., **2009**, Preparation and characterization of amino - functionalized magnetic nanogels via photopolymerization for MRI applications, *Colloids Surf., B*, 71, 243–247.
- Gota, C.; Okabe, K.; Funatsu, T.; Harada, Y.; Uchiyama, S., **2009**, Hydrophilic fluorescent nanogel thermometer for intracellular thermometry, *J. Am. Chem. Soc.*, 131, 2766–2767.
- Govender, T.; Stolnik, S.; Garnett, M. C.; Illum, L.; Davis, S. S., **1999**, PLGA nanoparticles prepared by nanoprecipitation: drug loading and release studies of a water soluble drug, *J. Controlled Release*, 57, 171–185.
- Greenley R.Z., **1980**, *J. Macromol. Sci. Chem.*, A14, 445.
- Goncalves, C.; Pereira, P.; Gama, M., **2010**, Self-assembled hydrogel nanoparticles for drug delivery applications, *Materials*, 3, 1420–1460.
- Güven O.; Eltan E., **1980**, Molecular association in aqueous solutions of high molecular weight poly(N-vinyl-2-pyrrolidone), *Makromol. Chem.*, 182, 3129–3134.
- Haag, R., **2004**, Supramolecular drug-delivery systems based on polymeric core-shell architectures, *Angew. Chem. Int. Ed.*, 43, 278–282.
- Han, E. H.; Wilensky, L. M.; Schumacher, B. L.; Chen, A. C.; Masuda, K.; Sah, R. L., **2010**, Tissue engineering by molecular disassembly and reassembly: biomimetic retention of mechanically functional aggrecan in hydrogel, *Tissue Eng., Part C: Met.*, 16, 1471–1479.
- Hart E. J., **1951**, Mechanism of the  $\gamma$ -ray induced oxidation of formic acid in aqueous solution, *J. Am. Chem. Soc.*, 73, 68–73.

- Hart E. J., **1959**, Development of the radiation chemistry of aqueous solutions, *J. Chem. Educ.* 36, 266.
- Hart E. J.; Gordon S.; Thomas J.K., **1964**, Rate constants of hydrated electron reactions with organic compounds, *J. Phys. Chem.*, 68, 1271.
- Heegaard, P.; Boas, U., **2004**, Dendrimer conjugates for selective solubilization of protein aggregates, *PCT Int. Appl.*, 43 pp.
- Henke A.; Kadlubowski S.; Ulanski P.; Rosiak J. M.; Arndt K-F., **2005**, Radiation-induced cross-linking of polyvinylpyrrolidone-poly(acrylic acid) complexes, *Nucl. Instrum. Methods Phys. Res., Sect. B*, 236, 391–398.
- Hill, D. J. T.; Whittaker, A. K.; Zainuddin, **2011**, Water diffusion into radiation crosslinked PVA-PVP network hydrogels, *Radiat. Phys. Chem.*, 80, 213–218.
- Hirakura, T.; Yasugi, K.; Nemoto, T.; Sato, M.; Shimoboji, T.; Aso, Y.; Morimoto, N.; Akiyoshi, K., **2010**, Hybrid hyaluronan hydrogel encapsulating nanogel as a protein nanocarrier: New system for sustained delivery of protein with a chaperone-like function, *J. Controlled Release*, 142, 483–489.
- Holowka, E. P.; Sun, V. Z.; Kamei, D. T.; Deming, T. J., **2006**, Polyarginine segments in block copolypeptides drive both vesicular assembly and intracellular delivery, *Nature Mat.*, 6, 52–57.
- Holtz, J. H.; Asher, S. A., **1997**, Polymerized colloidal crystal hydrogel films as intelligent chemical sensing materials, *Nature*, 389, 829–832.
- Ikeda, Masato; Ochi, Rika; Hamachi, Itaru, **2010**, Supramolecular hydrogel-based protein and chemosensor array, *Lab on a Chip*, 10, 3325-3334.

- Janata E.; Schuler R. H., **1982**, Rate constant for scavenging  $e_{aq}^-$  in  $N_2O$ -saturated solutions, *J. Phys. Chem.*, 86, 2079–2084.
- Jones, M. C.; Leroux, J. C., **1999**, Polymeric micelles-a new generation of colloidal drug carriers, *Eur. J. Pharm. Biopharm.*, 48, 101–111.
- Kabanov A. V.; Vinogradov S. V., **2009**, Nanogels as pharmaceutical carriers: Finite networks of infinite capabilities, *Angew. Chem. Int. Ed.*, 48, 5418–5429.
- Kadlubowski, S.; Grobelny, J.; Olejniczak, W.; Cichomski, M.; Ulanski, P., **2003**, Pulses of fast electrons as a tool to synthesize poly(acrylic acid) nanogels. Intramolecular cross-linking of linear polymer chains in additive-free aqueous solution, *Macromolecules*, 36, 2484–2492.
- Kang, S.; Munkhjargal, O.; Kim, S.; Park, A.; Shim, Y.; Lee, W., **2010**, Preparation and characterization of nano-sized hydrogels (nanogels) using inverse-mini-emulsion polymerization method for protein drug delivery, *Yakche Hakhoechi*, 40, 73–78.
- Kim, H. R.; Andrieux, K.; Couvreur, P., **2007**, PEGylated polymer-based nanoparticles for drug delivery to the brain, *Colloid Interface Sci. Ser.*, 3, 409–428.
- Kim, H. K.; Shim, W. S.; Kim, S. E.; Lee, K.; Kang, E.; Kim, J.; Kim, K.; Kwon, I. C.; Lee, D. S., **2009**, Injectable in situ-forming pH/thermo-sensitive hydrogel for bone tissue engineering, *Tissue Engineering, Part A*, 15, 923–933.
- Kiser, P. F.; Wilson, G; Needham, D., **1998**, A synthetic mimic of the secretory granule for drug delivery. *Nature*, 394, 459–462.
- Kochanny, Jr. G. L.; Timnick A.; Hochanadel C. J.; Goodman C. D., **1963**, Radiation chemistry studies of water as related to the initial linear energy transfer of 11-Mev to 23-Mev protons, *Radiation Research*, 19, 462–473.

- Koshi, Y.; Nakata, E.; Yamane, H.; Hamachi, I., **2006**, A fluorescent lectin array using supramolecular hydrogel for simple detection and pattern profiling for various glycoconjugates, *J. Am. Chem. Soc.*, 128, 10413–10422.
- Kwon, G. S.; Kataoka, K., **1995**, Block-copolymer micelles as long-circulating drug vehicles, *Adv. Drug Deliv. Rev.*, 16, 295–309.
- Langer, R.; Folkman, J., **1976**, Polymers for sustained-release of proteins and other macromolecules, *Nature*, 263, 797–800.
- Lee P. I., **1984**, Novel approach to zero-order drug delivery via immobilized nonuniform drug distribution in glassy hydrogels, *J. Pharm. Sci.*, 73, 1344–1347.
- Lee, C. C.; Gillies, E. R.; Fox, M. E.; Guillaudeu, S. J.; Frechet, J. M. J.; Dy, E. E.; Szoka, F. C., **2006**, A single dose of doxorubicin-functionalized bow-tie dendrimer cures mice bearing C-26 colon carcinomas, *Proc. Natl. Acad. Sci. U.S.A.*, 103, 16649–16654.
- Lemieux, P.; Vinogradov, S. V.; Gebhart, C. L.; Guerin, N.; Paradis, G.; Nguyen, H. K.; Ochiatti, B.; Suzdaltseva, Y. G.; Bartakova, E. V.; Bronich, T. K.; St-Pierre, Y.; Alakhov, V. Y.; Kabanov, A. V., **2000**, Block and graft copolymers and Nanogel (TM) copolymer networks for DNA delivery into cell, *J. Drug Target.*, 8, 91–105.
- Leon, J. W.; Bennett, J. R.; Qiao, T. A.; Harder, J. W.; Mourey, T. H.; Slater, G. L.; Dai, L., **2007**, Nanogel-based contrast agents for optical molecular imaging and preparation of nanogel., *U.S. Pat. Appl. Publ.*, 20070237821.
- Li, W; Wang, W.; Qian, S.; Yao, S., **2002**, Nano poly(N-isopropylacrylamide) microgel polymerization initiated by light, *Fushe Yanjiu Yu Fushe Gongyi Xuebao*, 20, 118–122.



- Li, J.; Liu, B.; Li, J., **2006**, Controllable self-assembly of CdTe/Poly (N-isopropylacrylamide-acrylic acid) microgels in response to pH stimuli, *Langmuir*, 22, 528–531.
- Li, Y.; Yang, J.; Wu, W.; Zhang, X.; Zhuo, R., **2009**, Degradable nanogels as a nanoreactor for growing silica colloids, *Langmuir*, 25, 1923–1926.
- Li, C.; Liu, S., **2010**, Responsive nanogel-based dual fluorescent sensors for temperature and Hg<sup>2+</sup> ions with enhanced detection sensitivity, *J. Mat. Chem.*, 20, 10716–10723.
- Li, H.; Pang, Z.; Jiao, Z.; Lin, F., **2010**, Synthesis and application of a microgel-supported acylating reagent by coupled ring-opening metathesis polymerization and activators re-generated by electron transfer for atom transfer radical polymerization, *J. Combinatorial Chem.*, 12, 255–259.
- Li, X. Y.; Kong, X. Y.; Zhang, J.; Wang, Y. J.; Wang, Y. J.; Shi, S.; Guo, G.; Luo, F.; Zhao, X.; Wei, Y. Q.; Qian, Z. Y., **2011**, A novel composite hydrogel based on chitosan and inorganic phosphate for local drug delivery of camptothecin nanocolloids, *J. Pharm. Sci.*, 100, 232–241.
- Liu, H.; Li, J., **2008-a**, Photochemical synthesis and characterization of polyethyleneimine-coated magnetic nanogel used as cancer-targeted carrier, *Gaodeng Xuexiao Huaxue Xuebao*, 29, 1703–1706.
- Liu, H.; Li, J., **2008-b**, Preparation and characterization of poly(PEGMA) modified superparamagnetic nanogels used as potential MRI contrast agents, *Iranian Polymer Journal*, 17, 721–727.
- Liu, L.; Liu, Y.; Hu, Z., **2009-a**, Preparation of core-shell structure fluorinated reactive microgel, *Tuliao Gongye*, 39, 32–34.

- Liu, W.; Huang, Y.; Peng, C.; Liu, H., **2009-b**, Synthesis and swelling properties of multiresponsive chitosan microgel, *Huagong Xuebao (Chinese Edition)*, 60, 2101–2106.
- Liu, J.; Song, H.; Zhang, L.; Xu, H.; Zhao, X., **2010**, Self-assembly-peptide hydrogels as tissue-engineering scaffolds for three-dimensional culture of chondrocytes in vitro, *Macromolecular Bioscience*, 10, 1164–1170.
- Lopes C.M.A.;Felisberti M.I., **2003**, Mechanical behaviour and biocompatibility of poly(1-vinyl-2-pyrrolidinone)–gelatin IPN hydrogels, *Biomaterials*, 24, 1279–1284.
- Lopez-Leon T.; Ortega-Vinuesa J. L.; Bastos-Gonzalez D.; Elaissari A., **2006**, Cationic and anionic poly(N-isopropylacrylamide) based submicron gel particles: electrokinetic properties and colloidal stability, *J. Phys. Chem. B*, 110, 4629–4636.
- Ma, C.; Prabhu, S., **2011**, Characterization of a novel lyophilized chitosan hydrogel complex for the controlled release of a highly water soluble drug, Niacinamide, *Int. J. Drug Delivery*, 3, 55–63.
- Maeda, H.; Wu, J.; Sawa, T.; Matsumura, Y.; Hori, K., **2000**, Tumor vascular permeability and the EPR effect in macromolecular therapeutics: a review, *J. Controlled Release*, 65, 271–284.
- Malik, N.; Evagorou, E. G.; Duncan, R., **1999**, Dendrimer-platinate: A novel approach to cancer chemotherapy, *Anticancer Drugs*, 10, 767–776.
- Magnet, S.; Charleux, B.; Delaittre, G.; Save, M., **2008**, Process for preparation of microgel particles by controlled radical polymerization in aqueous dispersion using nitroxide control agents, *PCT Int. Appl.*, 46.
- Matsumoto, A.; Miwa, Y.; Iga, Y.; Aota, H., **2008**, Free-radical multiallyl crosslinking polymerization preceded by in situ nanogel- or microgel-like

methacrylate-network-polymer precursor formation, *Nettowaku Porima*, 29, 12–22.

Matsumura, Y.; Hamaguchi, T.; Ura, T.; Muro, K.; Yamada, Y.; Shimada, Y.; Shirao, K.; Okusaka, T.; Ueno, H.; Ikeda, M.; Watanabe, N., **2004**, Phase I clinical trial and pharmacokinetic evaluation of NK911, a micelle-encapsulated doxorubicin, *Br. J. Cancer*, 91, 1775–1781.

Meza, R.; Gargallo, L., **1977**, Unperturbed dimensions of polyvinylpyrrolidone in pure solvents and in binary mixtures, *Eur. Polym. J.*, 13, 235.

Mi, P.; Ju, X.; Xie, R.; Wu, H.; Ma, J.; Chu, L., **2010**, A novel stimuli-responsive hydrogel for K<sup>+</sup>-induced controlled-release, *Polymer*, 51, 1648–1653.

Morris G. E.; Vincent B.; Snowden M. J., **1997**, adsorption of lead ions onto N-isopropylacrylamide and acrylic acid copolymer microgels, *J. Colloid Interface Sci.*, 190, 198–205.

Nishiyama, N.; Kataoka, K., **2006**, Current state, achievements, and future prospects of polymeric micelles as nanocarriers for drug and gene delivery, *Pharmacol. Ther.*, 112, 630–648.

Nochi, T.; Yuki, Y.; Takahashi, H.; Sawada, S.; Mejima, M.; Kohda, T.; Harada, N.; Kong, I. G.; Sato, A.; Kataoka, N.; Tokuhara, D.; Kurokawa, S.; Takahashi, Y.; Tsukada, H.; Kozaki, S.; Akiyoshi, K.; Kiyono, H., **2010**, Nanogel antigenic protein-delivery system for adjuvant-free intranasal vaccines, *Nature Mat.*, 9, 572–578.

Nolan C. M.; Reyes C. D.; Debord J. D.; Garcia A. J.; Lyon L. A., **2005**, Phase transition behavior, protein adsorption, and cell adhesion resistance of poly(ethylene glycol) cross-linked microgel particles, *Biomacromolecules*, 6, 2032–2039.

Nur, H.; Snowden, M. J.; Cornelius, V. J.; Mitchell, J. C.; Harvey, P. J.; Bence, L. S., **2009**, Colloidal microgel in removal of water from biodiesel, *Colloids Surf., A.*, 335, 133–137.

- Nur, H.; Pinkrah, V. T.; Mitchell, J. C.; Bence, L. S.; Snowden, M. J., **2010**, Synthesis and properties of polyelectrolyte microgel particles, *Adv. Colloid Interface Sci.*, 158, 15–20.
- Nurkeeva, Z. S.; Khutoryanskiy, V. V.; Mun, G. A.; Bitekenova, A. B.; Kadlubowski, S.; Shilina, Y. A.; Ulanski, P.; Rosiak, J. M., **2004**, Interpolymer complexes of poly(acrylic acid) nanogels with some non-ionic polymers in aqueous solutions, *Colloids Surf., A.*, 236, 141–146.
- Oh, J. K.; Tang, C.; Gao, H.; Tsarevsky, N. V.; Siegwart, D. J.; Sherwood, G.; Peteanu, L.; Matyjaszewski, K., **2006**, Synthesis and functionalization of degradable nanogel particles prepared by inverse miniemulsion AGET ATRP, *Polym. Prepr.*, 47, 945–946.
- Oh, J. K.; Bencherif, S. A.; Matyjaszewski, K., **2009**, Atom transfer radical polymerization in inverse miniemulsion: A versatile route toward preparation and functionalization of microgels/ nanogels for targeted drug delivery applications, *Polymer*, 50, 4407–4423.
- Oishi, M.; Hayashi, H.; Iijima, M.; Nagasaki, Y., **2007**, Endosomal release and intracellular delivery of anticancer drugs using pH-sensitive PEGylated nanogels, *J. Mat. Chem.*, 17, 3720–3725.
- Oishi, M.; Nagasaki, Y., **2008**, pH-responsive PEGylated nanogels as smart nanodevice for cancer diagnosis and therapy, *Polym. Prepr.*, 49, 461–462.
- Otsuka, H.; Nagasaki, Y.; Kataoka, K., **2003**, PEGylated nanoparticles for biological and pharmaceutical applications, *Adv. Drug Deliv. Rev.*, 55, 403–419.
- Panyam, J.; Labhasetwar, V., **2003**, Biodegradable nanoparticles for drug and gene delivery to cells and tissue, *Adv. Drug Deliv. Rev.*, 55, 329–347.
- Park, H.; Temenoff, J. S.; Holland, T. A.; Tabata, Y.; Mikos, A. G., **2005**, Delivery of TGF-beta.1 and chondrocytes via injectable, biodegradable hydrogels

for cartilage tissue engineering applications, *Biomaterials*, 26, 7095–7103.

Patel, Hitesh A.; Patel, Jayvadan K., **2010**, Nanogel as a controlled drug delivery system, *Int. J. Pharm. Sci. Rev. Res.*, 4, 37–41.

Peng, M.; Wang, H.; Chen, Y., **2008**, Encapsulation of microgels with polystyrene (PS): A novel method for the preparation of hollow PS particles, *Mat. Lett.*, 62, 1535–1538.

Peng, H.; Stolwijk, J. A.; Sun, L.; Wegener, J.; Wolfbeis, O. S., **2009**, A nanogel for ratiometric fluorescent sensing of intracellular pH values, *Angew. Chem., Int. Ed.*, 49, 4246–4249.

Photos, P. J.; Bacakova, L.; Discher, B.; Bates, F. S.; Discher, D. E., **2003**, Polymer vesicles in vivo: Correlations with PEG molecular weight, *J. Controlled Release*, 90, 323–334.

Qiu L.Y.; Bae Y.H., **2006**, Polymer architecture and drug delivery, *Pharm. Res.*, 23, 1–30.

Quan, C.; Sun, Y.; Cheng, H.; Cheng, S.; Zhang, X.; Zhuo, R., **2008**, Thermosensitive P(NIPAAm-co-PAAc-co-HEMA) nanogels conjugated with transferrin for tumor cell targeting delivery, *Nanotechnology*, 19, 1–8.

Quevedo, J. A.; Patel, G.; Pfeffer, R., **2009**, Removal of Oil from Water by Inverse Fluidization of Aerogels, *Ind. Eng. Chem. Res.*, 48, 191–201.

Rahimi, M.; Yousef, M.; Cheng, Y.; Meletis, E. I.; Eberhart, R. C.; Nguyen, K., **2009**, Formulation and characterization of a covalently coated magnetic nanogel, *J. Nanosci. Nanotechnol.*, 9, 4128–4134.

Ravin, H. A.; Seligman, A. M.; Fine, **1952**, Polyvinyl Pyrrolidone as a plasma expander-studies on its excretion, distribution and metabolism, *J. N. Engl. J. Med.*, 247, 921–929.

- Riesz, P., **1965**, The radiolysis of acetone in air-free aqueous solutions, *J. Phys. Chem.*, 69, 1366–1373.
- Robinson B. V.; Sullivan F. M.; Borzelleca J. F.; Schwartz S. L., **1990**, PVP, A critical review of kinetics and toxicology of polyvinylpyrrolidone (Povidone), Lewis Publishers, Inc., MI, USA.
- Rosiak J.; Olejniczak J.; Pékala W., **1990**, Fast reaction of irradiated polymers—I. Crosslinking and degradation of polyvinylpyrrolidone, *Int. J. Radiat. Appl. Instrum., Part C, Radiat. Phys. Chem.*, 36, 747–755.
- Rosiak J.; Olejniczak J., **1993**, Medical applications of radiation formed hydrogels, *Radiat. Phys. Chem.*, 42, 903–906.
- Rosiak, J. M., **2007**, Nano- and microgels of poly(vinyl methyl ether) obtained by radiation techniques, *Eurasian Chem. Tech. J.*, 9, 165–176.
- Ryu, J.; Chacko, R. T.; Jiwanich, S.; Bickerton, S.; Babu, R. P.; Thayumanavan, S., **2010**, Self-cross-linked polymer nanogels: a versatile nanoscopic drug delivery platform., *J. Am. Chem. Soc.*, 132, 17227–17235.
- Sabharwal, S.; Mohan, H.; Bhardwaj, Y. K.; Majali, A. B., **1999**, Radiation induced crosslinking of poly(vinyl methyl ether) in aqueous solutions, *Radiat. Phys. Chem.*, 54, 643–653.
- Sakurada, I.; Ikada, Y., **1963**, Effects of  $\gamma$ -radiation on polymers in solution. V. Intramolecular crosslinking of poly(acrylic acid) in dilute aqueous solution, *Bull. Inst. Chem. Res., Kyoto Univ.*, 41, 114–122.
- Sakurada, I.; Ikada, Y., **1964**, Effects of  $\gamma$ -radiation on polymers in solution. VIII. Radiation effects on poly(vinyl alcohol) in aqueous solutions below the critical concentration for gel formation, *Bull. Inst. Chem. Res., Kyoto Univ.*, 42, 32–41.
- Sanson, N.; Rieger, J., **2010**, Synthesis of nanogels/ microgels by conventional and controlled radical crosslinking copolymerization, *Polymer Chemistry*, 1, 965–977.

- Saxena A.; Mozumdar S.; Johri A. K., **2006**, Ultra-low sized cross-linked polyvinylpyrrolidone nanoparticles as non-viral vectors for in vivo gene delivery, *Biomaterials*, 27, 5596–5602.
- Schmidt, T.; Janik, I.; Kadlubowski, S.; Ulanski, P.; Rosiak, J. M.; Reichelt, R.; Arndt, K.-F., **2005**, Pulsed electron beam irradiation of dilute aqueous poly(vinyl methyl ether) solutions, *Polymer*, 46, 9908–9918.
- Spinks J. W.; Woods R. J., 1964, *An introduction to radiation chemistry*, John Wiley & Sons, New York, 237–308.
- Şen M.; Yakar A., **2001**, Controlled release of Terbinafine Hydrochloride from pH sensitive poly(N-vinyl 2 pyrrolidone/itaconic acid) hydrogels, *Int. J. Pharm.*, 228, 33–41.
- Sinha-Ray S.; Zhang Y.; Placke D.; Megaridis C. M.; Yarin A. L., **2010**, Resins with "nano-raisins", *Langmuir*, 26, 10243–10249.
- Staudinger, H.; Husemann E., **1935**, *Ber. Dtsch. Chem. Ges.*, 68, 1618–1634.
- Sun, X.; Chiu, Y. Y.; Lee, L. J., **1997**, Microgel formation in the free radical crosslinking copolymerization of methyl methacrylate (MMA) and ethylene glycol dimethacrylate (EGDMA), *Chem. Res.*, 36, 1343–1351.
- Sun, H.; Zhang, L.; Zhu, X.; Kong, C.; Zhang, C.; Yao, S., **2009**, Poly(PEGMA) magnetic nanogels: preparation via photochemical method, characterization and application as drug carrier, *Sci. China Ser. B*, 52, 69–75.
- Sun, W.; Zhu, H., **2010**, Progress of folate-PAMAM dendrimer conjugates as drug carriers in targeted drug delivery system, *Zhongguo Yiyao Gongye Zazhi*, 41, 538–542.
- Sundaram P. V.; Venkatesh R., **1998**, Retardation of thermal and urea induced inactivation of alpha-chymotrypsin by modification with carbohydrate polymers, *Protein Eng.*, 11, 699–705.

- Svenson, S.; Tomalia, D. A., **2005**, Commentary-Dendrimers in biomedical applications-reflections on the field, *Adv. Drug Deliv. Rev.*, 57, 2106–2129.
- Tanaka, T. and Fillmore, D. J., **1979**, Kinetics of swelling of gels, *J. of Chem. Phys.*, 70, 1214–1218.
- Tomoda, Y.; Tsuda, M., **1962**, Some aspects of the crosslinking and degradation of gelatin molecules in aqueous solutions irradiated by Co60  $\gamma$ -rays, *Tokyo Kogyo Shikensho Hokoku*, 57, 517–520.
- Tong, R.; Cheng, J., **2007**, Anticancer polymeric nanomedicines, *Polymer Rev.*, 47, 345–381.
- Ulanski, P.; Janik, I.; Rosiak, J. M., **1998**, Radiation formation of polymeric nanogels, *Radiat. Phys. Chem.*, 52, 289–294.
- Ulanski, R.; Rosiak, J. M., **1999**, The use of radiation technique in the synthesis of polymeric nanogels, *Nucl. Instrum. Methods Phys. Res., Sect. B*, 151, 356–360.
- Ulanski, P.; Kadlubowski, S.; Rosiak, J. M., **2002**, Synthesis of poly(acrylic acid) nanogels by preparative pulse radiolysis, *Radiat. Phys. Chem.*, 62, 533–537.
- Ulanski P.; Rosiak J.M., **2004**, Polymeric nano/microgels, *Encyclopedia of Nanoscience and Nanotechnology*, Amer. Sci. Publ. (Ed. H.S. Nalwa), 8, 845–871.
- Van Der Linden, H., Herber, S., Olthuis, W., and Bergveld, P., **2002**, Development of stimulus-sensitive hydrogels suitable for actuators and sensors in microanalytical devices, *Sens. Mat.*, 14, 129–139.
- Van Tomme, Sophie R.; Hennink, Wim E., **2007**, Biodegradable dextran hydrogels for protein delivery applications, *Expert Rev. Med. Devices*, 4, 147–164.
- Vereshchinskii, I.V.; Pikaev, A.K, **1964**, Introduction to Radiation Chemistry, Davey, New York, 61–140.



- Viljoen, C.; Verbeek, C. J. R.; Pickering, K. L., **2007**, The use of aqueous urea as chemical denaturant in processing CGM into a biodegradable polymer material, *Adv. Mater. Process.* IV, 29, 181–184.
- Vinogradov, S. V.; Bronich, T. K.; Kabanov, A. V., **2002**, Nanosized cationic hydrogels for drug delivery: preparation, properties and interactions with cells, *Adv. Drug Deliv. Rev.*, 54, 135–147.
- Vinogradov, S. V.; Batrakova, E. V.; Kabanov, A. V., **2004**, Nanogels for oligonucleotide delivery to the brain, *Bioconjug. Chem.*, 15, 50–60.
- Wada, A.; Tamaru, S.; Ikeda, M.; Hamachi, I., **2009**, MCM–enzyme–supramolecular hydrogel hybrid as a fluorescence sensing material for polyanions of biological significance, *J. Am. Chem. Soc.*, 131, 5321–5330.
- Wang X.; Wang Y.; Chen Z.; Shin D. M., **2009**, Advances of cancer therapy by nanotechnology, *Cancer Res. Treat*, 41, 1–11.
- Wardman P., **1978**, Application of pulse radiolysis methods to study the reactions and structure of biomolecules, *Rep. Prog. Phys.*, 41, 259.
- Weiss J., **1944**, Radiochemistry of aqueous solutions, *Nature*, 153, 748.
- Wichterle, O.; Lim, D., **1960**, Hydrophilic gels for biological use, *Nature*, 185, 117–118.
- Wieder, K. J.; Palczuk, N. C.; van Es, T.; Davis, F. F., **1979**, Some properties of polyethylene glycol: Phenylalanine ammonia-lyase adducts, *J. Biol. Chem.*, 254, 12579–12587.
- Wu, X.; Pelton, R. H.; Hamielec, A. E.; Woods, D. R.; McPhee, W., **1994**, The kinetics of poly(N-isopropylacrylamide) microgel latex formation, *Colloid. Polym. Sci.*, 272, 467–77.
- Wu, H.; Zhang, H.; Fan, L.; Wang, J.; Ren, B., **2007**, Synthesis and properties of temperature-sensitive poly(N-isopropylacrylamide/acrylamide) nanogel, *Jiefangjun Yaoxue Xuebao*, 23, 245–249.

- Wu, W.; Mitra, N.; Yan, E. C. Y.; Zhou, S., **2010-a**, Multifunctional hybrid nanogel for integration of optical glucose sensing and self-regulated insulin release at physiological pH., *ACS Nano*, 4, 4831–4839.
- Wu, W.; Shen, J.; Banerjee, P.; Zhou, S., **2010-b**, Core-shell hybrid nanogels for integration of optical temperature-sensing, targeted tumor cell imaging, and combined chemo-photothermal treatment, *Biomaterials*, 31, 7555–7566.
- Yan, J.; Pedrosa, V. A.; Simonian, A. L.; Revzin, Al., **2010**, Immobilizing enzymes onto electrode arrays by hydrogel photolithography to fabricate multi-analyte electrochemical biosensors, *ACS Appl. Mater. Interfaces*, 2, 748–755.
- Yoshimura, Ibuki; Miyahara, Yoshifumi; Kasagi, Noriyuki; Yamane, Hiroki; Ojida, Akio; Hamachi, Itaru, **2004**, Molecular recognition in a supramolecular hydrogel to afford a semi-wet sensor chip, *J. Am. Chem. Soc.*, 126, 12204–12205.
- Yu, K.; Zhang, L. F.; Eisenberg, A., **1996**, Novel morphologies of “crew-cut” aggregates of amphiphilic diblock copolymers in dilute solution, *Langmuir*, 12, 5980–5984.
- Yu, S. Y.; Hu, J. H.; Pan, X. Y.; Yao, P.; Jiang, M., **2006**, Stable and pH-sensitive nanogels prepared by self-assembly of chitosan and ovalbumin, *Langmuir*, 22, 2754–2759.
- Yu, Q.; Zhou, M.; Ding, Y.; Jiang, B.; Zhu, S., **2007**, Development of networks in atom transfer radical polymerization of dimethacrylates, *Polymer*, 48, 7058–7064.
- Zelikin A. N.; Such G. K.; Postma A.; Caruso F., **2007**, Poly(vinylpyrrolidone) for bioconjugation and surface ligand immobilization, *Biomacromolecules*, 8, 2950–2953.

Zhang J. G.; Xu S. Q.; Kumacheva E., **2004**, Polymer microgels: reactors for semiconductor, metal, and magnetic nanoparticles, *J. Am. Chem. Soc.*, 126, 7908–7914.

Zhang, Y.; Ji, C., **2010**, Electro-induced covalent cross-linking of chitosan and formation of chitosan hydrogel films: Its application as an enzyme immobilization matrix for use in a phenol sensor, *Anal. Chem.*, 82, 5275–5281.

Zillessen, A.; Bartsch, E., **2010**, Synthesis of photo-cross-linkable microgel colloids for cluster formation studies, *Langmuir*, 26, 89–96.

## **CURRICULUM VITAE**

Name and Surname : Semiha Duygu IŞIK

Place of Birth : Ankara, Turkey

Date of Birth : 20/03/1985

Marital Status : Single

### **Education and Academic Carrier**

High School : 1999 – 2003, Gazi Anatolian High School

Under Graduate (B. Sc.) : 2003 – 2008, Hacettepe University,  
Department of Chemistry

Graduate – M. Sc. : 2008 – present, Hacettepe University,  
Department of Chemistry, Polymer Chemistry Division

Foreign Language : English

### **Experience at Work**

2007 : Summer Training, Eczacıbaşı – Zentiva Health Products,  
R&D Center

2007 – 2008 : Graduation work, Hacettepe University,  
Department of Chemistry, Organic Chemistry Division

2009 – present : Research Assistant, Hacettepe University,  
Department of Chemistry, Polymer Chemistry Division